



US Army Corps of Engineers®



# Hydrodynamic, Salinity, and Morphological Modeling Study of a Sediment Diversion

An Application of the Adaptive Hydraulics Model/SEDLIB Sediment Transport Library

MRG&P Report No. 27 • March 2019



## MRG&P

Mississippi River Geomorphology & Potamology Program



# **Hydrodynamic, Salinity, and Morphological Modeling Study of a Sediment Diversion**

An Application of the Adaptive Hydraulics Model/SEDLIB Sediment Transport Library

Gary L. Brown and Kimberly C. Pevey

*Coastal and Hydraulics Laboratory  
U.S. Army Engineer Research and Development Center  
3909 Halls Ferry Road  
Vicksburg, MS 39180-6199*

Final report

Approved for public release; distribution is unlimited.

Prepared for U.S. Army Corps of Engineers, New Orleans District  
7400 Leake Ave  
New Orleans, LA, 70118

Under Project 118958, "Louisiana Coastal Area Medium Diversion at White Ditch"

## **Abstract**

A water diversion designed to channel sediment-rich water from the Mississippi River into Breton Sound marsh was evaluated through application of a numerical model. The model was validated to data collected from April to December 2010. After model validation was complete, simulations to understand the effects of the proposed diversion on hydrodynamics, salinity, sedimentation, and land building were conducted. Model salinity results indicate that the proposed diversion will rapidly freshen most of Breton Sound and maintain fresh water conditions in the Sound until the diversion is closed. After closure, the time of recovery of salinity in Breton Sound is a function of the prevailing wind-driven currents and Mississippi River discharges through the eastern passes. With respect to the land building potential, model results indicate that the diversion has the capability to create land, but that the diversion cannot operate at full capacity for the full life cycle of the project. Deposition of sand at the diversion channel mouth creates a backwater effect that causes the water surface elevation in the outfall channel to exceed prescribed design constraints. The outfall channel mouth will therefore need to be periodically dredged and placed to form new land elsewhere in the marsh.

# Contents

<b>Abstract</b> .....	<b>ii</b>
<b>Figures and Tables</b> .....	<b>v</b>
<b>Preface</b> .....	<b>viii</b>
<b>Unit Conversion Factors</b> .....	<b>ix</b>
<b>1 Introduction</b> .....	<b>1</b>
Background.....	1
Objective .....	3
Technical approach .....	4
<b>2 Model Development</b> .....	<b>5</b>
Model description.....	5
Mesh development.....	6
Boundary conditions .....	9
<i>Tides</i> .....	9
<i>Winds</i> .....	12
<i>Flow boundary conditions</i> .....	15
<i>Salinity</i> .....	16
<i>Additional parameterization</i> .....	16
Model validation .....	16
<i>Hydrodynamics</i> .....	18
<i>Discharge</i> .....	29
<i>Salinity</i> .....	35
<b>3 Salinity Impacts Due to Diversion</b> .....	<b>46</b>
<b>4 Morphologic Modeling</b> .....	<b>50</b>
Approach .....	50
Morphologic model set up .....	53
<i>Sediment properties</i> .....	53
<i>Boundary conditions</i> .....	55
<i>Tide and wind</i> .....	57
<i>Relative sea level rise</i> .....	57
<i>Primary productivity</i> .....	59
Results .....	60
<i>Qualitative validation to Caernarvon outfall</i> .....	60
<i>Diversion operations and the energy budget constraint</i> .....	63
<i>50 yr projections of land gain associated with BSD operations</i> .....	64
<b>5 Conclusions</b> .....	<b>72</b>
<b>References</b> .....	<b>73</b>



**Report Documentation Page**

# Figures and Tables

## Figures

Figure 1-1. Location of study area in southern Louisiana.....	1
Figure 1-2. Inset image of study area (image courtesy of Google). .....	2
Figure 2-1. Model domain (outlined in yellow) showing area of interest (AOI) in red.....	7
Figure 2-2. AOI inset mesh showing mesh elements (image courtesy Google).....	7
Figure 2-3. Multi-beam data collected by ERDC (image courtesy Google). .....	8
Figure 2-4. Location of tidal gauges and model boundary. ....	10
Figure 2-5. Water surface elevation comparison for Southwest Pass.....	11
Figure 2-6. Water surface elevation comparison for Bay Gardene. ....	11
Figure 2-7. Water surface elevation comparison for Dauphin Island. ....	12
Figure 2-8. Wind gauge locations. ....	13
Figure 2-9. East (+)/West (-) wind magnitudes at Shell Beach. ....	14
Figure 2-10. North (+)/South (-) wind magnitudes at Shell Beach. ....	14
Figure 2-11. Mississippi River hydrograph for validation period. ....	15
Figure 2-12. Caernarvon Diversion inflow for the validation period. ....	16
Figure 2-13. ERDC-CHL 2010 data collection site locations. ....	17
Figure 2-14. ERDC-CHL 2013 data collection site locations. ....	19
Figure 2-15. Water surface elevation comparison for Site 1. ....	20
Figure 2-16. Water surface elevation comparison for Site 2. ....	20
Figure 2-17. Water surface elevation comparison for Site 3.....	21
Figure 2-18. Water surface elevation comparison for Site 4.....	21
Figure 2-19. Water surface elevation comparison for Site 5.....	22
Figure 2-20. Water surface elevation comparison for Site 8.....	22
Figure 2-21. Water surface elevation comparison for Site 9.....	23
Figure 2-22. Water surface elevation comparison for Site 10.....	23
Figure 2-23. Water surface elevation comparison for Caernarvon Outfall. ....	24
Figure 2-24. Water surface elevation comparison for Black Bay. ....	24
Figure 2-25. Water surface elevation comparison for Cow Bayou.....	25
Figure 2-26. Water surface elevation comparison for Crooked Bayou.....	25
Figure 2-27. Water surface elevation comparison for Dauphin Island. ....	26
Figure 2-28. Water surface elevation comparison for Bay Gardene. ....	26
Figure 2-29. Water surface elevation comparison for Mississippi Sound. ....	27
Figure 2-30. Water surface elevation comparison for Port Fourchon. ....	27
Figure 2-31. Water surface elevation comparison for Reggio Canal. ....	28
Figure 2-32. Discharge comparison for Site 1.....	30
Figure 2-33. Discharge comparison for Site 2.....	31

Figure 2-34. Discharge comparison for Site 3.....	31
Figure 2-35. Discharge comparison for Site 4.....	32
Figure 2-36. Discharge comparison for Site 5.....	32
Figure 2-37. Discharge comparison for Site 8.....	33
Figure 2-38. Discharge comparison for Site 9.....	33
Figure 2-39. Discharge comparison for Site 10.....	34
Figure 2-40. Salinity comparison locations.....	36
Figure 2-41. Salinity comparison for Site 1.....	37
Figure 2-42. Salinity comparison for Site 2.....	37
Figure 2-43. Salinity comparison for Site 3.....	38
Figure 2-44. Salinity comparison for Site 4.....	38
Figure 2-45. Salinity comparison for Site 5.....	39
Figure 2-46. Salinity comparison for Site 8.....	39
Figure 2-47. Salinity comparison for Site 9.....	40
Figure 2-48. Salinity comparison for Site 10.....	40
Figure 2-49. Salinity comparison for CRMS 0121.....	41
Figure 2-50. Salinity comparison for CRMS 0129.....	41
Figure 2-51. Salinity comparison for CRMS 0131.....	42
Figure 2-52. Salinity comparison for CRMS 0132.....	42
Figure 2-53. Salinity comparison for CRMS 0135.....	43
Figure 2-54. Salinity comparison for CRMS 0136.....	43
Figure 2-55. Salinity comparison for CRMS 0146.....	44
Figure 2-56. Salinity comparison for CRMS 0147.....	44
Figure 2-57. Salinity comparison for Bay Gardene.....	45
Figure 3-1. Salinity contours 10 Days after diversion opening.....	47
Figure 3-2. Salinity contours 20 days after diversion opening.....	47
Figure 3-3. Salinity contours 30 days after diversion opening.....	48
Figure 3-4. Salinity contours 40 days after diversion opening.....	48
Figure 3-5. Time history of salinity at Bay Gardene.....	49
Figure 3-6. Time history of salinity at Site 5.....	49
Figure 4-1. Inset mesh for morphologic modeling.....	52
Figure 4-2. Zoom of inset mesh for morphologic modeling at diversion outfall.....	52
Figure 4-3. Modeled annual water and sediment inflow hydrograph for the diversion.....	55
Figure 4-4. Modeled annual water and sediment inflow hydrograph for Caernarvon Diversion.....	56
Figure 4-5. Modeled annual mass flux for BSD and CD.....	56
Figure 4-6. Applied tide and wind boundary conditions for morphological modeling.....	57

Figure 4-7. Relative sea level rise curves applied to morphological modeling scenarios. ....	59
Figure 4-8. Primary productivity algorithm used in morphological modeling scenarios.....	61
Figure 4-9. Ground elevation at year 0 of morphological model simulation - medium RSLR. ....	61
Figure 4-10. Ground elevation at year 10 of morphological model simulation - medium RSLR. ....	62
Figure 4-11. Ground elevation at year 20 of morphological model simulation - medium RSLR. ....	62
Figure 4-12. Observed pattern of land gain (source: Lake Ponchartrain Basin Foundation).....	63
Figure 4-13. Bed displacement after 5 yr of operation of BSD.....	65
Figure 4-14. Bed displacement after 10 yr of operation of BSD.....	65
Figure 4-15. Bed displacement after 15 yr of operation of BSD.....	66
Figure 4-16. Bed displacement after 20 yr of operation of BSD.....	66
Figure 4-17. Water surface elevation at BSD outfall. ....	67
Figure 4-18. Projected land gain associated with the operation of BSD for different rates of RSLR.....	67
Figure 4-19. Spatial distribution of land gain due to the operation of BSD-low RSLR (Note: does not include land from dredge placement).....	70
Figure 4-20. Spatial distribution of land gain due to the operation of BSD - medium RSLR (Note: does not include land from dredge placement). ....	70
Figure 4-21. Spatial distribution of land gain due to the operation of BSD - high RSLR (Note: does not include land from dredge placement). ....	71

## Tables

Table 2-1. Location of tidal boundary reference gauges.....	10
Table 2-2. Wind station symbols and locations. ....	13
Table 2-3. ERDC-CHL 2010 data collection site locations. ....	18
Table 2-4. ERDC-CHL 2013 data collection locations. ....	18
Table 4-1. Silt and clay sediment grain class properties.....	55
Table 4-2. Values of the rate of acceleration of eustatic sea level rise for each of the Modified NRC curves.....	59
Table 4-3. Thickness of dredge placement needed to build land.....	68
Table 4-4. Land building efficiency and percent of land due to dredge placement. ....	71

## Preface

This study was prepared for the U.S. Army Corps of Engineers (USACE), New Orleans District (MVN), under Project 118958, “Louisiana Coastal Area Medium Diversion at White Ditch.” The publication of this report was funded by the Mississippi River Geomorphology and Potamology (MRG&P) Program. The MRG&P is part of the Mississippi River and Tributaries Program and is managed by the USACE, Mississippi Valley Division (MVD), and Districts. The Acting Technical Director was Dr. James W. Lewis. The MVD Commander was MG Richard G. Kaiser. The MVD Director of Programs was Mr. James Bodron.

The study was conducted in 2013 by personnel of the U.S. Army Engineer Research and Development Center (ERDC), Coastal and Hydraulics Laboratory (CHL), Vicksburg, MS, in cooperation with the MVN. Project manager for the MVN was Mr. Andrew MacInnes.

The study was conducted under the general supervision of Mr. José Sánchez, Director of CHL, and Dr. Robert McAdory, Chief, Estuarine Engineering Branch.

At the time of publication of this report, Mr. Jeffrey R. Eckstein was the Deputy Director of CHL, and Dr. Ty V. Wamsley was the Director.

COL Ivan P. Beckman was the Commander of ERDC, and Dr. David W. Pittman was the Director.

## Unit Conversion Factors

Multiply	By	To Obtain
acres	4,046.873	square meters
cubic feet	0.02831685	cubic meters
cubic inches	1.6387064 E-05	cubic meters
cubic yards	0.7645549	cubic meters
degrees (angle)	0.01745329	radians
degrees Fahrenheit	(F-32)/1.8	degrees Celsius
feet	0.3048	meters
microns	1.0 E-06	meters
miles (U.S. statute)	1,609.347	meters
miles per hour	0.44704	meters per second
pounds (force)	4.448222	newtons
square feet	0.09290304	square meters
yards	0.9144	meters



# 1 Introduction

## Background

The U.S. Army Corps of Engineers (USACE), New Orleans District (MVN), requested that the U.S. Army Engineer Research and Development Center (ERDC), Coastal and Hydraulics Lab (CHL), perform a numerical modeling study to estimate impacts on the Breton Sound estuary from a diversion of the Mississippi River.

Breton Sound is located south of New Orleans and is situated between the Mississippi River Gulf Outlet to the east and the Mississippi River to the west (Figure 1-1 and Figure 1-2). Breton Sound is a complex deltaic environment that has been undergoing formation over the last 4000 years and is composed of many different deltaic geomorphic features including lakes, marshes, barrier islands, natural levees, and abandoned river channels (Roberts 1997; Snedden et al. 2007a). Sediment starvation, relative sea level rise, storm passage, and channelization have all contributed to significant wetland loss to coastal Louisiana. Breton Sound has suffered land loss as a result of each of these causes.

Figure 1-1. Location of study area in southern Louisiana.

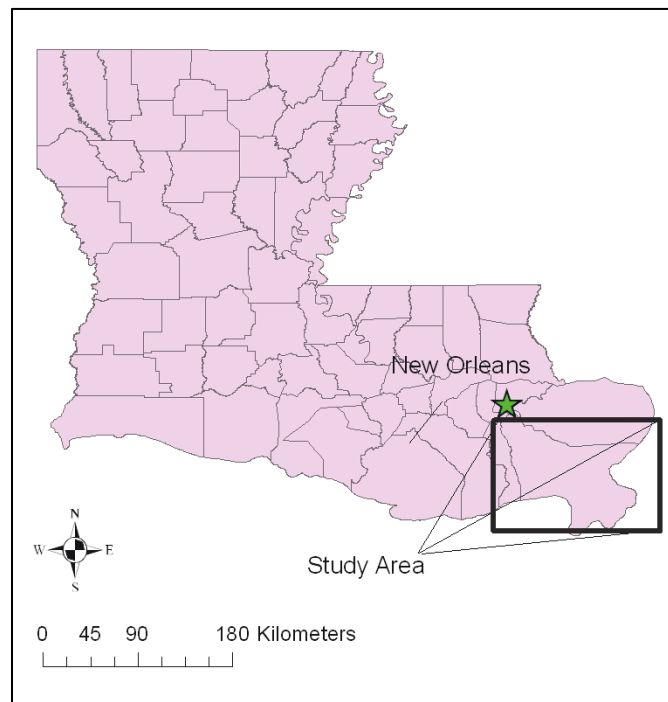
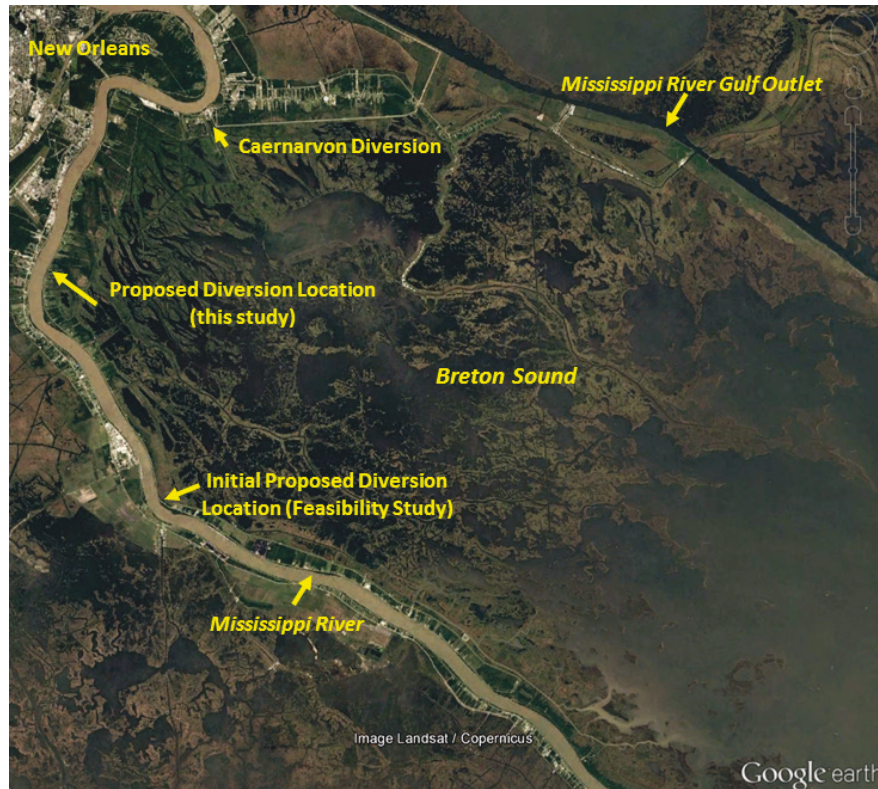


Figure 1-2. Inset image of study area (image courtesy of Google).



The Breton Sound marsh is presently being fed by the Caernarvon Diversion, a freshwater diversion that can transfer up to 8,000 cubic feet per second (cfs) of freshwater into the estuary via five 15-foot (ft) box culverts. Each box culvert has a sluice gate that can be opened incrementally to pass water through the diversion at a variable flow rate. The maximum flow rate is determined by the head difference across the diversion.

The Caernarvon Diversion was completed in 1991 and first operated in August of that year. The fresh water from the Mississippi River travels through approximately 19 to 25 miles of brackish wetlands before reaching the Breton Sound and then an additional 31 miles before reaching the Gulf of Mexico. Before Hurricane Katrina, this flow was divided between two main paths, which accounted for approximately 99% of the freshwater flow (Snedden et al. 2007b). The two main channels are Lake Leary and Bayou Terre aux Boeufs to the east and Manuels Canal and River aux Chenes to the west. Of these two, the eastern route is responsible for the most flow (Lane et al. 2007). The water depths in these channels are maintained to approximately 10 to 11.5 ft and 3 to 5 ft in the adjacent lakes (Lane et al. 2007). When flow in the two main channels exceeds 3,500 cfs, the water

surpasses the conveyance capacity of the channels and is transported by sheet flow through the vegetated marsh (Snedden et al. 2007b).

Land loss in the Breton Sound basin during 1956–1978 was approximately 1,660 acres/year (yr) and during 1978–1990 the loss rate was estimated at 1,020 acres/yr (Barras et al. 1994). Hurricanes Katrina and Rita in 2005 had a significant impact on the marsh as land loss in the Breton Sound basin for 2004–2005 was estimated at 26,240 acres (14%) (Barras 2006).

In 2010, a feasibility study in the Louisiana Coastal Area (LCA) Program for a medium diversion at White Ditch was completed that recommended a plan to build a structure capable of diverting up to 35,000 cfs into Breton Sound. The diversion would operate fully during March and April and run a small maintenance flow during the rest of the year. The location for the tentatively selected plan during the feasibility study was just north of Phoenix, LA. However, during initial phases of preliminary engineering design (PED), the diversion location was moved upstream approximately 9 miles to the southern limit of Braithwaite, LA (see Figure 1-2). This new location was selected because preliminary analyses indicated that locating the diversion at the new site would result in much more diverted sand than a diversion at the original site and would require a much shorter outfall channel than the outfall channel associated with the original site.

In 2014, the cost share partner suspended all work on LCA projects (including the medium diversion at White Ditch) with the exception of the Mississippi River Hydrodynamic and Delta Management (MRHDM) Study, and PED was terminated. This study documents the initial PED modeling work. The diversion modeled channels approximately 35,000 cfs of fresh water into the west side of the Breton Sound marsh, near River aux Chenes. Work was continued on a Mid-Breton sediment diversion under the MRHDM study and is documented in Brown et al. (2019).

## **Objective**

The study described herein focuses on determining the changes in hydrodynamics, salinity, and sedimentation resulting from diversion operation. The application of a numerical model along with substantial data collection was required to determine the capability of the diversion to accomplish its intended purpose of building new marsh and maintaining the existing marsh in Breton Sound. The tool chosen for this

study was the Adaptive Hydraulics (AdH) numerical model (see Section 2 for more details).

## **Technical approach**

A previous numerical modeling study on the Caernarvon Diversion served as the starting point for the study documented in this report. The data collected for the Caernarvon Diversion study included bathymetric surveys in the two main channels of the Breton Sound estuary as well as water level, discharge, and salinity data. These data were collected for the period from April to December 2010.

The Caernarvon Diversion AdH model included a Gulf of Mexico saline tidal boundary, Mississippi River freshwater inflow, and also included the Caernarvon Diversion freshwater inflow. Wind forcing from 10 gauges was interpolated and applied across the model.

While the data collected for the previous Caernarvon Diversion study were included, additional data were required for the present study. The data collection effort included extensive bathymetric surveying of the Breton Sound marsh near the proposed diversion. Seven gauges were installed to collect water level, discharge, salinity, and turbidity samples over a period of approximately 4 months in 2013.

The model was validated to the previous Caernarvon Diversion data collection period (April to December 2010) since it was the most data-rich timeframe available. After model validation was complete, simulations to understand the effects of the proposed diversion on hydrodynamics, salinity, sedimentation, and land building (long-term morphologic change) were conducted.

## 2 Model Development

### Model description

A two-dimensional (2D) depth-averaged application of the numerical model (AdH) was applied to analyze the hydrodynamic, salinity, and morphodynamic responses of the Breton Sound estuary and environs to the implementation of a sediment diversion. To perform the morphodynamic analyses, the SEDLIB Sediment Transport Library was invoked.

AdH is a finite element model that is capable of simulating three-dimensional (3D) Navier-Stokes equations, 2D and 3D shallow water equations, and groundwater equations (Berger 2013). It can be run in a serial or multiprocessor mode on personal computers, UNIX, Silicon Graphics, and CRAY operating systems. The uniqueness of AdH is its ability to dynamically refine the domain mesh in areas where more resolution is needed to properly resolve complex flow and transport phenomena. AdH can simulate the transport of conservative constituents, such as salt, as well as sediment transport that is coupled to bed and hydrodynamic changes (via SEDLIB). The ability of AdH to allow the domain to wet and dry within the marsh areas as the tide changes is necessary to effectively model a shallow marsh environment. This tool is being developed at ERDC-CHL and has been applied for a wide variety of applications including flow and sediment transport in complex sections of the Mississippi River, tidal conditions in southern California, and flow field changes caused by vessel traffic in the Houston Ship Channel, as well as many other applications.

The AdH model has been linked to SEDLIB, which is a multi-grain class, cohesive and cohesionless sediment type, sediment transport library developed at the CHL. Models based on this code have previously been used to investigate the effects of sediment diversions at both the Old River Control Structure (Heath et al. 2015) and the West Bay Diversion (Sharp et al. 2013). The model has been run in 2D depth-averaged mode, with quasi-3D sediment behavior. This quasi-3D behavior includes semi-analytic corrections to the model equations that approximate important 3D sediment processes such as sediment stratification, sediment mass flux, and bendway effects (Brown 2012).

For this study, the 2D depth-averaged shallow water module of AdH was applied for all simulations. AdH solves for depth and depth-averaged velocity and constituent transport throughout the model domain. Due to the shallow nature of the Breton Sound estuary, the flow is assumed to be vertically well mixed and therefore not subject to significant salinity stratification effects. (More details of the 2D shallow water module of AdH and its computational philosophy can be found at <https://chl.erdc.dren.mil/chladh/>.) All model simulations were run on the ERDC high-performance computers: Diamond (SGI Altix Ice) and Garnet (Cray XE6) and AFRL's Sprit (SGI Ice X).

## Mesh development

The mesh was developed using the Surface-water Modeling System, a graphical user interface developed by ERDC for increasing the modeling productivity for a variety of USACE numerical models, including AdH. The large-domain (hydrodynamic and salinity) mesh developed for this study covers a large portion of southern Louisiana including portions of the Mississippi River, Breton Sound, Chandeleur Sound, and the Gulf of Mexico, and extends east to Pensacola, FL. The Mississippi River is the primary freshwater inflow and is specified nearly 50 miles upstream of New Orleans, LA. The tidal boundary is over 335 miles long and extends into the Gulf of Mexico. The model mesh contains approximately 257,000 nodes and 503,000 elements and covers an area of over 24,100 square miles. The model mesh was originally developed for the previous Caernarvon Diversion study and was modified to increase resolution and more accurately define channels and lakes in the vicinity of the proposed diversion location region. The entire model domain is shown in Figure 2-1. The mesh resolution in Breton Sound is depicted in Figure 2-2.

The bathymetric data were obtained from multiple sources with more recent surveys taking precedence over older data. In the Breton Sound estuary, multi-beam and single-beam bathymetric surveys conducted by CHL (May 2010 and November 2012) were used to define the main channels (see Figure 2-3). The model mesh contains material types specified as either marsh or water. Where data were unavailable in the water regions, the elevation was initially set to -1.5 meters (m) North American Vertical Datum of 1988 (NAVD88) 2004.65. During validation, these values were adjusted on an as-needed basis. The marsh elevations in the study area were obtained from a lidar dataset collected in January 2011.



Figure 2-1. Model domain (outlined in yellow) showing area of interest (AOI) in red.



Figure 2-2. AOI inset mesh showing mesh elements (image courtesy Google).





Figure 2-3. Multi-beam data collected by ERDC (image courtesy Google).



The remainder of the mesh utilized the SL-15 Advanced CIRCulation (ADCIRC) mesh data developed from the Louisiana Coastal Protection and Restoration study (Bunya et al. 2010), National Atmospheric and Oceanic Administration (NOAA) surveys (updated 2011–2012), and the USACE comprehensive surveys of the Mississippi River (2003–2004). Marsh elevations were obtained from the U.S. Geological Survey (USGS) 3 m National Elevation Dataset.

A higher level of refinement (smaller, more detailed mesh) was required to account for major flow paths identified by the bathymetric data collection effort in the study area. Modifications were achieved by digitizing channels using high-resolution aerial imagery of the Breton Sound marsh at 500 cfs and 8000 cfs flow through the Caernarvon Diversion. Historical imagery, particularly high sediment flux events, was inspected to determine the major pathways for water movement. To get data for other regions such as the Fort Saint Philip diversion and Bayou Lamoque, 1 m imagery from Global Mapper was digitized.

## Boundary conditions

Boundary conditions were developed from 2010 data for the validation and alternative analyses. The boundary conditions required for each simulation were hourly discharge rates for the Mississippi River at Belle Chasse (filtered to remove the tidal signal), Caernarvon Diversion discharge, a Gulf of Mexico tidal boundary condition, and wind data from several stations within or near the model domain.

### Tides

The Gulf of Mexico boundary condition is a tidal boundary condition based on tidal harmonics and measured data. The tidal boundary extends 335 miles from south of Houma, LA, to east of Pensacola, FL. Tidal harmonics from the ADCIRC model tidal database and water levels from a NOAA station at Southwest Pass at Louisiana Pilot's Station East (8760922) were used to develop the tidal boundary condition.

A total of nine harmonic constituents (K1, O1, Q1, M2, S2, N2, K2, M4, and M6) were acquired from the ADCIRC tidal database for seven locations along the boundary (including the endpoints). The harmonic constituents for the boundary nodes in between were interpolated from this dataset.

The water surface elevations were then reconstructed from the harmonic constituents, and a shift (constant from node to node) was applied to the entire boundary. The shift was required since the reconstructed signal has a mean of zero and the model elevations are in NAVD88, meters. Since the exact shift was unknown, a best approximation was utilized. The shift included the NOAA VDatum shift from Mean Sea Level (MSL) to NAVD88 for Southwest Pass (constant 0.1915 m) and the non-harmonic portion of the Southwest Pass NOAA gauge (time-varying).

While it is understood that the VDatum shift and non-harmonic shift will vary greatly over the length of the boundary, the simplest approach was employed so as not to introduce any additional errors by attempting to apply a more complex boundary condition. In this approach, the distance of the boundary from the study area is thought to allow the dominant source of the non-harmonic signal, wind forcing, to be accounted for by the physics within the model.

Water surface elevation comparisons indicate that this approach was highly successful. Analysis between the field data and the model results was conducted for several gauges; three are shown below (Southwest Pass, Bay Gardene, and Dauphin Island). Bay Gardene and Dauphin Island were chosen based on the availability of a datum reference to NAVD88. For the analysis, the mean of the field data and mean of the model data were calculated. The mean of the field data was then shifted by the difference between the two in order to analyze the amplitudes of the tidal signal more clearly. The shift for Bay Gardene was -0.03 m, and the shift for Dauphin Island was 0.15 m, indicating that the overall tidal boundary has an appropriate mean elevation. The locations of these gauges and their respective organizations are listed in Table 2-1 and shown in Figure 2-4. Comparisons between the field data are shown in Figure 2-5 through Figure 2-7.

Table 2-1. Location of tidal boundary reference gauges.

Station Name - Number	Source	Datum	Latitude	Longitude
Bay Gardene - 07374527	USGS	NAVD88	28° 55.9'	89° 24.4'
Dauphin Island - 8735180	NOAA	NAVD88	30° 15.0'	88° 04.5'
Southwest Pass - 8760922	NOAA	MSL	29° 35.1'	89° 36.4'

Figure 2-4. Location of tidal gauges and model boundary.

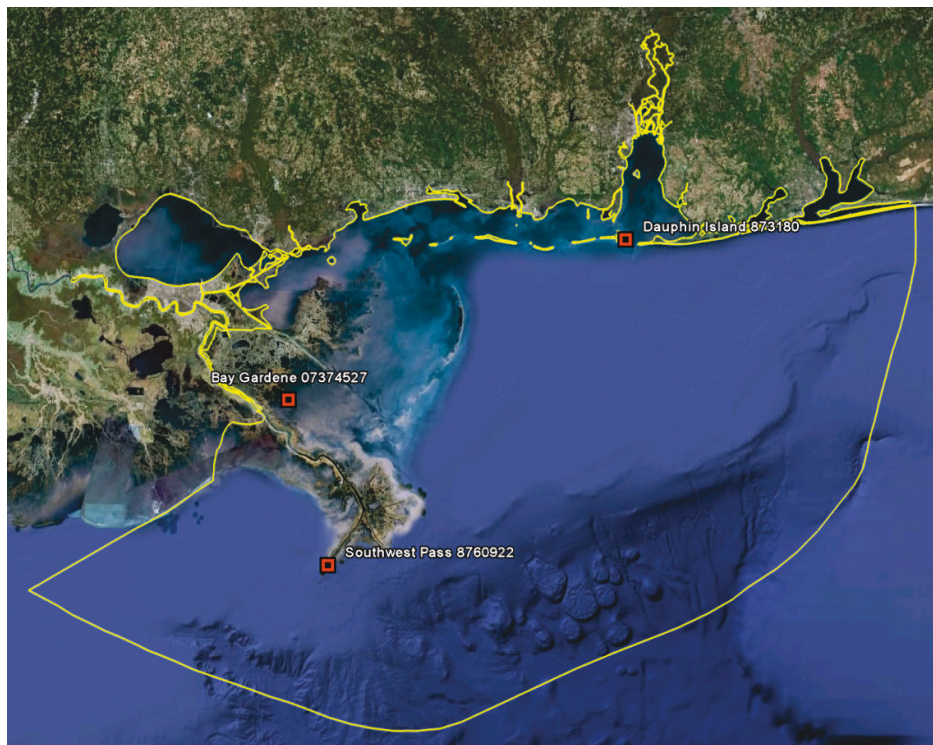


Figure 2-5. Water surface elevation comparison for Southwest Pass.

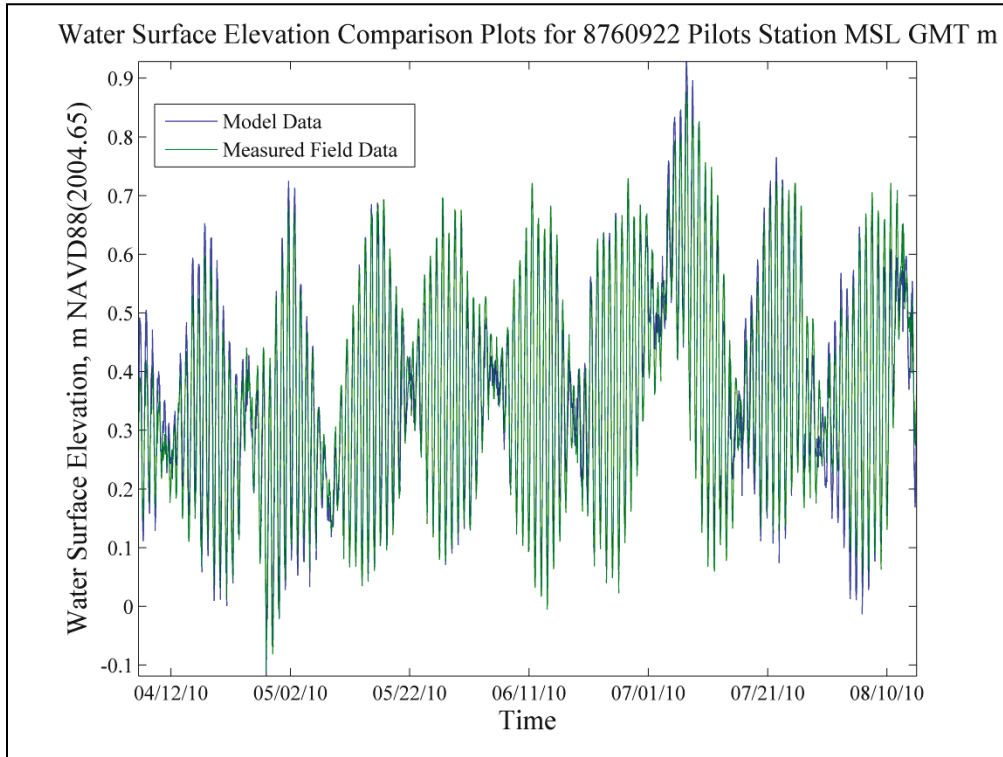


Figure 2-6. Water surface elevation comparison for Bay Gardene.

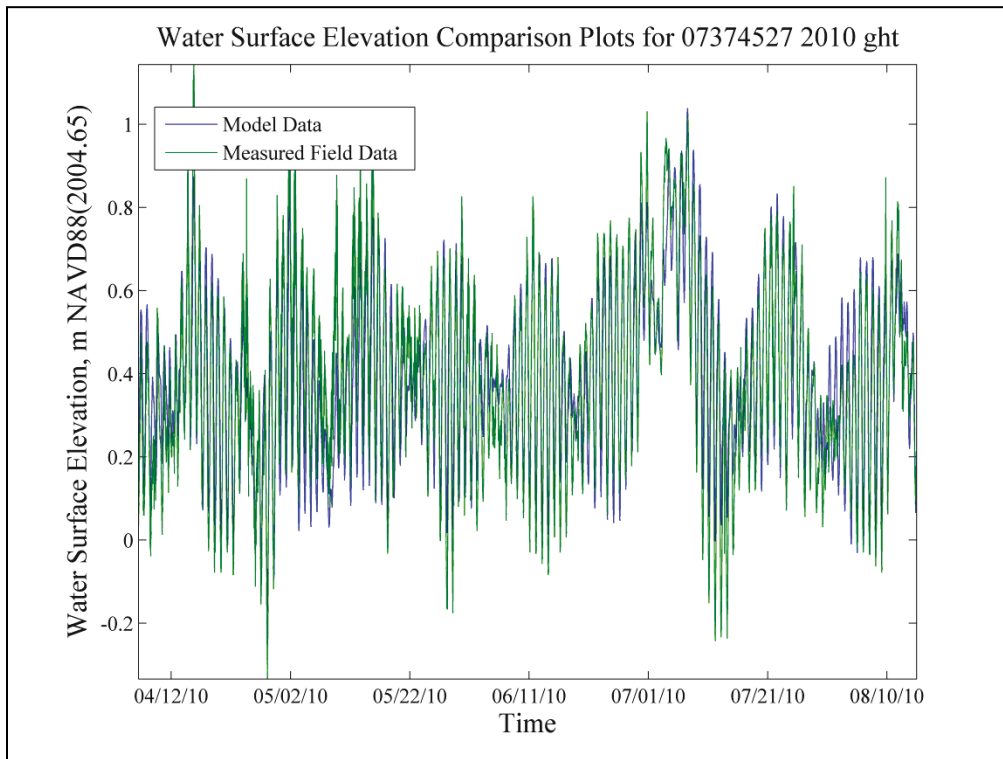
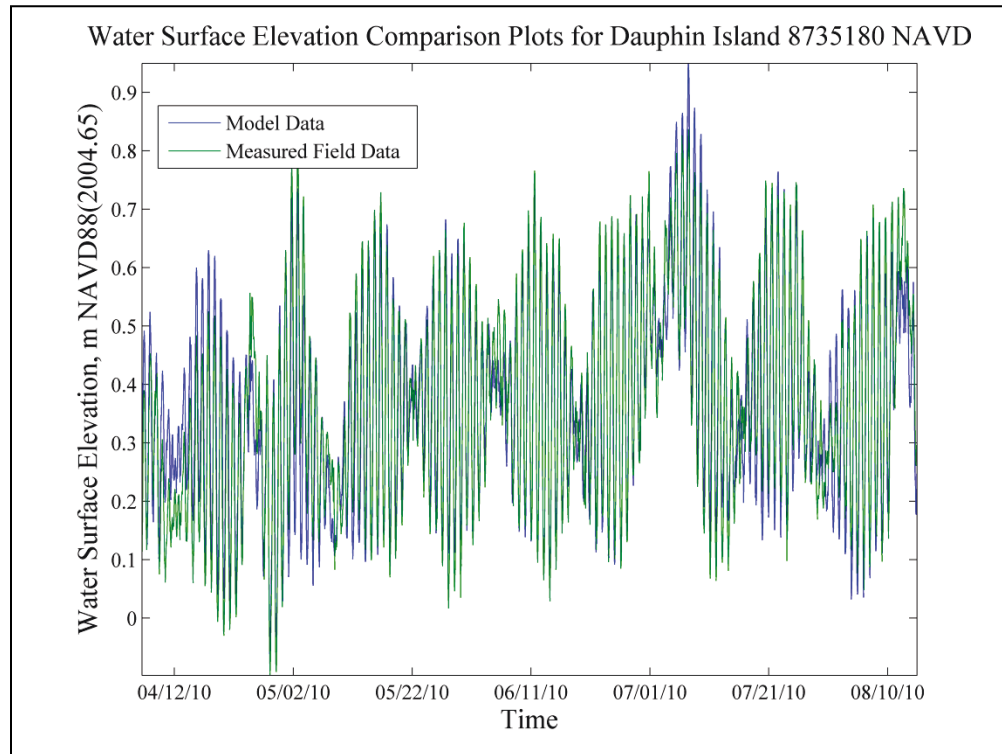




Figure 2-7. Water surface elevation comparison for Dauphin Island.



The above three gauges (and their means) show that the model is reproducing the field data in an accurate manner, regardless of the assumptions required by the tidal boundary. The non-harmonic signal, though applied uniformly across the boundary, is reproduced well by the model since the dominant wind forcing is accounted for appropriately.

### Winds

Hourly wind data were obtained from the NOAA National Data Buoy Center for several locations across the model domain. Station information can be found in Table 2-2 and Figure 2-8.

Significant data gaps were filled with data from the nearest gauge; minor data gaps were linearly interpolated. All wind data were filtered using a 4-hour filter. Figure 2-9 and Figure 2-10 show the wind data for the east/west direction and north/south direction, respectively, for the gauge nearest the study area (Shell Beach, NOAA National Ocean Service gauge no. 8761305) during the validation period between April 10 and June 30 in 2010. North and east are positive wind directions. Wind attenuation by tall standing marsh grasses and trees was included in the model.



Table 2-2. Wind station symbols and locations.

Station Name	Station Symbol/Number	Station Location (lat/lon)
Grand Isle, Louisiana	GISL1	29.263/-89.957
Western Lake Pontchartrain, Louisiana	LKPL1	30.315/-90.281
New Canal, Louisiana	NWCL1	30.027/-90.113
Pilot's Station East, Southwest Pass, LA	PSTL1	28.932/-89.407
Shell Beach, Louisiana	SHBL1	29.868/-89.673
Gulfport Outer Range	GPOM6	30.230/-88.982
Petit Bois	PTBM6	30.213/-88.500
Dauphin Island	DPIA1	30.248/-88.073
Orange Beach	42012	30.065/-87.555
Mars-Mississippi Canyon	42363	28.160/-89.220

Figure 2-8. Wind gauge locations.



Figure 2-9. East (+)/West (-) wind magnitudes at Shell Beach.

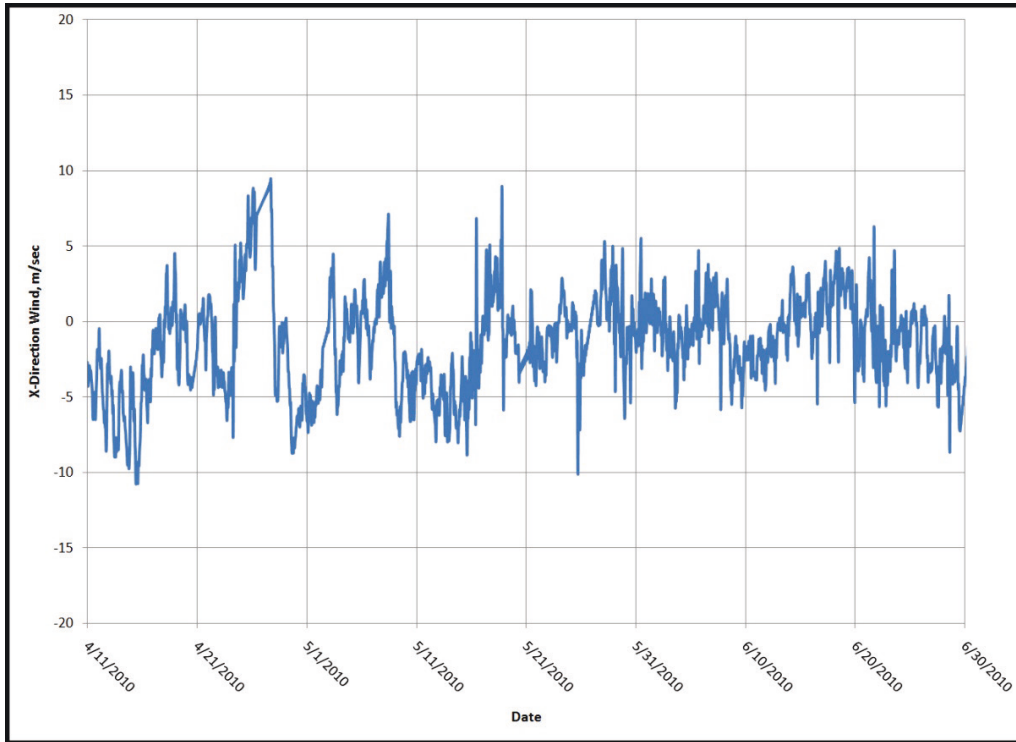
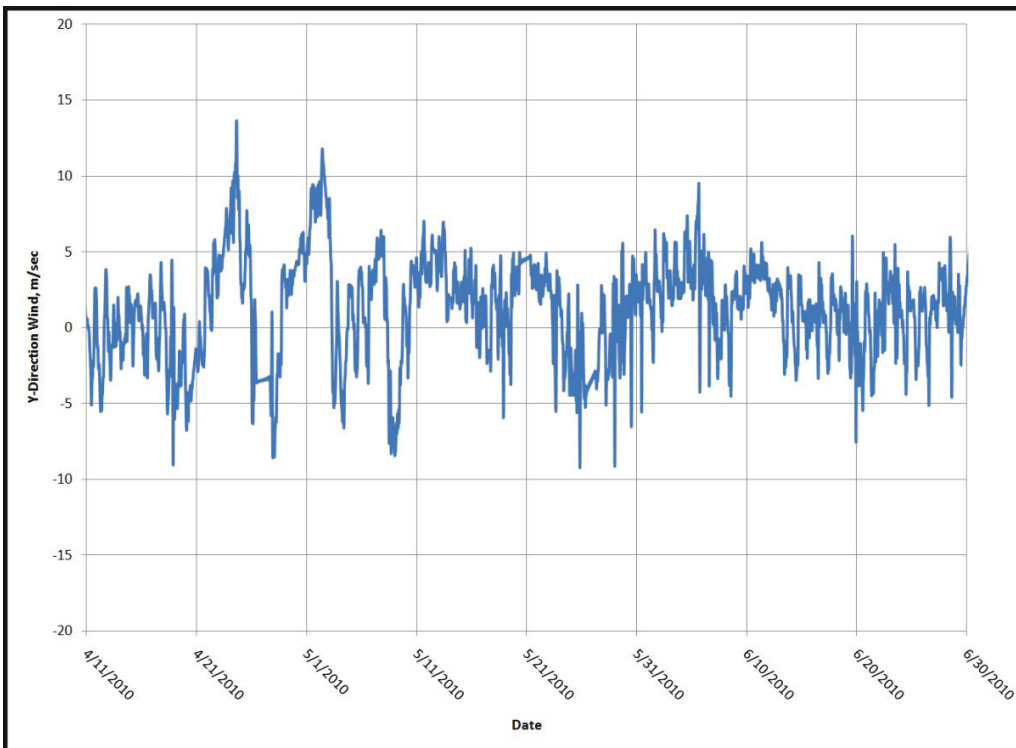


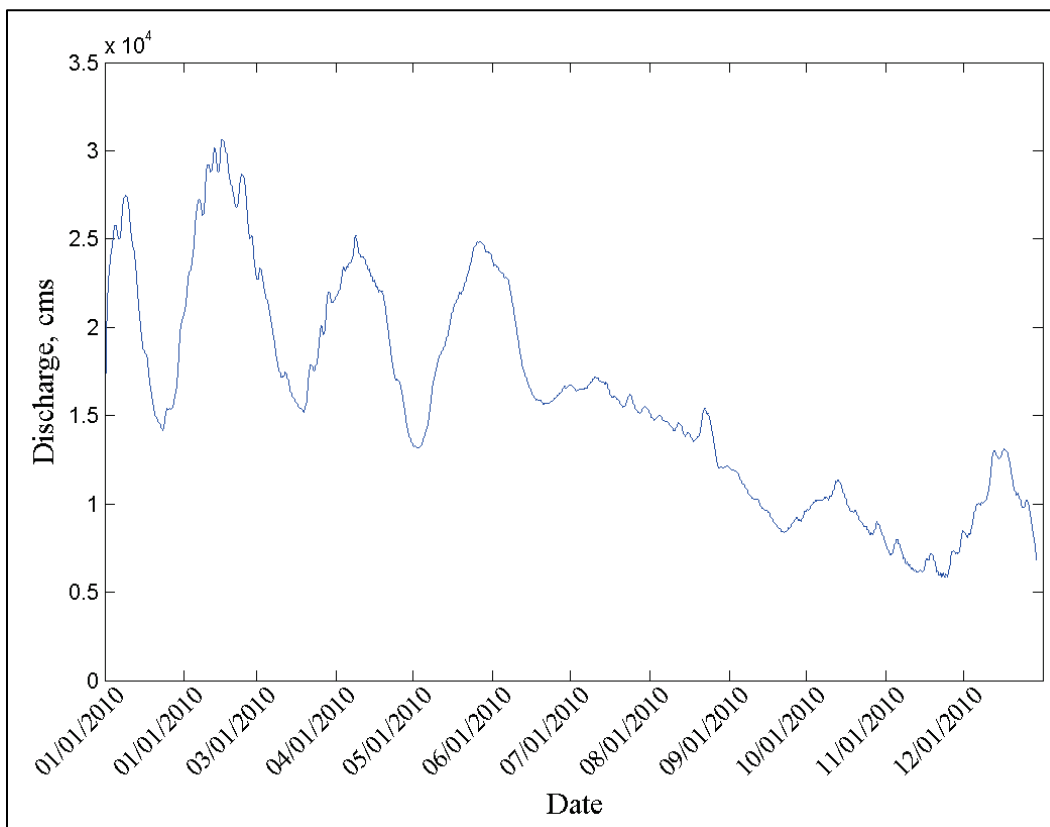
Figure 2-10. North (+)/South (-) wind magnitudes at Shell Beach.



### Flow boundary conditions

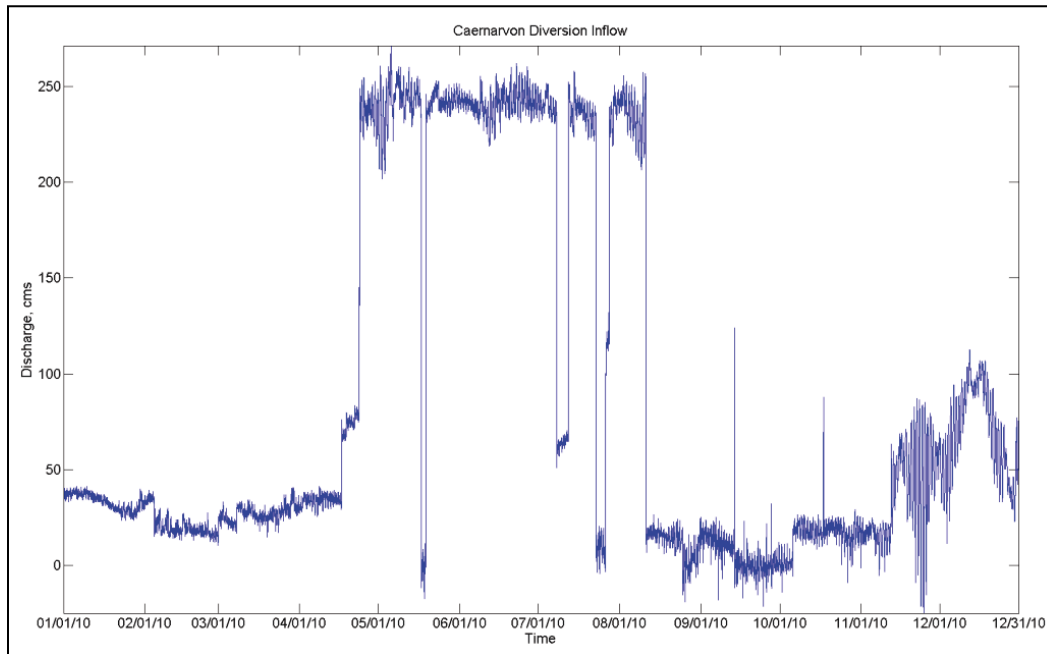
The 2010 Mississippi River hydrograph at Belle Chasse (USGS) was used for validation period (Figure 2-11). The Belle Chasse data were used because there is typically an observed, but as yet unexplained, *loss* of river discharge between Baton Rouge and Belle Chasse for high flows. Rather than attempting to account for these losses, it was decided to use the Belle Chasse observations, filter out the tidal signal, and apply these at the inflow boundary condition (located 50 miles upstream of New Orleans). This approach ensures that the proper river discharge reaches the existing diversions and outlets into the nearshore environs.

Figure 2-11. Mississippi River hydrograph for validation period.



The Caernarvon diversion hydrograph for 2010 was used for the validation simulation (Figure 2-12). The flow rate was at or near the maximum capacity rate of 8000 cfs from 23 April 2010 to 10 August 2010 in an attempt to mitigate any adverse impacts to the Breton Sound estuary from the Deepwater Horizon oil spill.

Figure 2-12. Caernarvon Diversion inflow for the validation period.



### Salinity

The initial salinity conditions were developed by assigning salinity values throughout the domain that corresponded to the initial observed values. The model was then run for a spin-up period of a month. In spite of his initialization period, however, the high residence time of Breton Sound during periods when Caernarvon Diversion is at low flow means that the initialization conditions persist until such time as the Sound is flushed of salt by Caernarvon operations (i.e., early June).

### Additional parameterization

Bed roughness for the wetted, submerged regions of the mesh was approximated with Manning's Equation. These included open water, channels, lakes, etc. For the marshes, an unsubmerged vegetated roughness method was used. This method requires as input assumed stem diameter and number of stems per unit area.

### Model validation

The model was validated to 15-minute water level and discharge data collected by CHL personnel between April and December 2010. Salinity data were also collected between April and December 2010. The data were influenced by the Deepwater Horizon oil spill with regard to the



Caernarvon Diversion operation. The diversion was fully opened to permit flows of approximately 8,000 cfs from mid-April to early August. This condition significantly impacted salinity validation as the 8,000 cfs flow condition kept much of the study area fresh until mid- to late-August.

The locations of CHL gages (labeled by site number) are shown in Figure 2-13 and are given in tabular form in Table 2-3. The gages were installed over a series of days beginning on 15 April 2010. Over the data collection period, some gages experienced technical problems or were damaged. These issues affected the amount of data collected. Therefore, the validation plots (water level, discharge, and salinity) may not all start on the same date, nor will the validation period be the same for all locations.

Figure 2-13. ERDC-CHL 2010 data collection site locations.



Table 2-3. ERDC-CHL 2010 data collection site locations.

Site Name	Latitude	Longitude
Site 1	29° 49' 13.4969" N	89° 55' 42.7892" W
Site 2	29° 49' 01.3788" N	89° 52' 49.2876" W
Site 3	29° 46' 47.6443" N	89° 47' 29.9527" W
Site 4	29° 45' 26.5775" N	89° 44' 49.6710" W
Site 5	29° 40' 29.9217" N	89° 36' 18.2911" W
Site 7	29° 43' 25.3753" N	89° 48' 55.5468" W
Site 8	29° 44' 43.2625" N	89° 47' 48.9865" W
Site 9	29° 40' 56.1433" N	89° 51' 39.0772" W
Site 10	29° 42' 03.5793" N	89° 54' 29.1630" W

Additional water level, discharge, and salinity data were collected late January through mid-May 2013. The locations of these gauges are given in Table 2-4 and Figure 2-14.

Table 2-4. ERDC-CHL 2013 data collection locations.

Site Name	Latitude	Longitude
Site 12	29° 34' 13.44" N	89° 45' 57.54" W
Site 13	29° 38' 10.75" N	89° 48' 13.70" W
Site 14	29° 35' 38.26" N	89° 44' 31.94" W
Site 15	29° 38' 12.79" N	89° 42' 41.80" W
Site 16	29° 39' 54.01" N	89° 44' 25.57" W
Site 17	29° 40' 17.28" N	89° 39' 08.13" W
Site 18	29° 42' 12.88" N	89° 42' 27.38" W

## Hydrodynamics

Validation of the system hydrodynamics was achieved by comparisons of the water surface elevation and discharge to collected field data. In addition to the field data collected by ERDC, comparisons were also made to several NOAA gauges.



Figure 2-14. ERDC-CHL 2013 data collection site locations.



Due to the difficulty of establishing reliable vertical control for remotely located observational gages, references to vertical datums are highly unreliable. Very few tide gauges give references to a land-based datum (such as NAVD88), and of those that do, there are still questions as to their accuracy (i.e., indications of subsidence over decades). For these reasons, the best approach is to analyze water surface elevation from each gauge with the means removed. This was accomplished by calculating the mean of the model and the mean of the field data for the analysis period, then shifting the field data to match the model. The water surface elevation validation results are given in Figure 2-15 through Figure 2-31. Given the complexity of the system and the limited amount of topographical and bathymetric data, the water surface elevation validation is reasonable.

Figure 2-15. Water surface elevation comparison for Site 1.

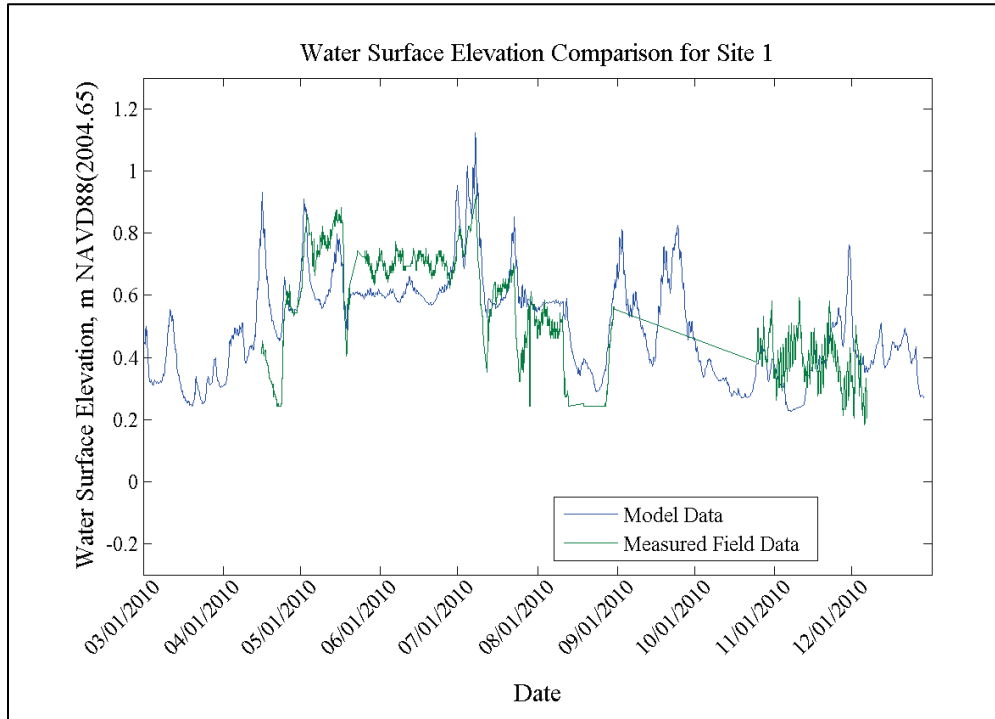


Figure 2-16. Water surface elevation comparison for Site 2.

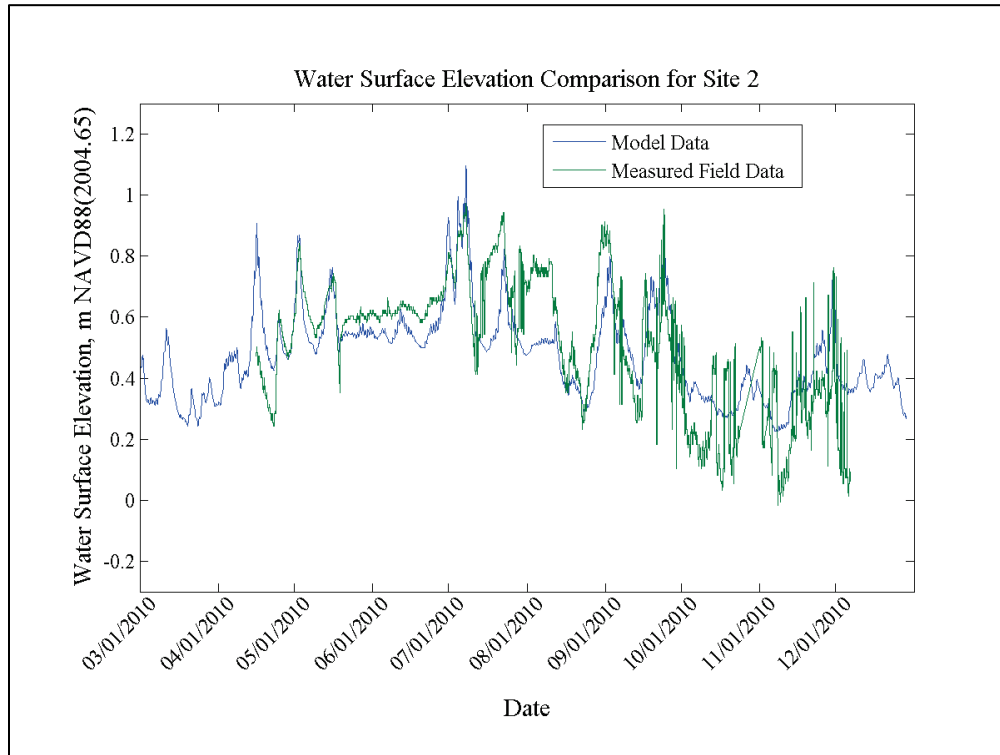


Figure 2-17. Water surface elevation comparison for Site 3.

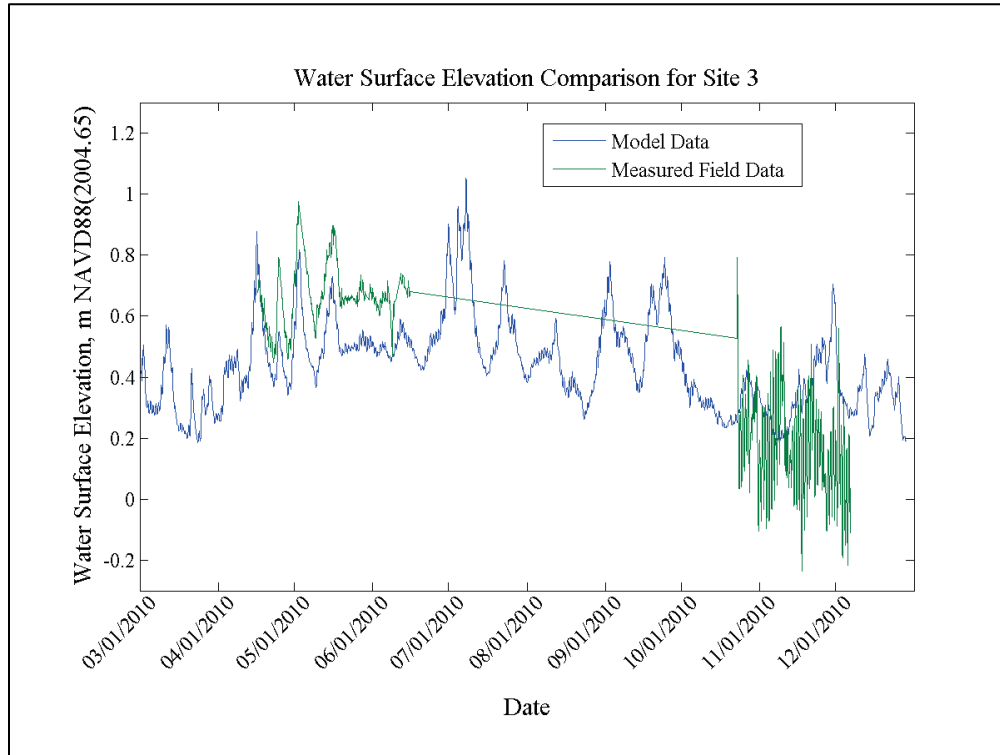


Figure 2-18. Water surface elevation comparison for Site 4.

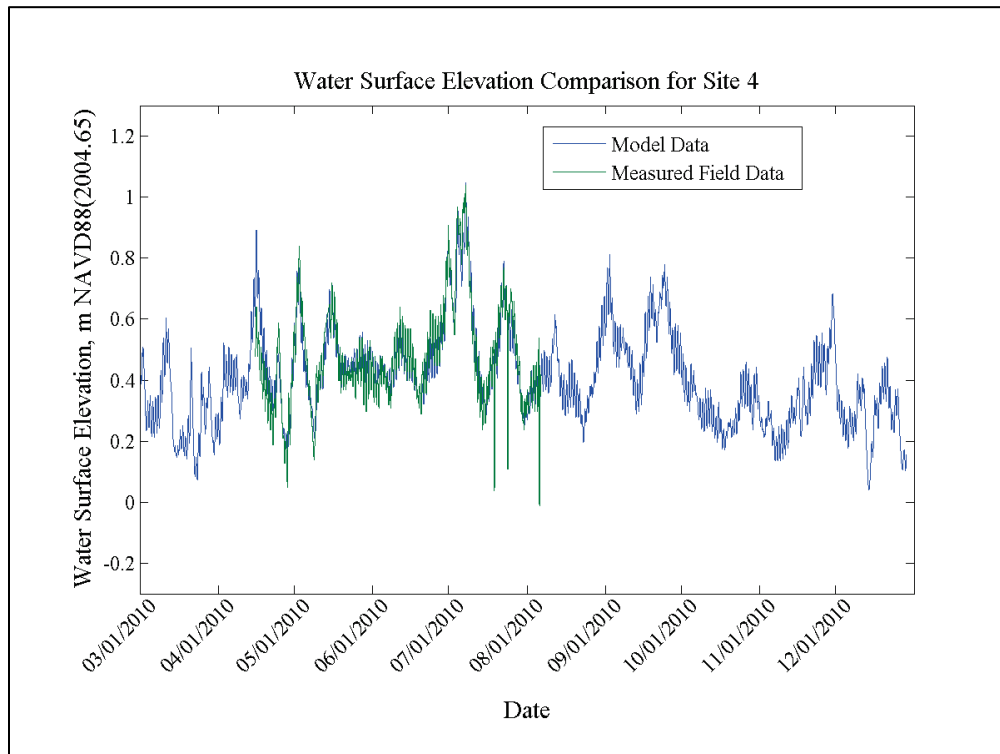


Figure 2-19. Water surface elevation comparison for Site 5.

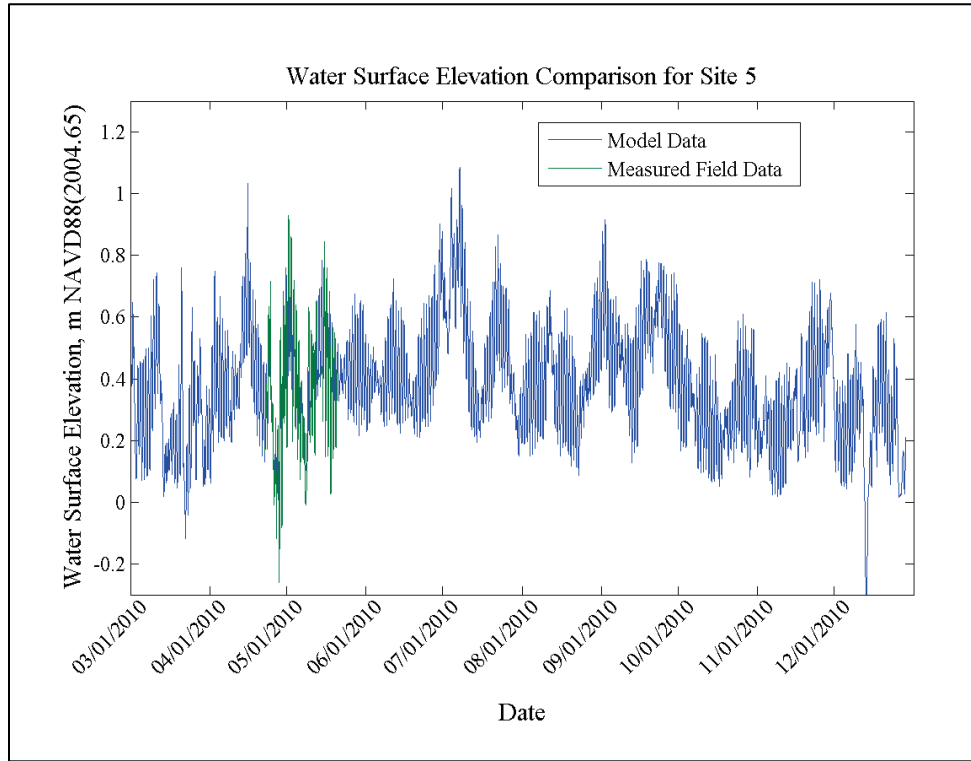


Figure 2-20. Water surface elevation comparison for Site 8.

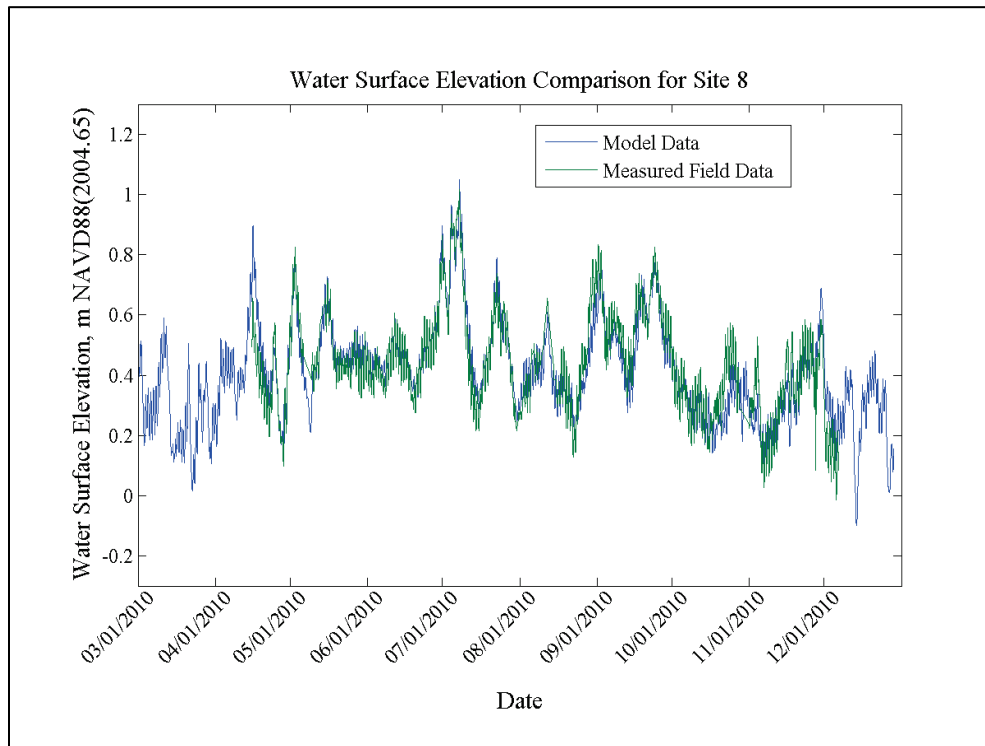


Figure 2-21. Water surface elevation comparison for Site 9.

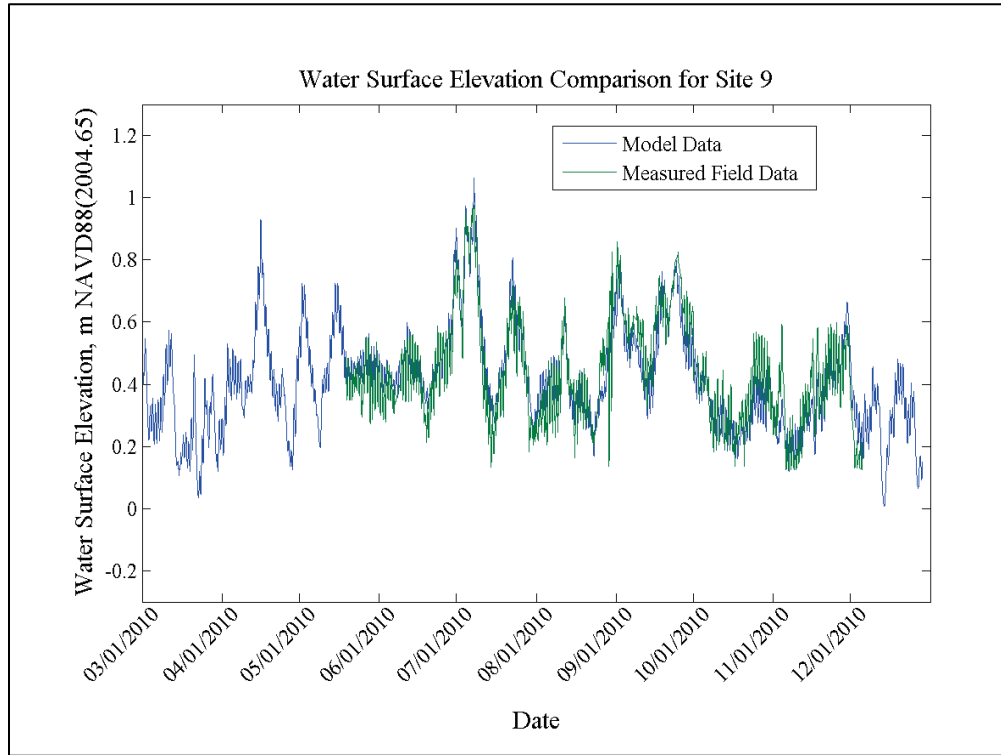


Figure 2-22. Water surface elevation comparison for Site 10.

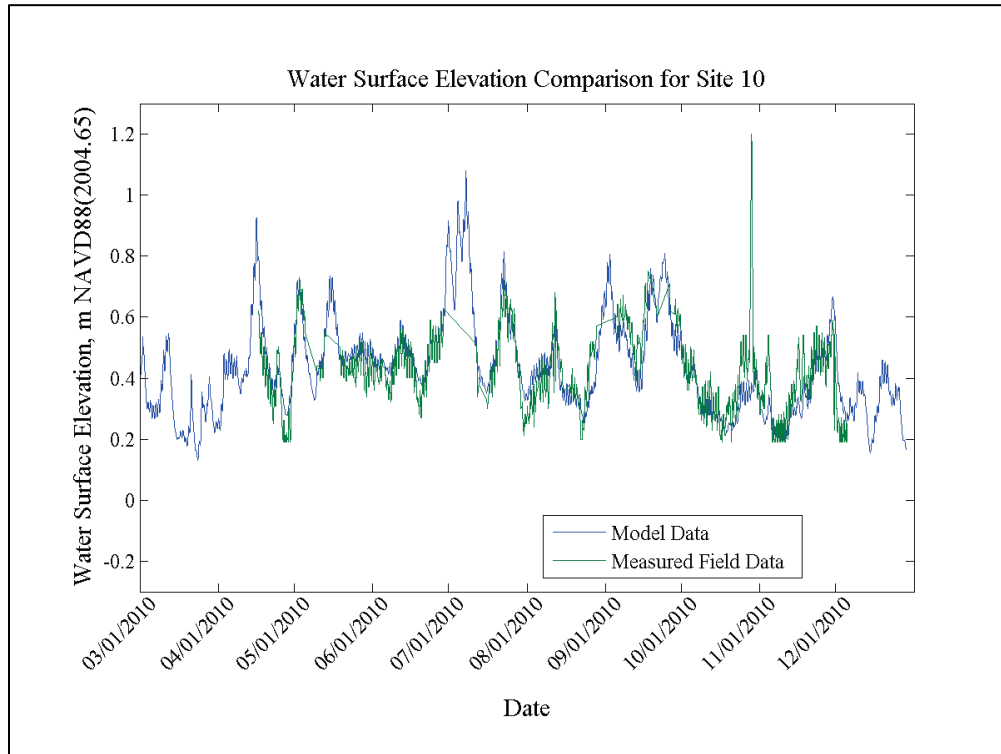


Figure 2-23. Water surface elevation comparison for Caernarvon Outfall.

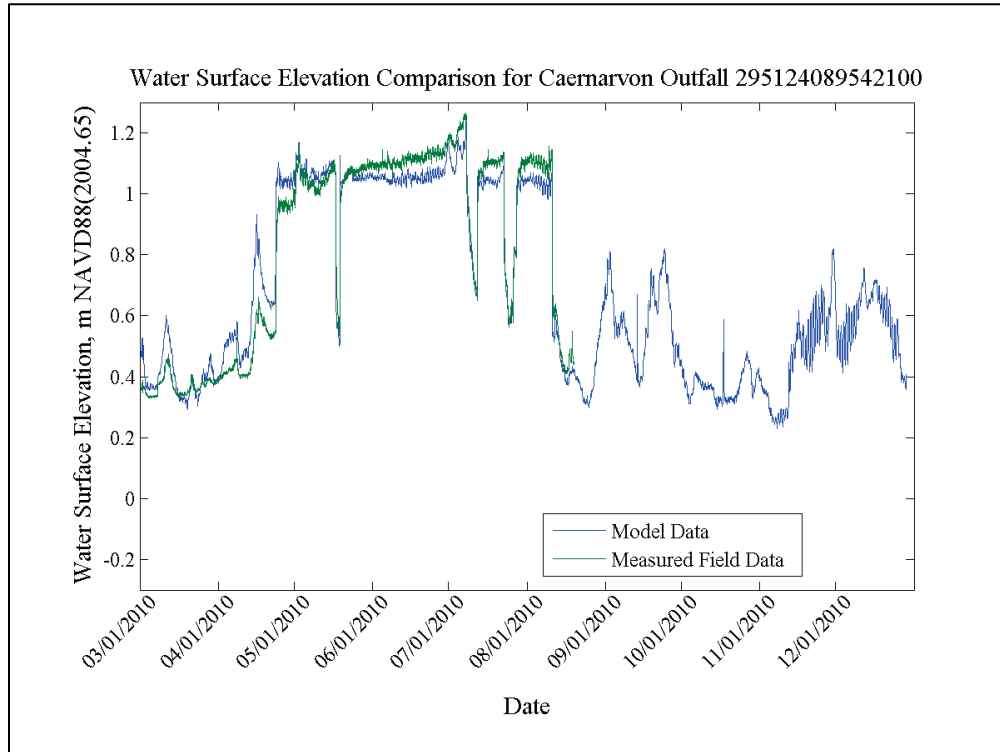


Figure 2-24. Water surface elevation comparison for Black Bay.

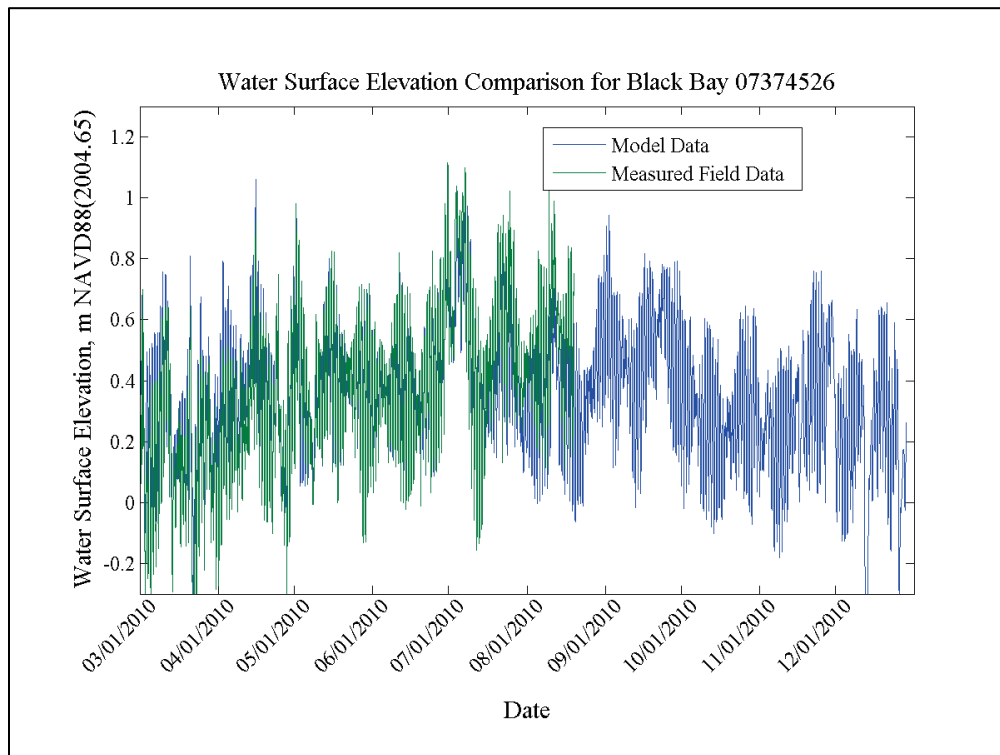


Figure 2-25. Water surface elevation comparison for Cow Bayou.

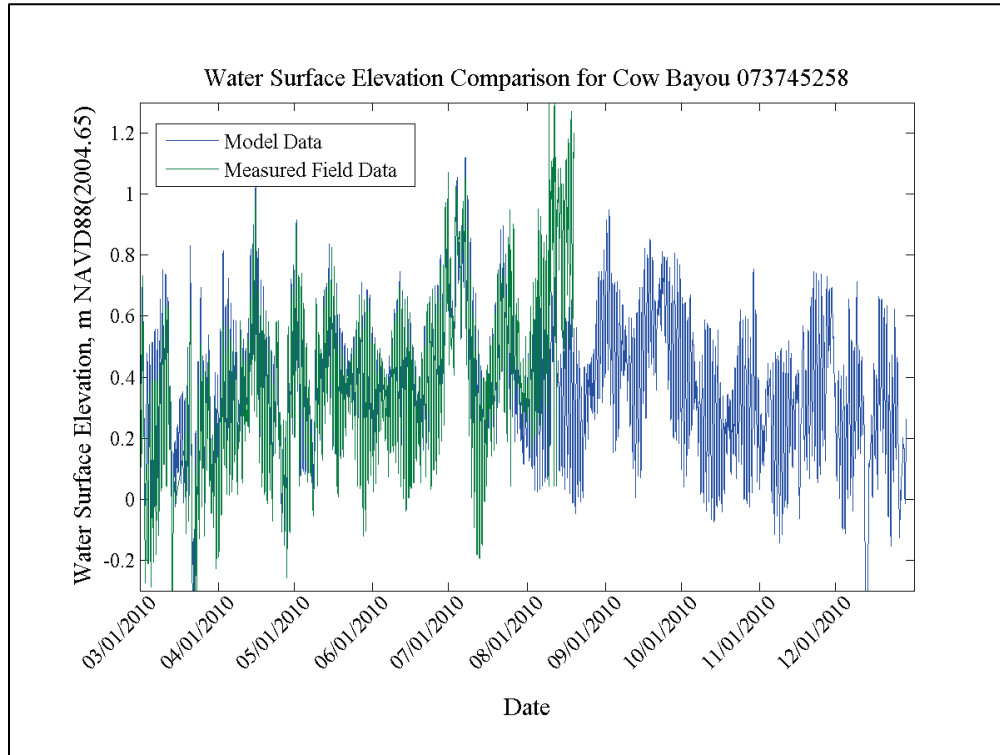


Figure 2-26. Water surface elevation comparison for Crooked Bayou.

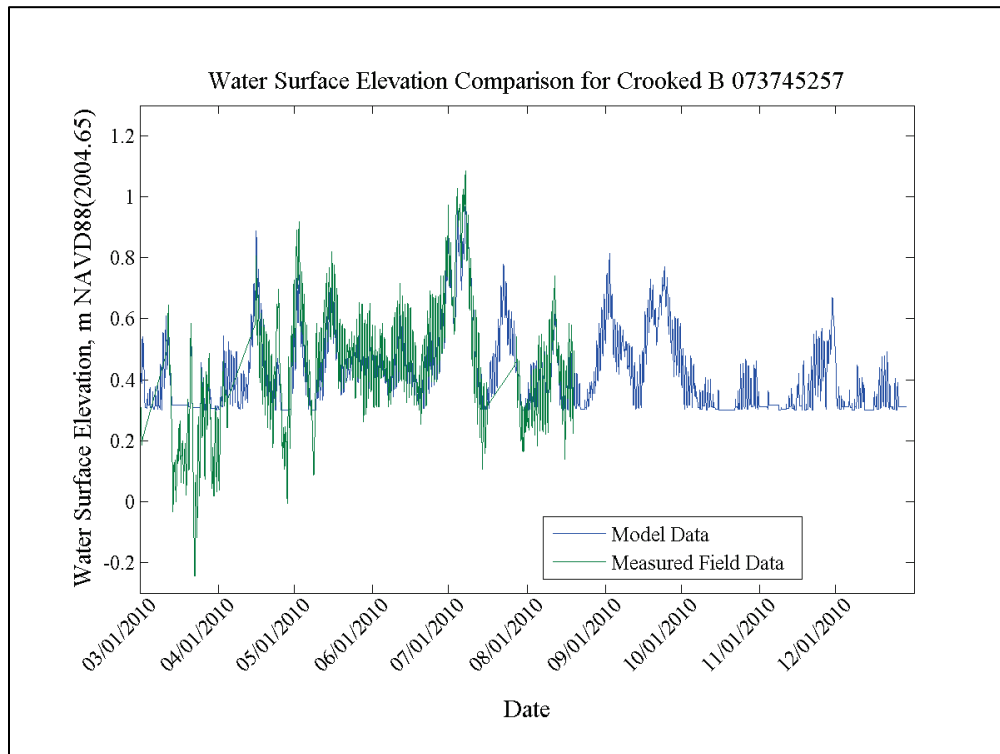


Figure 2-27. Water surface elevation comparison for Dauphin Island.

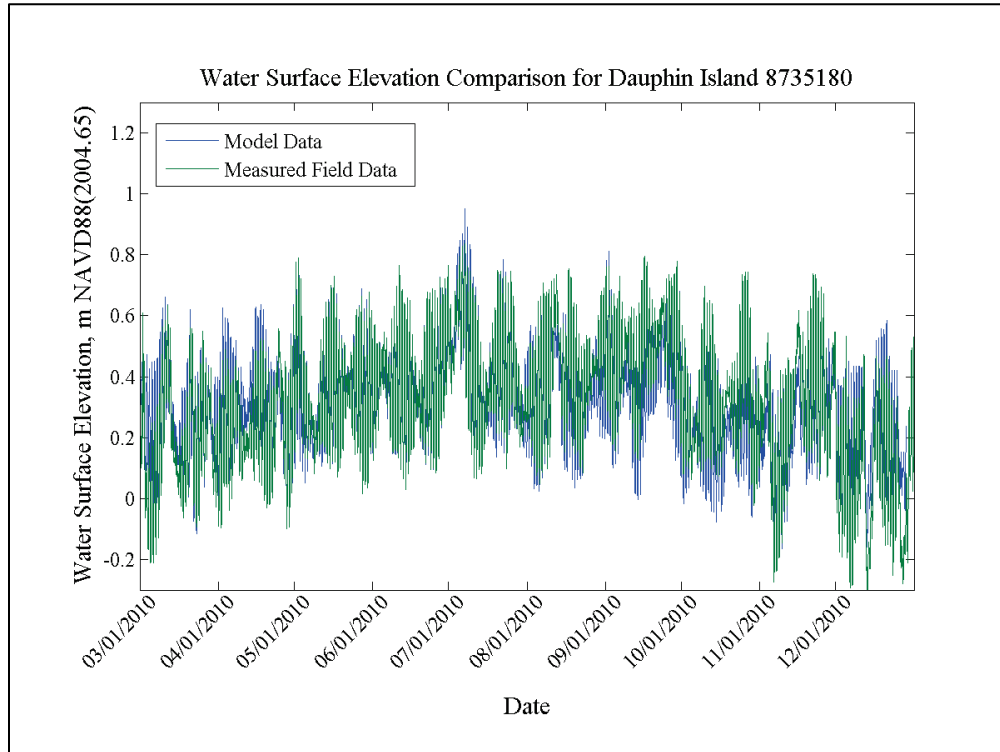


Figure 2-28. Water surface elevation comparison for Bay Gardene.

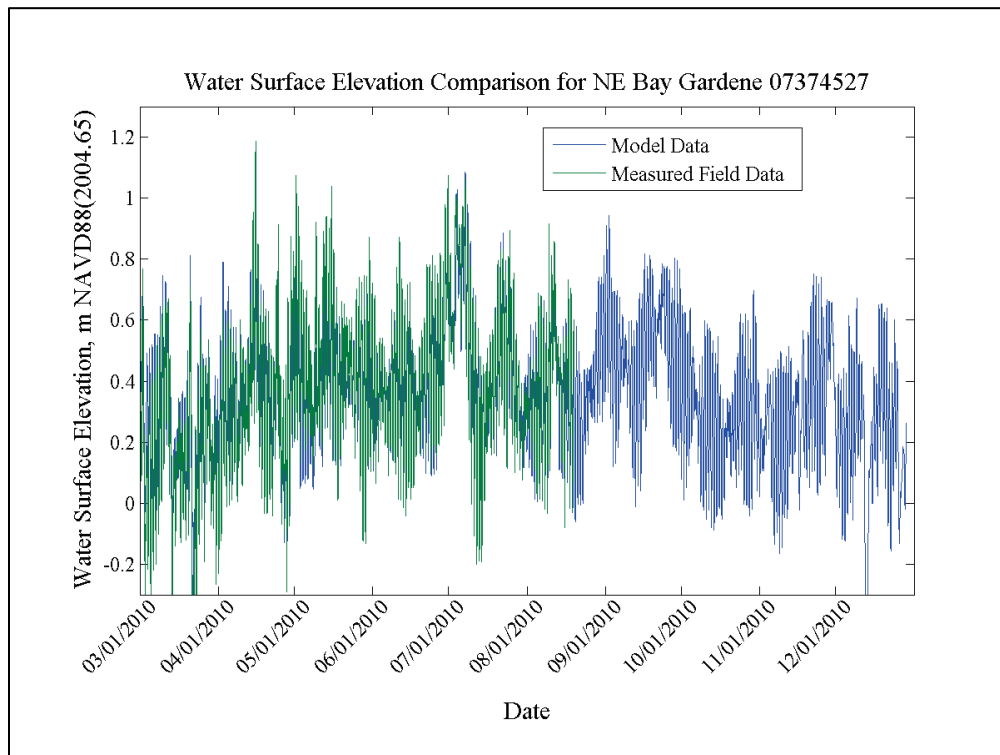




Figure 2-29. Water surface elevation comparison for Mississippi Sound.

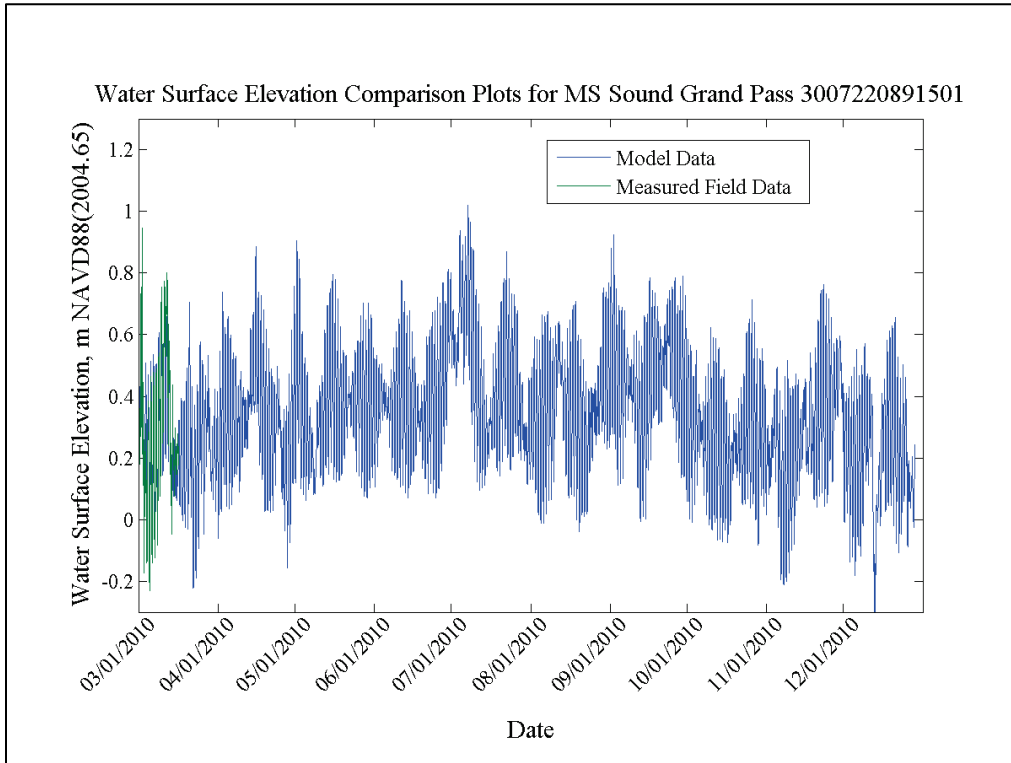


Figure 2-30. Water surface elevation comparison for Port Fourchon.

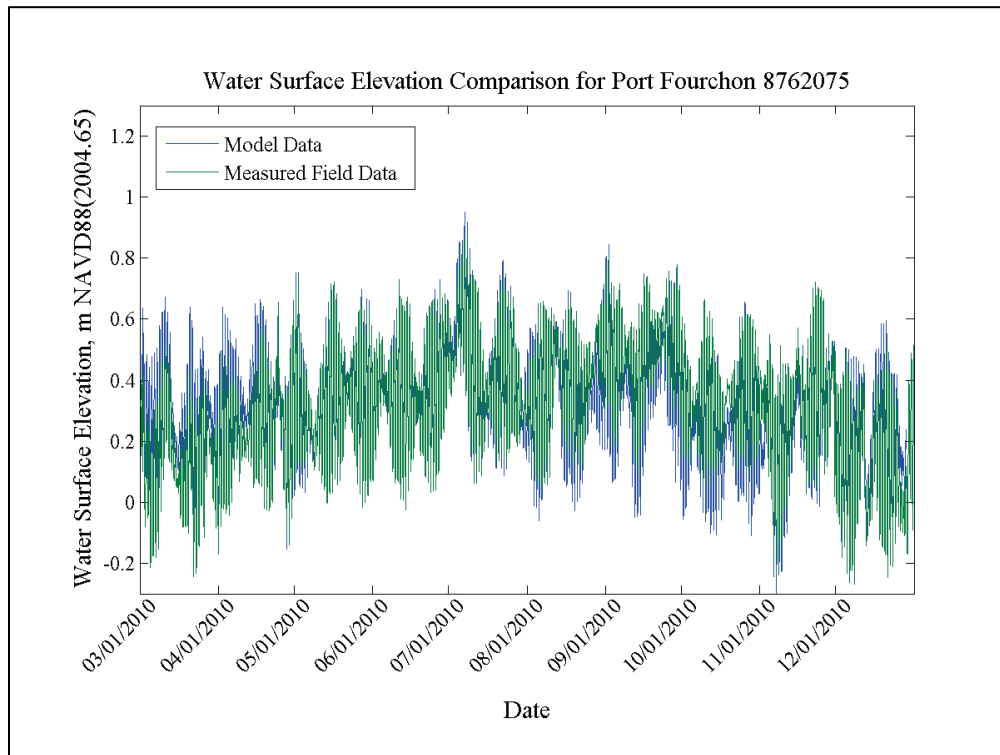
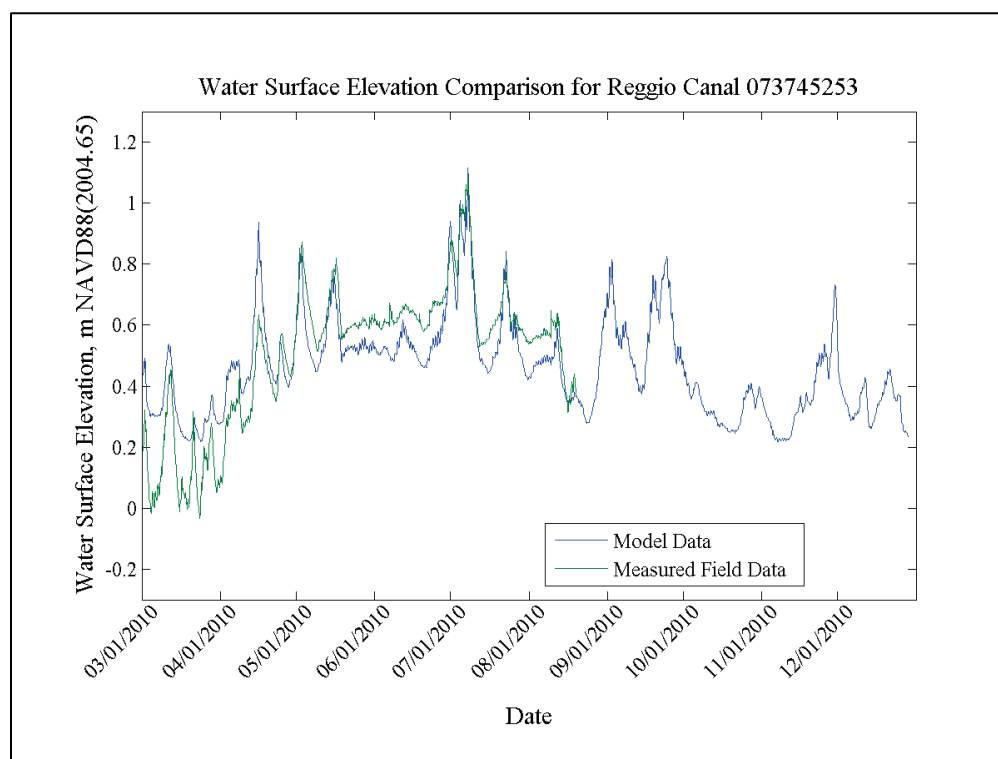


Figure 2-31. Water surface elevation comparison for Reggio Canal.



Sites 1, 2, 3, and 10 are located near the Caernarvon Diversion outfall and are protected from the tidal influence by miles of marshes. The fluctuations seen in these gauges are attributed primarily to wind influences. In these gauges, the tidal influences can still be seen in the smaller, minor fluctuations. Several sensitivity studies were conducted to optimize the correlation between the field and the model data by adjusting the wind attenuation on the submerged marshes. The wind attenuation on the marsh is constant across the Breton Sound marsh at 0.85.

The remaining gauges have more tidal influence. Several sensitivities were conducted to adjust the Manning's  $n$  friction in the channels and the marsh friction (applied as "Unsubmerged Vegetation" with the FR URV card in AdH). The channels in the study area have an applied friction of 0.018. The marsh is assumed to have 0.01 m diameter stems, with an average density of 20 stems per square meter. The resulting water surface elevations show that the model represents the field data appropriately throughout the remainder of the region. Some gauges have too much tidal influence (model amplitudes are higher than field amplitudes) while some gauges have too little. Given the complexity of the system, and the amount of bathymetric data available, the comparisons shown here indicate a well-validated model.

The water levels in the Caernarvon outfall channel are driven almost exclusively by the flow rate of the Caernarvon Diversion with wind and tidal forcing minimally affecting the levels. Figure 2-23 shows the model's ability to capture the dynamic nature of the diversion by accurately mimicking the effect of a sudden stoppage of flow (reference Figure 2-12 for Caernarvon Diversion flow rates). The wide range in water surface elevation seen at this gauge, and the model's ability to capture it, is also an indication of the model's accuracy in this area.

### Discharge

The discharges used for validation were calculated from velocities gathered from a mounted horizontal acoustic Doppler current profiler (HADCP) using Equation 2-1 below.

$$Q=cV_{HADCP}A_{avg} \quad (2-1)$$

Here,  $Q$  is the calculated discharge,  $c$  is the correlation coefficient,  $V_{HADCP}$  is the average velocity from the HADCP, and  $A_{avg}$  is the average cross-sectional area. To gather the data needed to establish the correlation coefficients for each site, a boat-mounted acoustic Doppler current profiler (ADCP) was used to measure total cross-sectional discharge. These ADCP cross-sectional discharge measurements were collected on several occasions, while the HADCP was mounted to a fixed station and gathered 15-minute data over the course of the study.

A linear relationship ( $c$  in Equation 2-1) between the average HADCP velocity and the cross-sectional discharge was generated for each site. Note that while some of the gauges had a wide range of velocities (both ebb and flood), several gauges were calibrated only to a small range of velocities due to the timing of the data collection. Additionally, the average cross-sectional area (constant over the course of the data collection) was used to calculate discharge, regardless of instantaneous water levels.

The discharge validation results are given in Figure 2-32 through Figure 2-39. Note that the Caernarvon Diversion was opened to its full capacity flow of approximately 8,000 cfs on 23 April 2010 as a mitigation measure in response to the Deepwater Horizon oil spill. The diversion operated at full capacity until 10 August 2010 when operation returned to normal.

Sites 1 and 2 are located in the channels to the west and east of the Caernarvon outfall channel, respectively (Figure 2-32 and Figure 2-33). Based on marsh geometry, the majority of the flow from the diversion passes through these two channels (reference Figure 2-12 for Caernarvon Diversion flow rate). However, simple addition indicates that the water is leaving the channel. It can be seen in the model that this is occurring. This conclusion has also been supported by local residents who have noted that the marsh floods during full operation of the diversion.

Site 1 shows some fluctuations (early to mid-June) that are believed to be false data. These fluctuations are not seen in the nearby Site 2 discharge, nor are they seen in the Caernarvon discharge. Additionally, the side-looking HADCP was calibrated to the cross-sectional velocity using a 3-hour window of data. If this window were not representative of typical flows, it may have introduced significant error.

Figure 2-32. Discharge comparison for Site 1.

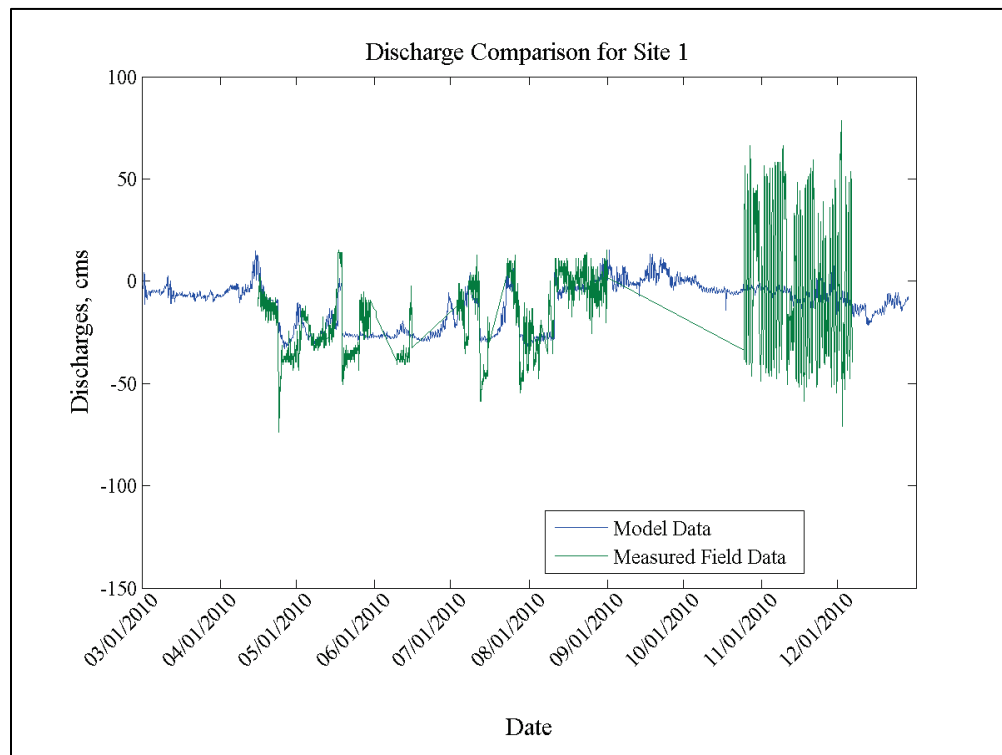


Figure 2-33. Discharge comparison for Site 2.

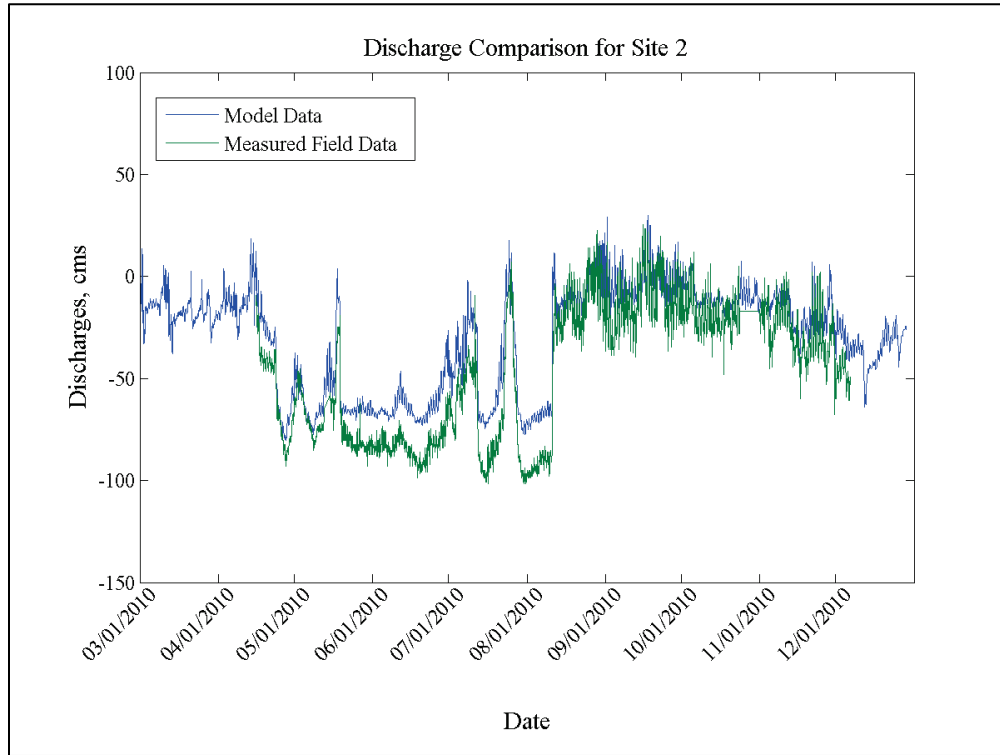


Figure 2-34. Discharge comparison for Site 3.

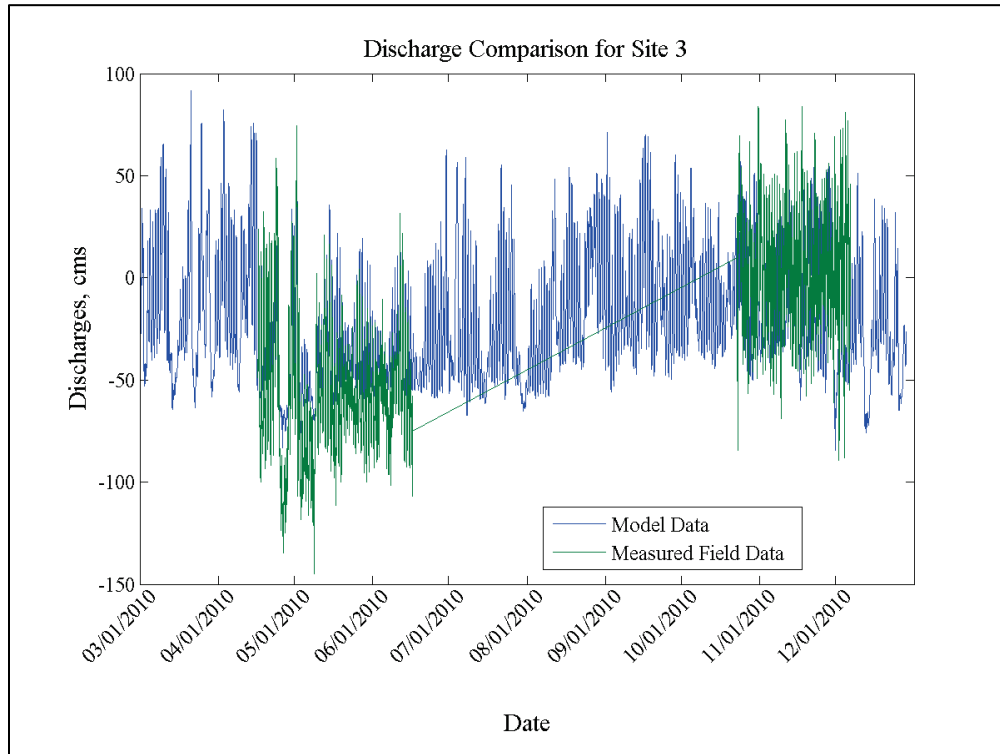


Figure 2-35. Discharge comparison for Site 4.

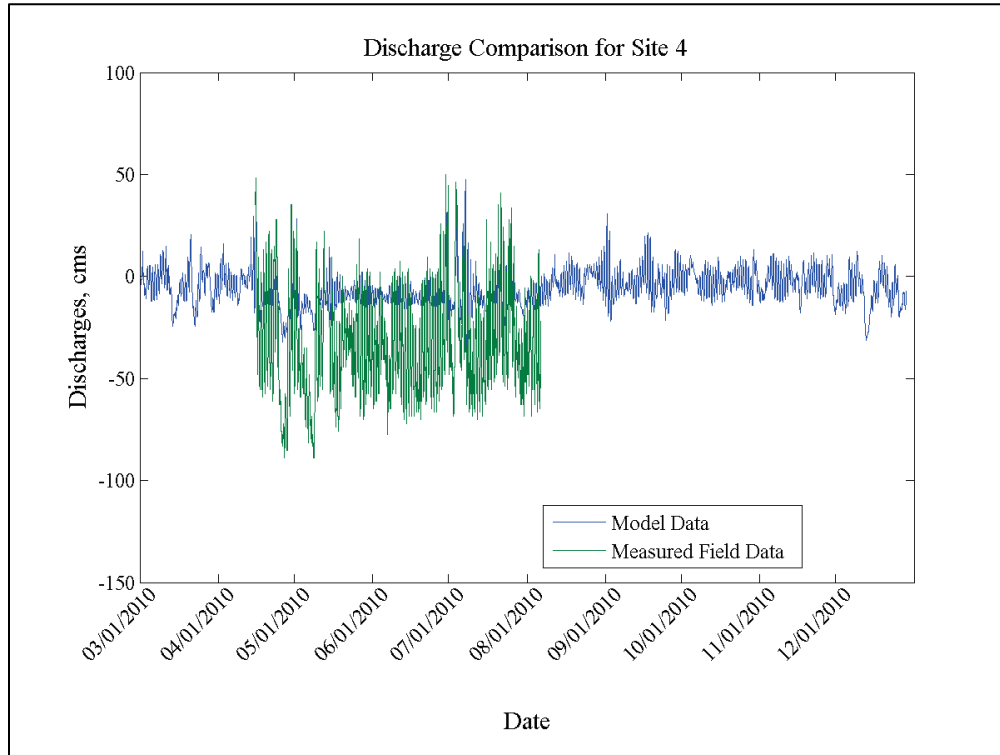


Figure 2-36. Discharge comparison for Site 5.

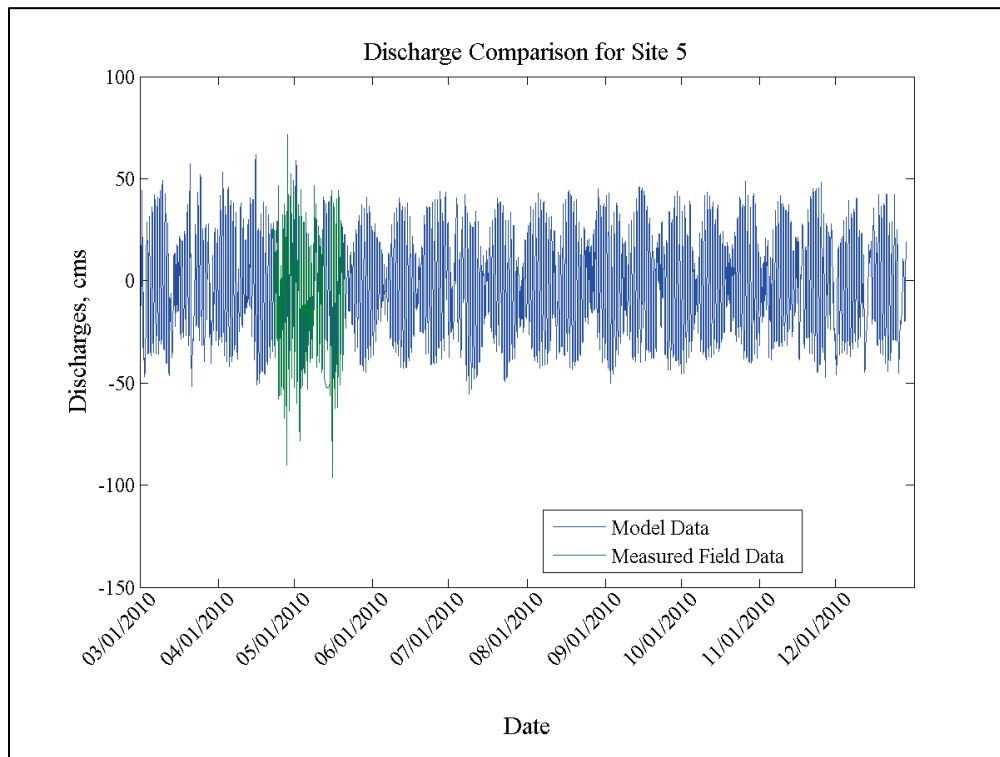


Figure 2-37. Discharge comparison for Site 8.

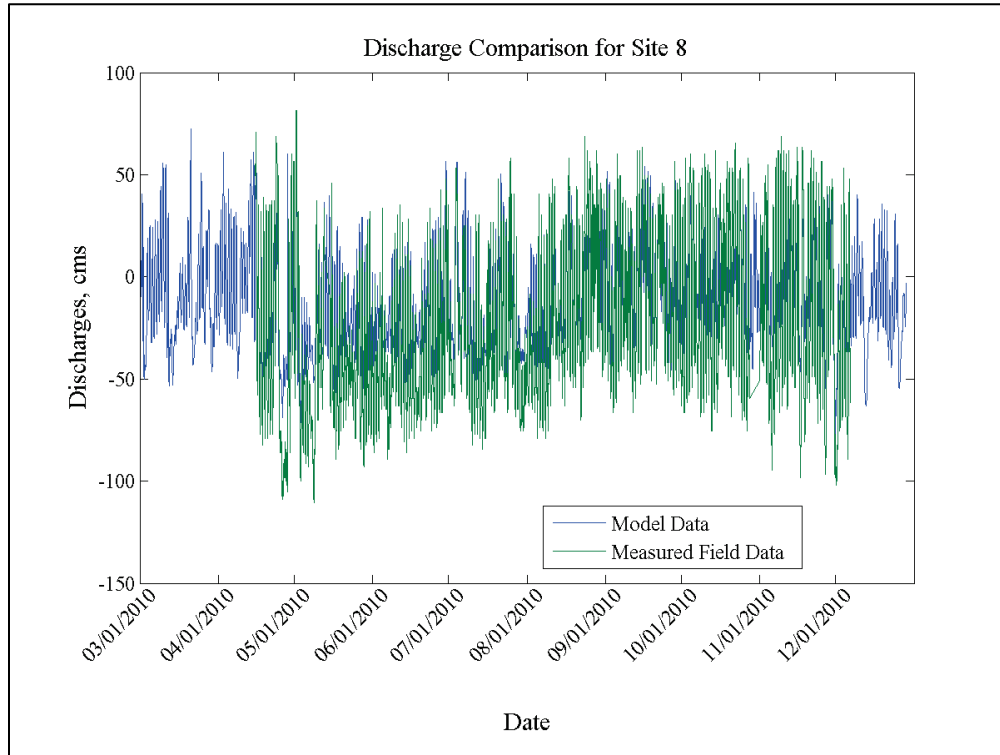


Figure 2-38. Discharge comparison for Site 9.

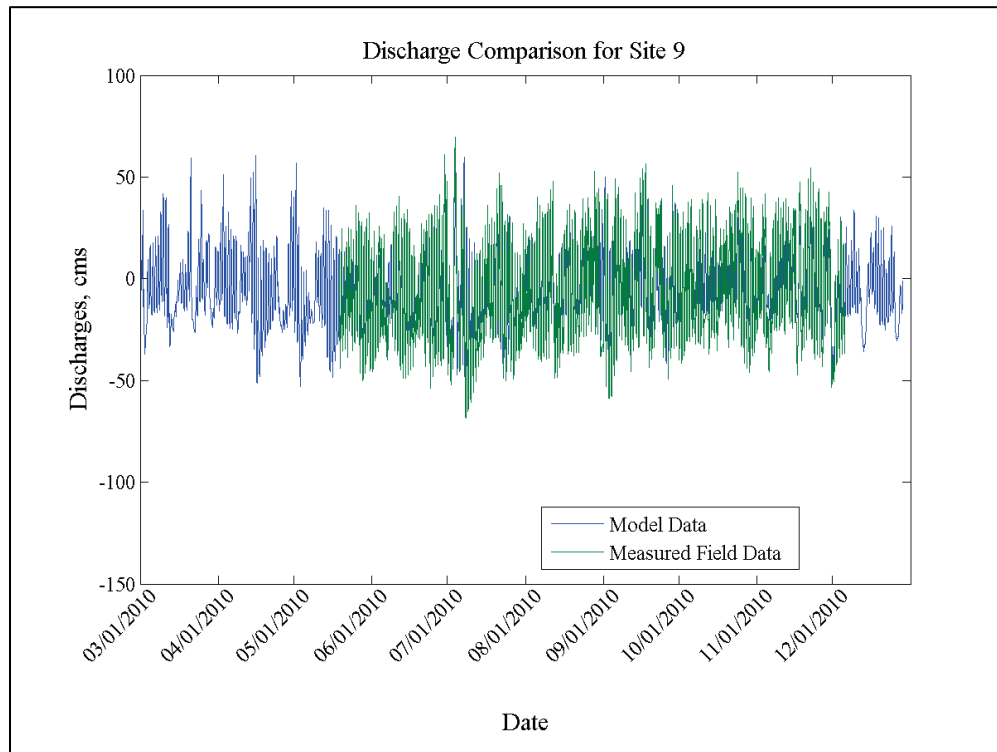
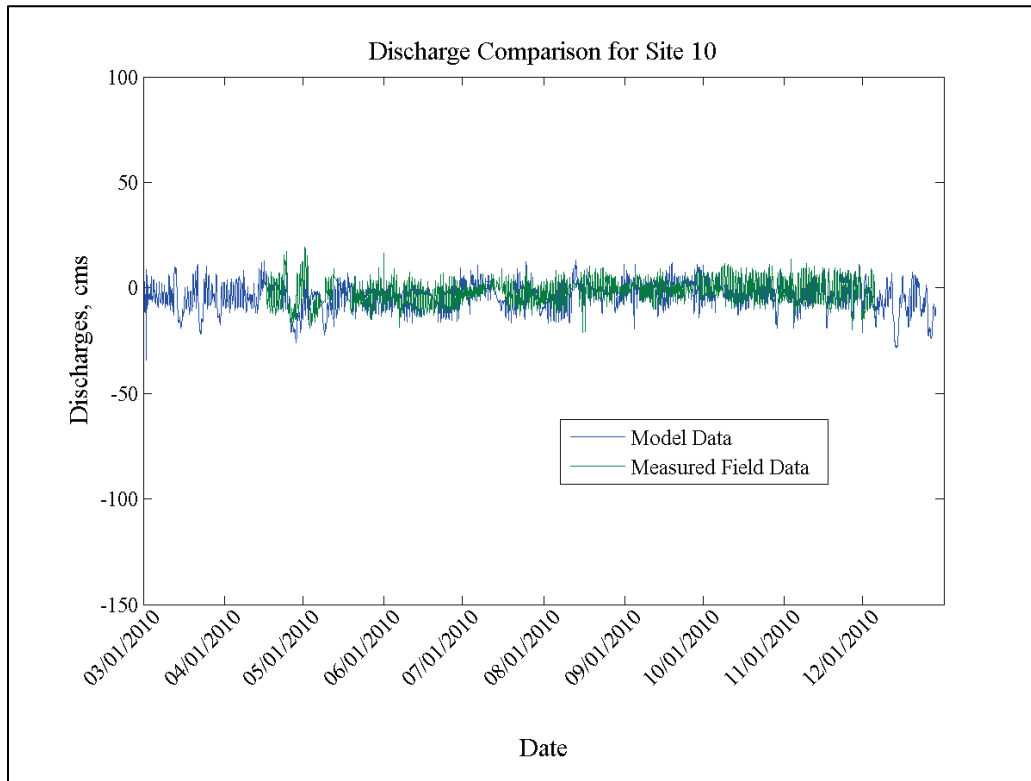


Figure 2-39. Discharge comparison for Site 10.



The outfall of Lake Leary, Site 3, shows good correlation with the field data, particularly during tidal flood. The ebb periods are slightly low on the discharge. In the region between Site 3, Site 4, and Site 8, the hydrodynamics are extremely complex. While main channels can be clearly identified in the aerial photography and bathymetry, during high sediment concentration events, the flow does not appear to follow the main channel. The model indicates this as well; in fact, it diverts too much ebb flow to the side channels. However, there is insufficient off-channel bathymetry to properly capture the unique circulation pattern occurring in this region. Many mesh changes were made in an attempt to understand the flow pattern, but without more detailed bathymetry information, it was not possible to fully capture this phenomenon. For this reason, the discrepancies found in Site 3, Site 4, and Site 8 during ebb flow are considered acceptable for this work.

Site 5 is located near the outfall of Bayou Terre Aux Boeufs. Though Site 4 is also located along Bayou Terra Aux Boeufs, Site 5 is unaffected by the discharge discrepancies. Site 5 is strongly influenced by tides as can be seen by the net discharge averaging near zero. Note that the calibration of Site 5 relied on only two data points at nearly the same flow rate.



The discharge at Site 9 on the Oak River (River Aux Chenes) correlates exceptionally well with the field data. Located north of Site 9, just off of Oak River, is Site 10. The correlation for Site 10 is less than optimal, but magnitude of the error is similar to the other gauges. Site 10 is located on what appears to be a main flow path for the Caernarvon Diversion outfall; however, satellite imagery during high sediment concentration flows indicate that the majority of the flow bypasses this side-channel. Many changes to the mesh were made in an attempt to properly capture the flow pattern. Because of the complex flow patterns in a region in which little or no bathymetry data were available, the current state of the model was deemed acceptable.

Overall, the model reproduces the field data with acceptable accuracy. The complexity of the system and the amount of bathymetric data available are the primary sources of uncertainty. However, the model can replicate field water surface elevation and discharges to an acceptable degree.

### **Salinity**

The salinity within the Breton Sound marsh is generally less than 10 parts per thousand during low Caernarvon flow and is almost completely fresh during high Caernarvon flow rates. The source of salinity for this region was investigated heavily.

During Mississippi River flooding, river discharge through Bohemia Spillway, the Fort Saint Philip crevasses, and Baptiste Collette significantly freshens lower Breton Sound. These fresh water inflows to Breton Sound are balanced by the influx of salinity from both the southern end of Chandeleur Islands and the Mississippi Sound and the northern end of the Chandeleur Islands.

There has not been a documented study directed solely at investigating residual (tidally averaged) flow trends within the Chandeleur Sound. However, several studies indicate that flow is generally toward the southwest (Johnson 2008), with reversals possible. These flow reversals tend to have seasonal trends (Johnson 2008) and are correlated with wind-driven circulation (Schroeder 1985).

The Coastal, Wetlands, Planning, Protection, and Restoration Act (CWPPRA) was enacted in 1990 to identify, prepare, and fund construction of coastal wetlands restoration projects in Louisiana

(CWPPRA 2014). The Coastwide Reference Monitoring System (CRMS) is a CWPPRA-funded project that monitors multiple physical and environmental parameters for use in evaluating the performance of CWPPRA projects. The data from these monitoring stations are readily available online (<http://lacoast.gov>).

The model salinity was compared to field data at the ERDC sites (Figure 2-13) as well as several CRMS stations and the Bay Gardene USGS station (Figure 2-40). The comparisons can be found in Figure 2-41 through Figure 2-57.

Figure 2-40. Salinity comparison locations.

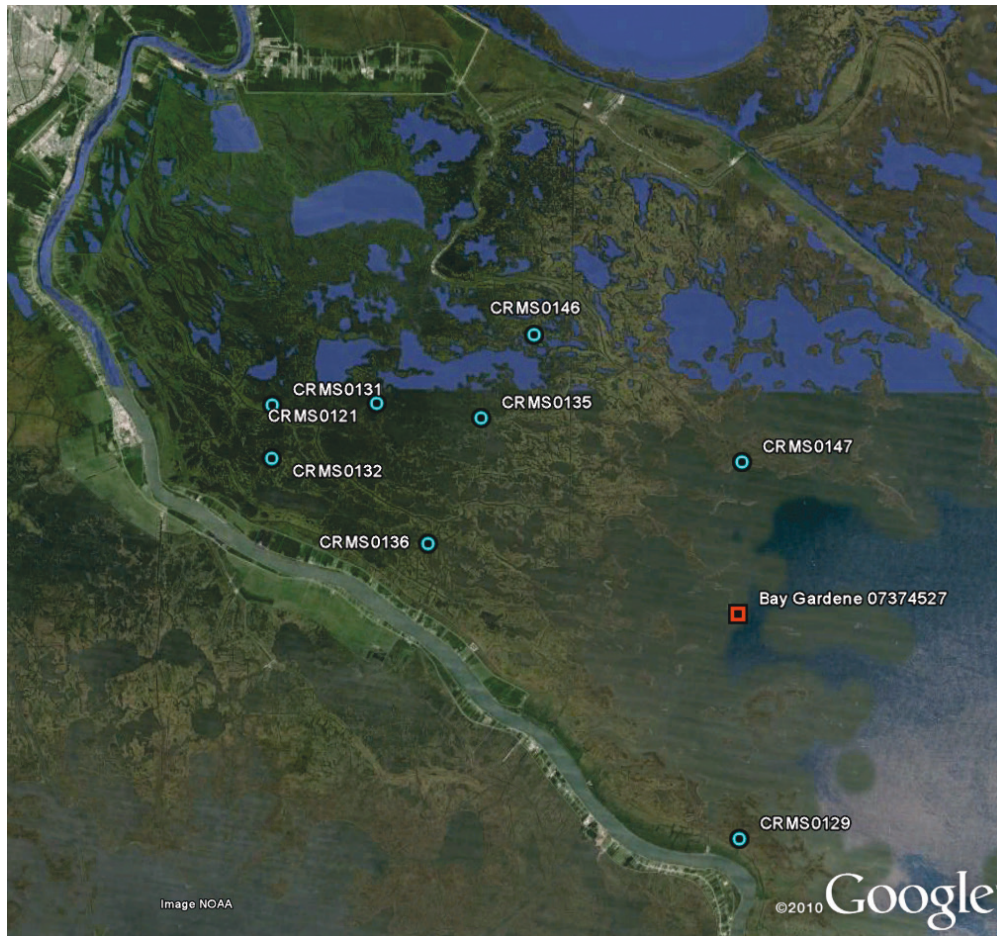


Figure 2-41. Salinity comparison for Site 1.

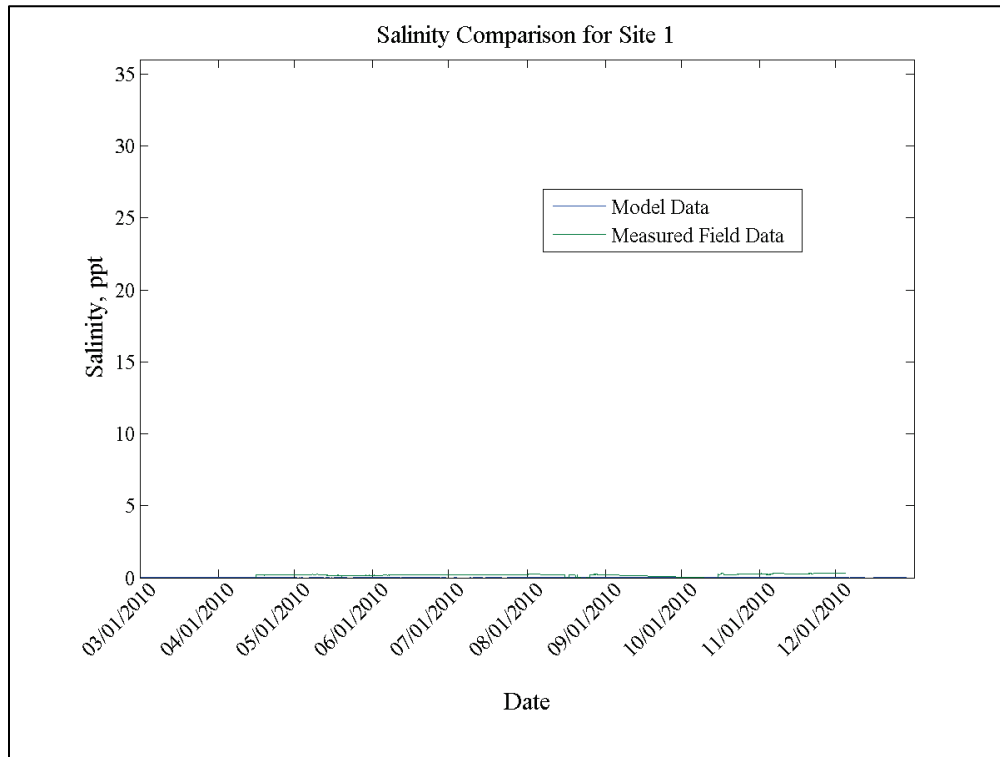


Figure 2-42. Salinity comparison for Site 2.

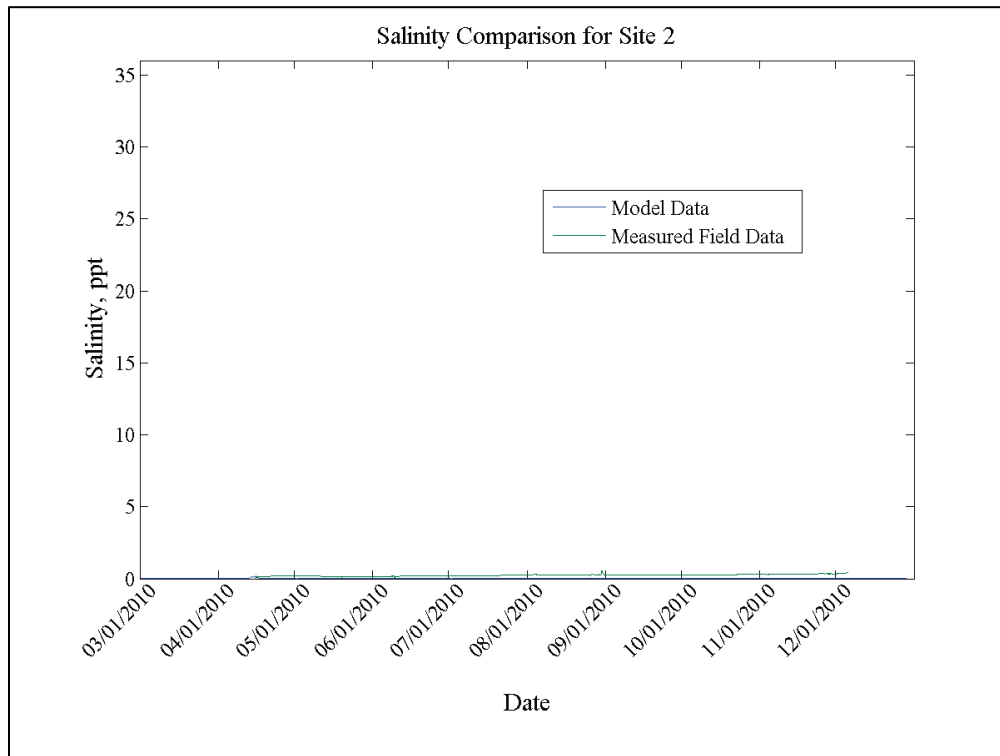


Figure 2-43. Salinity comparison for Site 3.

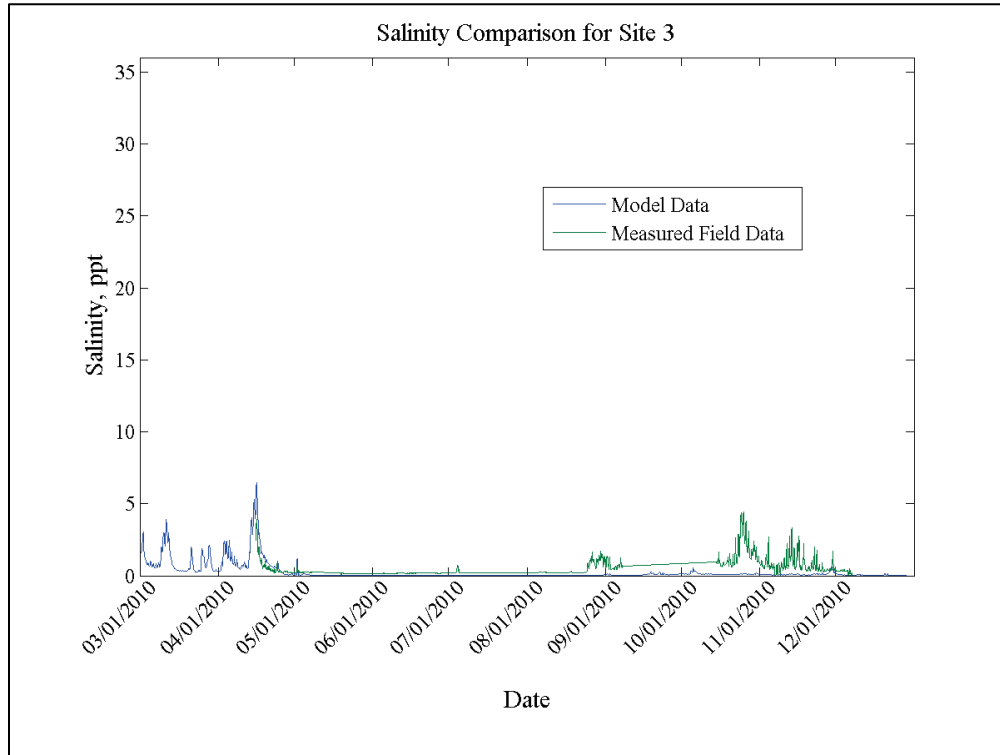


Figure 2-44. Salinity comparison for Site 4.

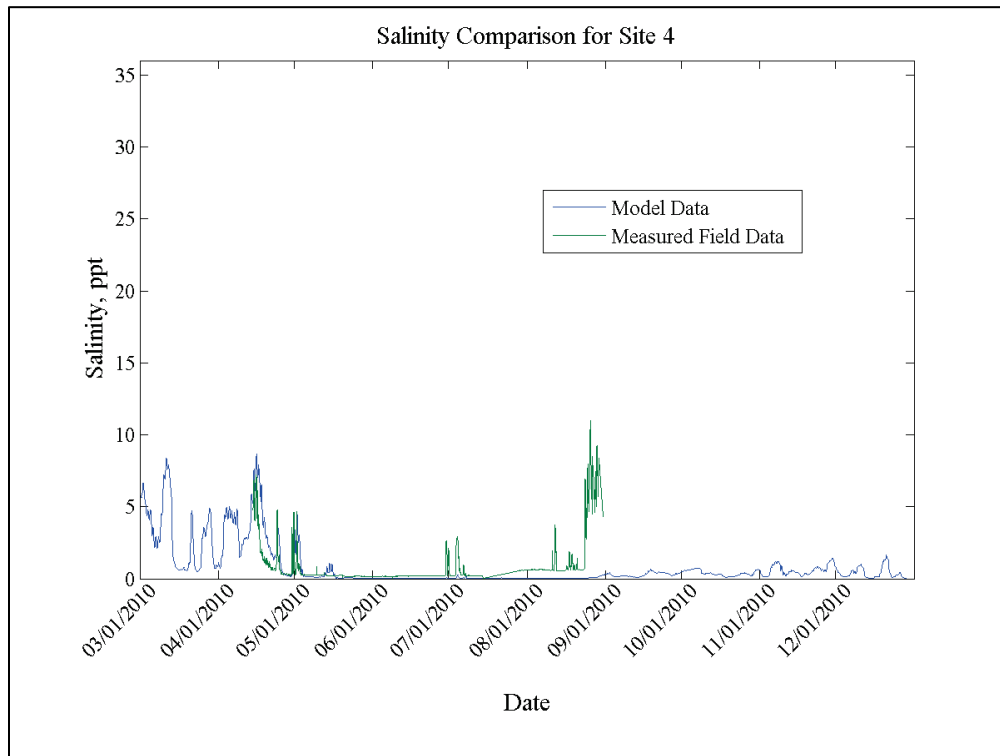


Figure 2-45. Salinity comparison for Site 5.

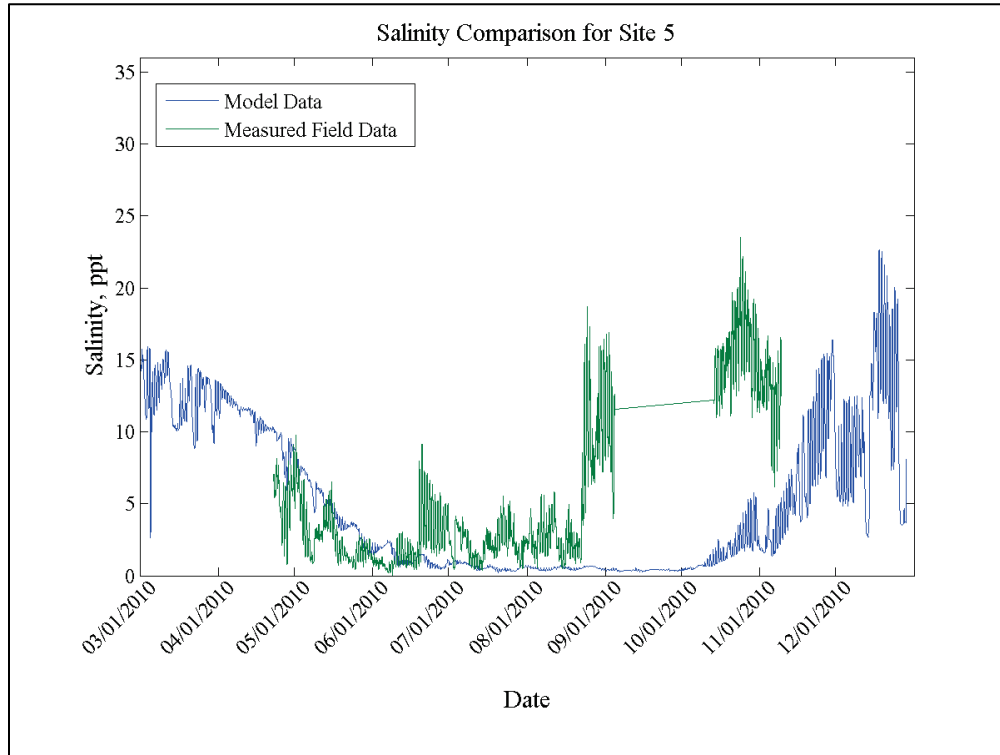


Figure 2-46. Salinity comparison for Site 8.

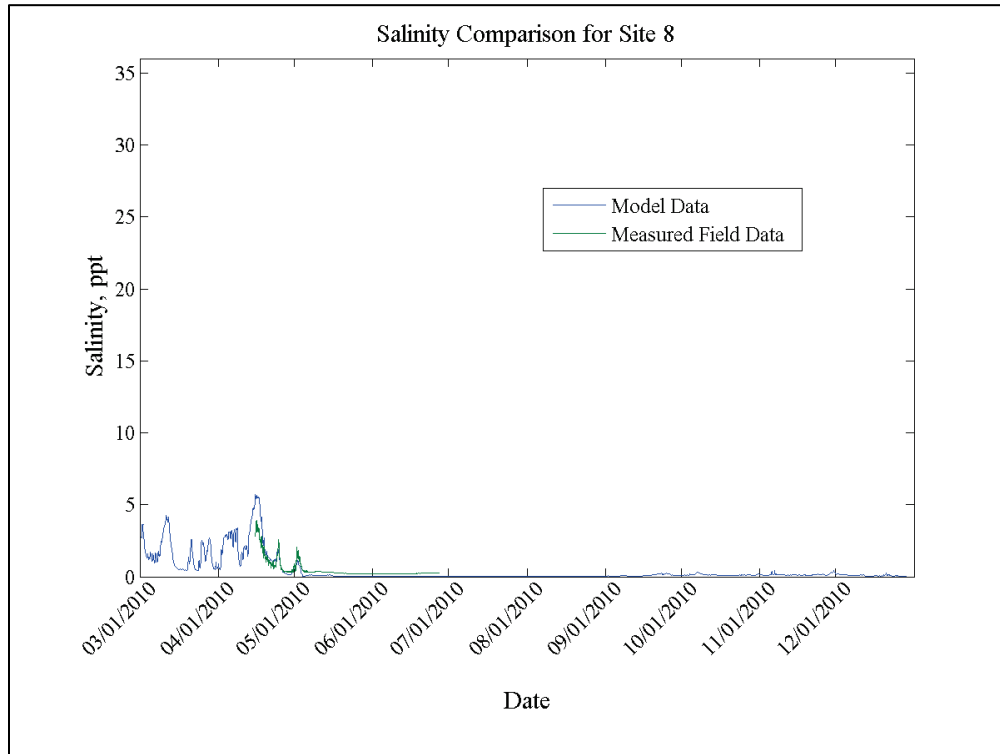


Figure 2-47. Salinity comparison for Site 9.

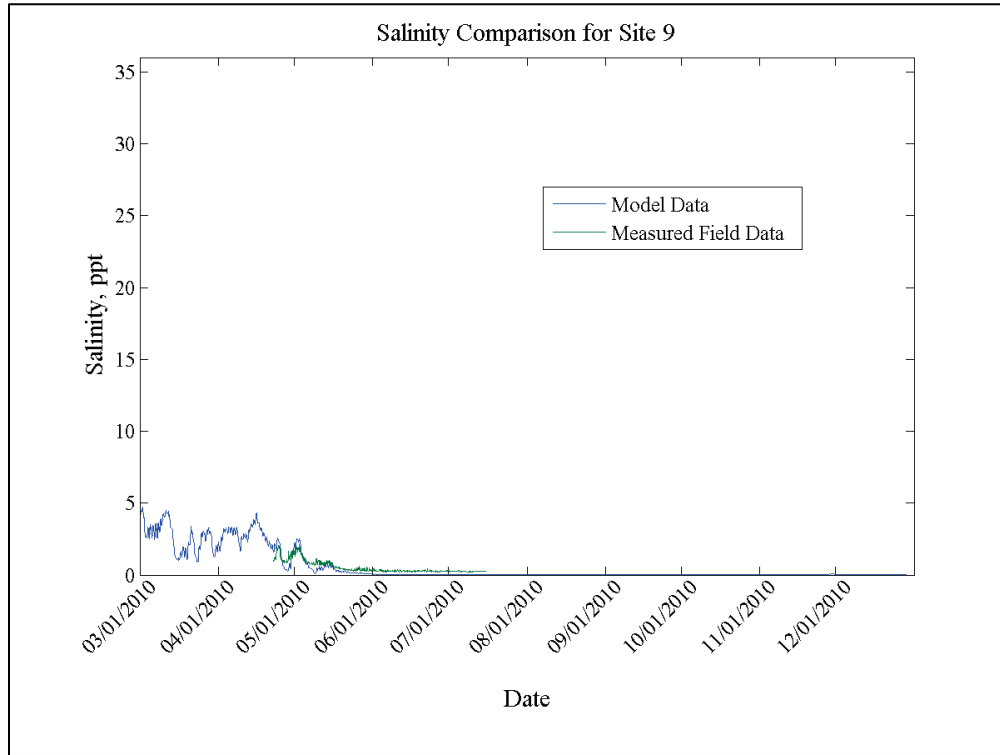


Figure 2-48. Salinity comparison for Site 10.

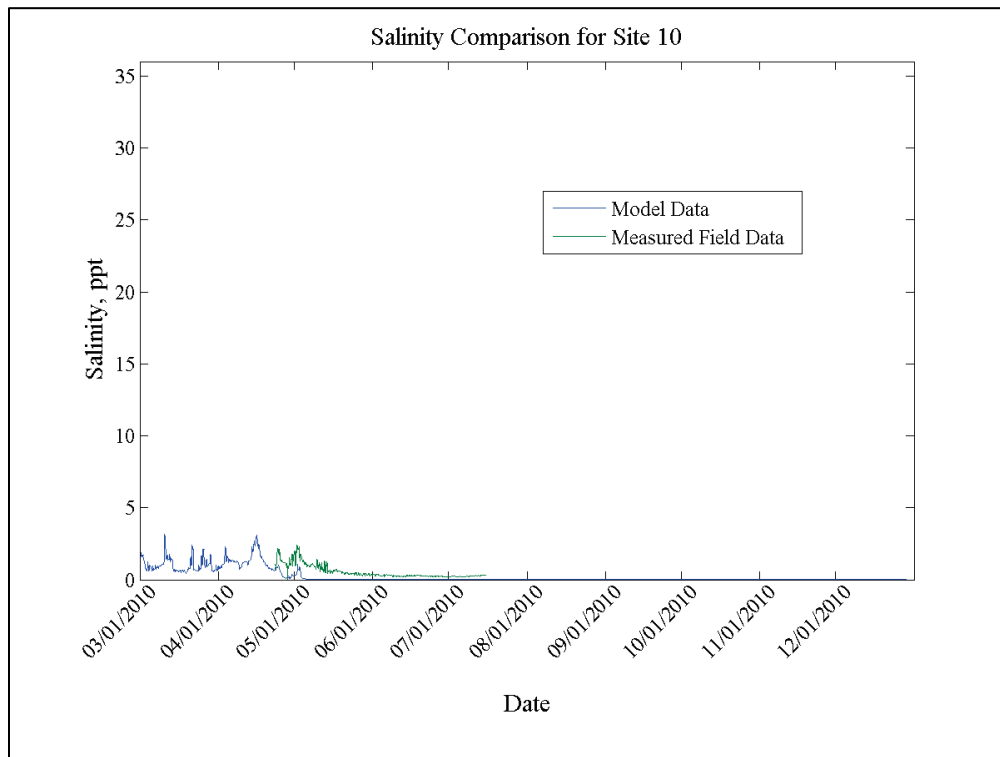


Figure 2-49. Salinity comparison for CRMS 0121.

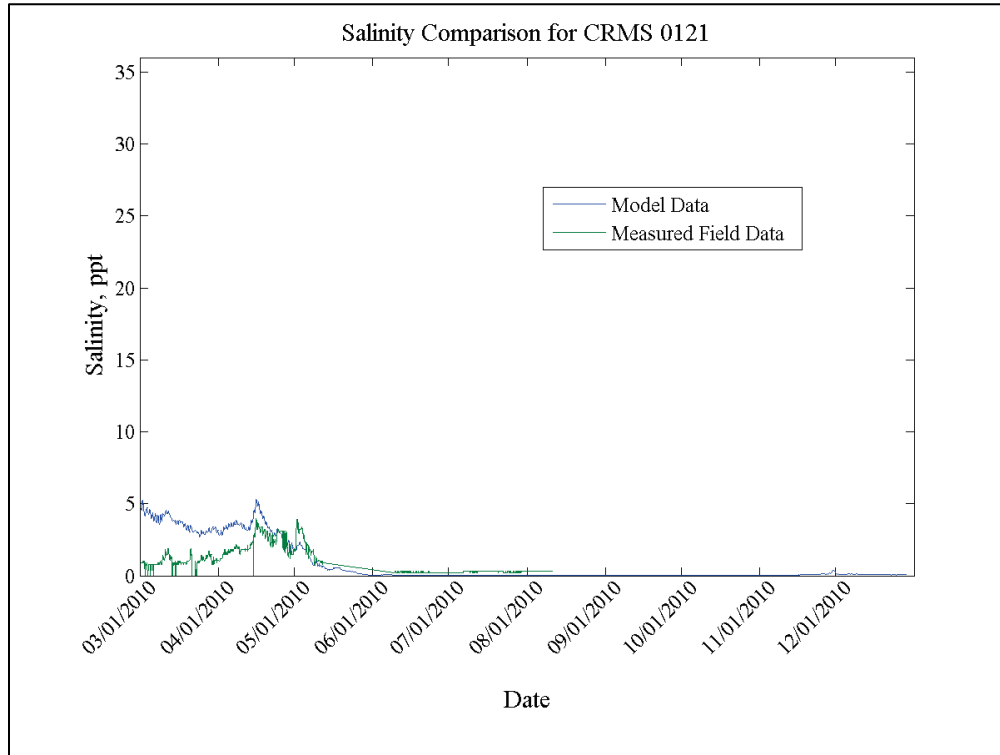


Figure 2-50. Salinity comparison for CRMS 0129.

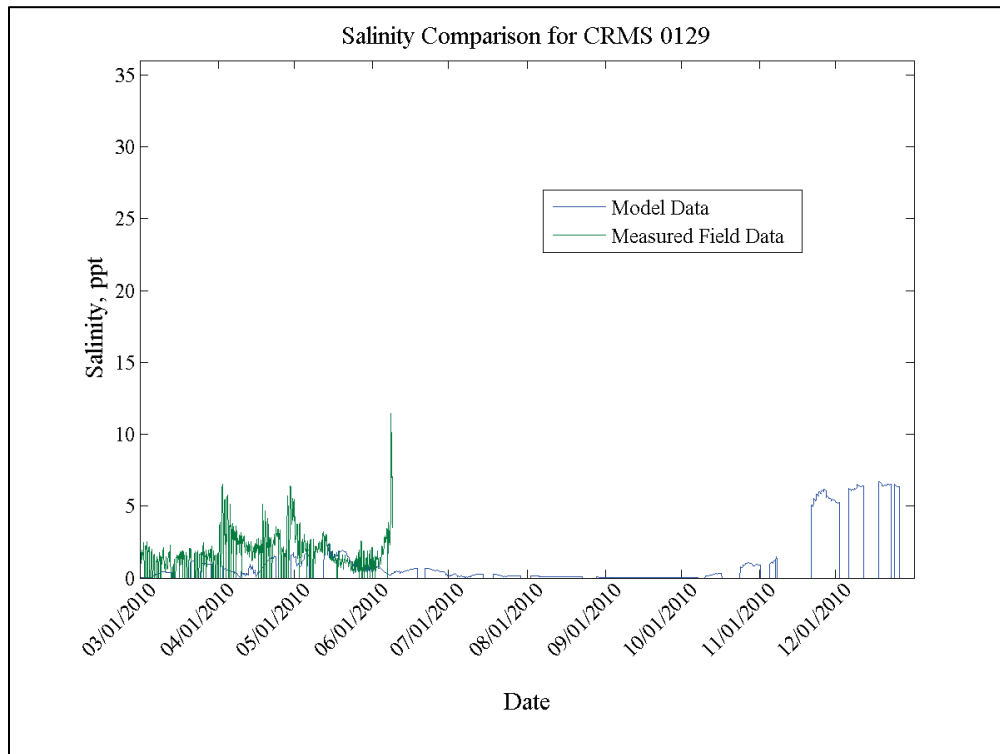




Figure 2-51. Salinity comparison for CRMS 0131.

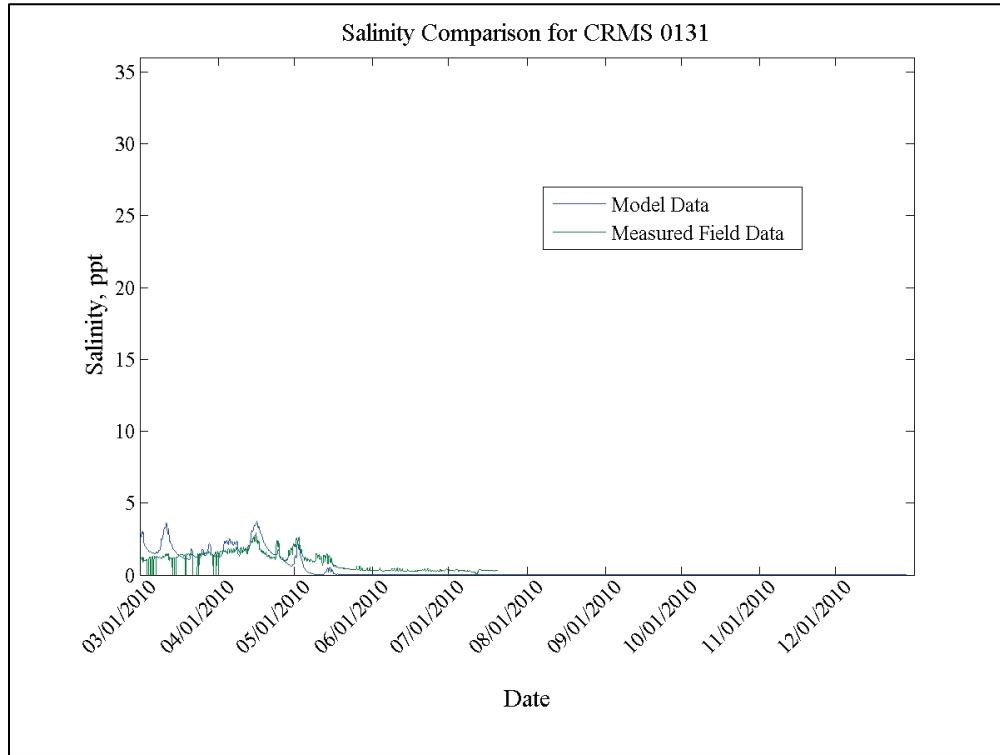


Figure 2-52. Salinity comparison for CRMS 0132.

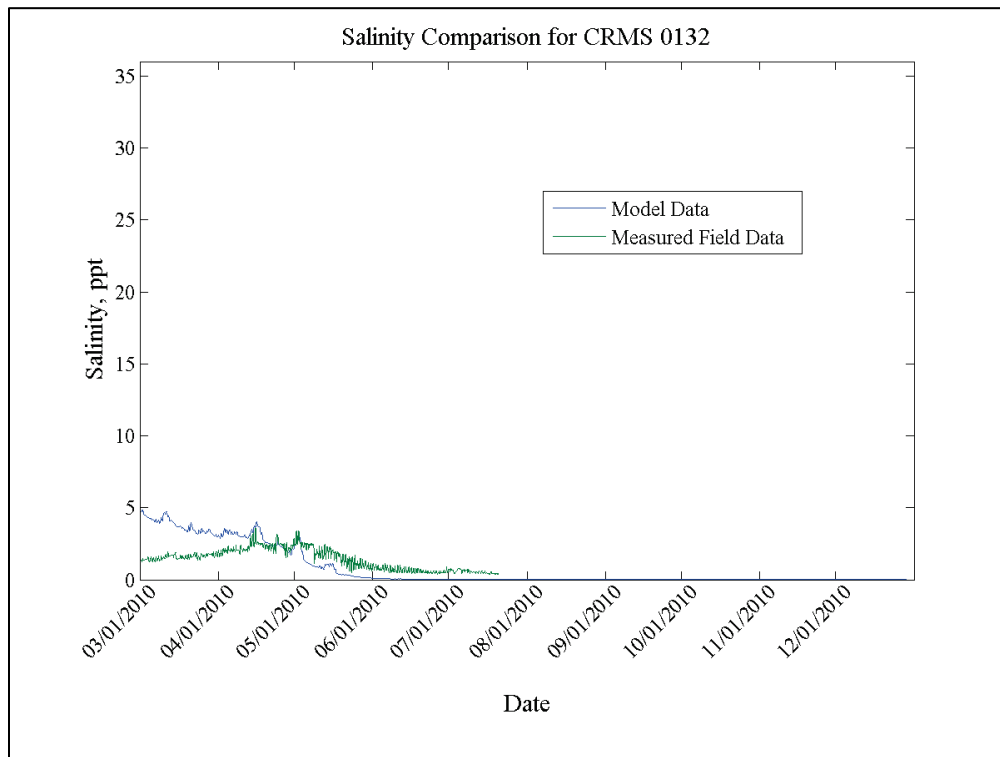


Figure 2-53. Salinity comparison for CRMS 0135.

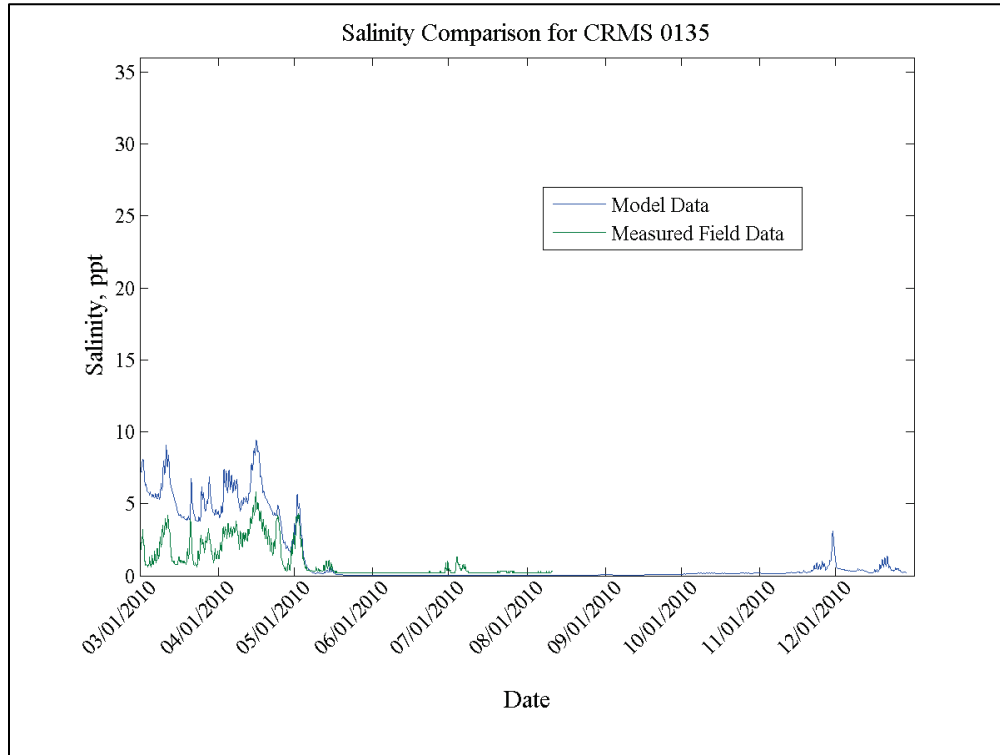


Figure 2-54. Salinity comparison for CRMS 0136.

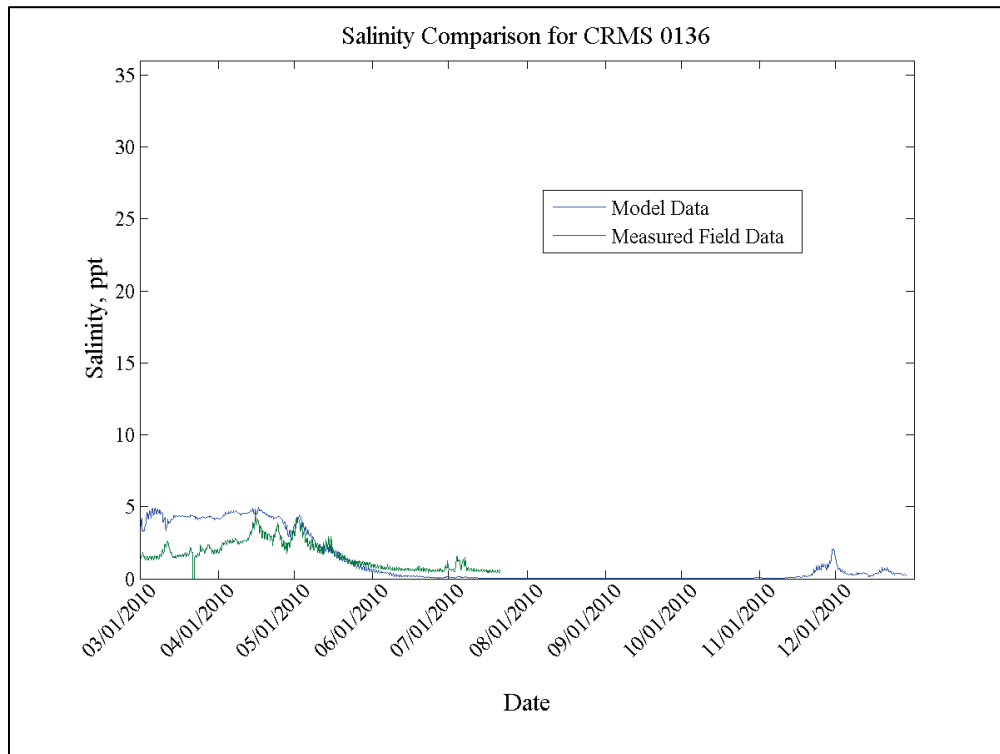


Figure 2-55. Salinity comparison for CRMS 0146.

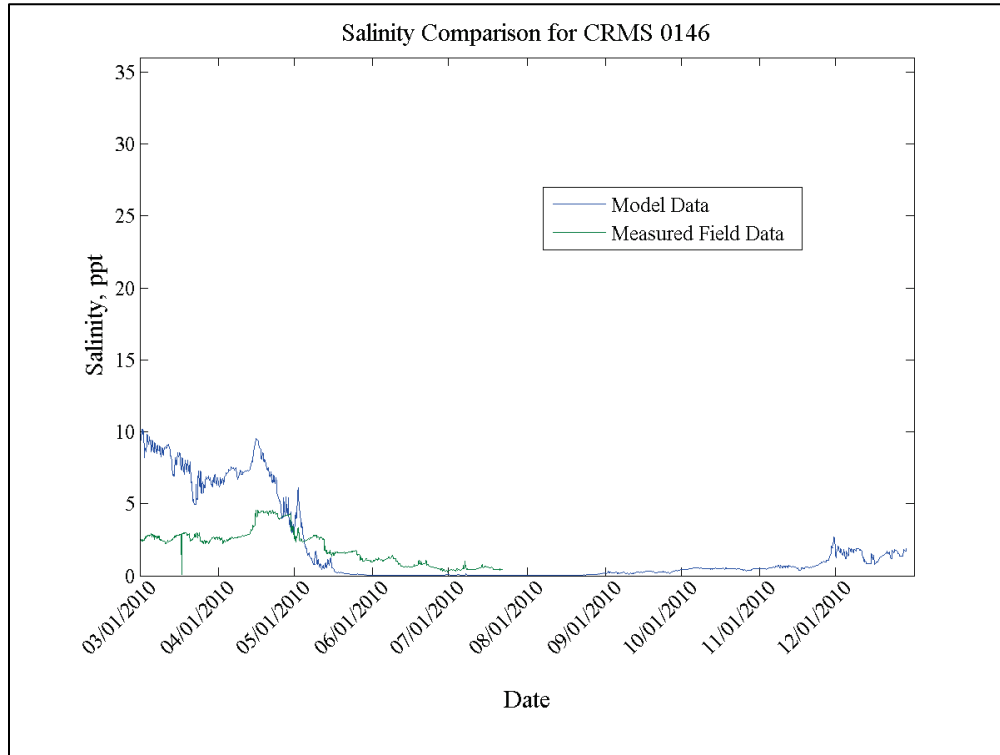


Figure 2-56. Salinity comparison for CRMS 0147.

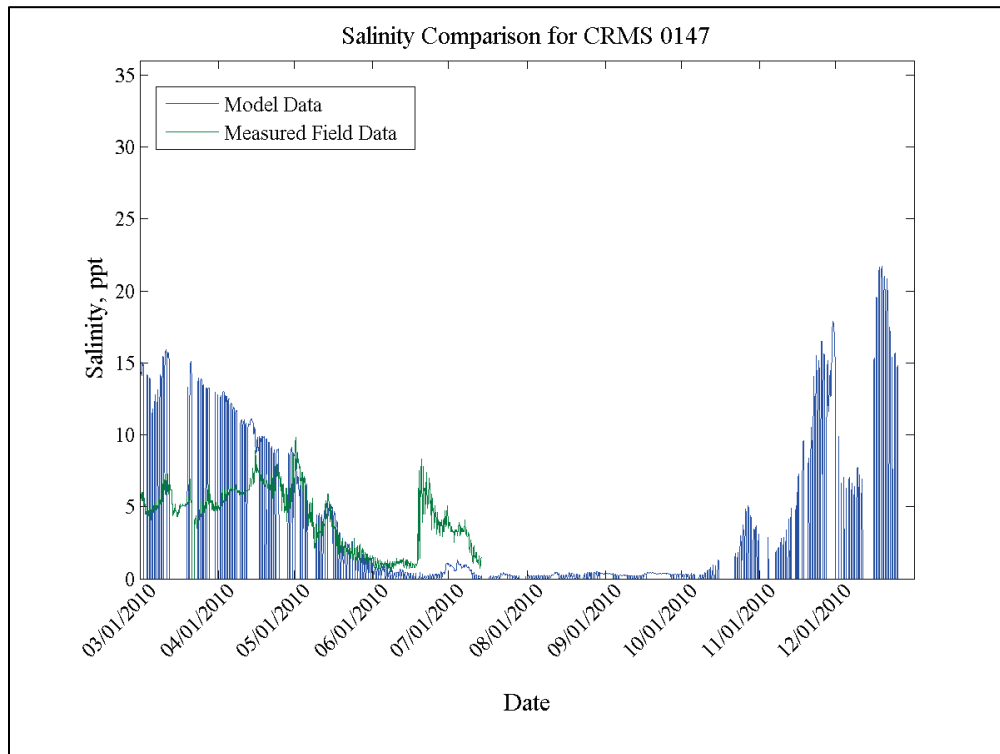
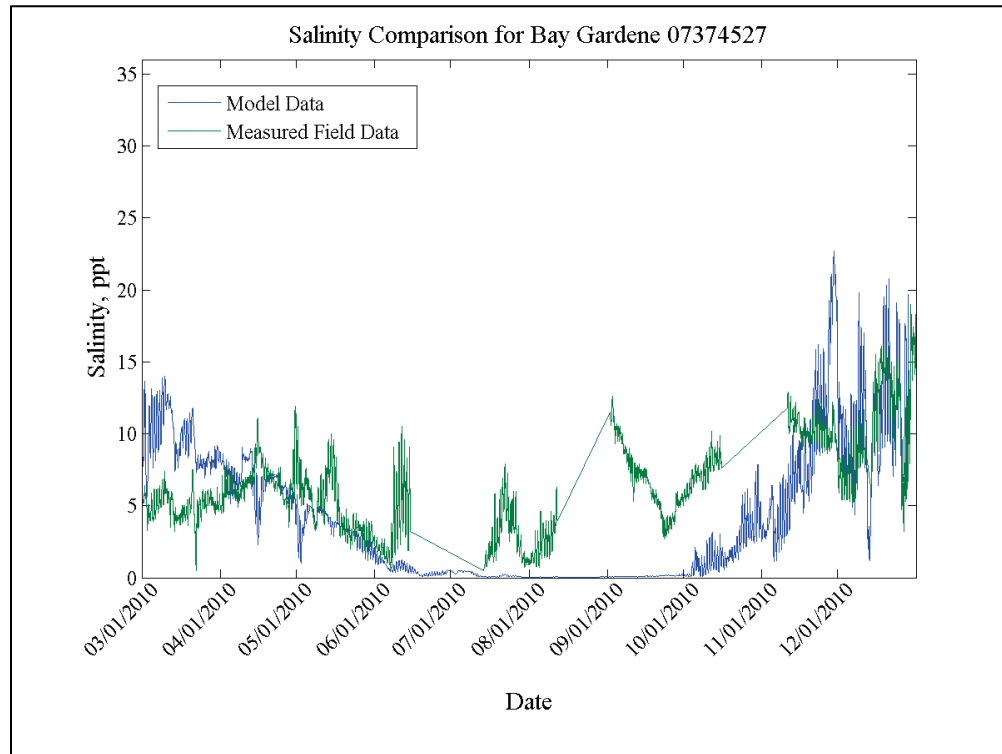


Figure 2-57. Salinity comparison for Bay Gardene.



The salinity comparisons show that the recovery of salinity after cessation of Caernarvon operations is delayed in the model (relative to the field observations) by approximately 2 months. Once salinity is restored to the estuary, it matches observations well. However, this delay is indicative of some discrepancy between the model and field, related to circulation in South Breton Sound and Chandeleur Sound. This discrepancy could be associated with any of several factors, including multi-dimensional factors not modeled by the 2D model (e.g., stratification, Ekman dispersion), or it could be related to uncertainties in boundary conditions (e.g., winds, discharge).

However, as of this writing, the source of this discrepancy has not been determined. Therefore, only qualitative results from the model are included in this report, results that are sufficiently robust that they can be trusted with the level of validation achieved thus far.

### 3 Salinity Impacts Due to Diversion

Changes in salinity were investigated by performing simulations of the model through the validation period for four different combinations of diversion operations: No diversions; Caernarvon Diversion (CD) only; modeled Breton Sound Diversion (BSD) only; CD and BSD.

The CD was operated as it was observed to operate during 2010. BSD was operated at 35,000 cfs, from March 20 to April 30.

Figures 3-1 to 3-4 depict salinity contours with both BSD open and closed for 10, 20, 30, and 40 days after the diversion opening, respectively. Two general observations can be made. The first is that the BSD freshens all but the eastern part of Breton Sound very quickly after opening (within the first 10 days). The second observation is that there is very little difference in the salinity contours between the with- and without-BSD simulations for South Breton Sound and Chandeleur Sound. This is because the coastal currents, driven by winds and Mississippi River discharges through the eastern passes, overwhelm the inflow from BSD.

Consider Figure 3-5 and Figure 3-6. These are time histories of salinity at Bay Gardene and Site 5, for all three of the scenarios that include diversion operations. Note that, in all cases, the timing and magnitude of salinity recovery are almost identical. This means that the recovery of salinity is a function of prevailing wind and Mississippi River conditions. Hence, two general statements can be made concerning the expected impact of BSD operations on Breton Sound.

- BSD can be expected to rapidly freshen all of Breton Sound (except the region east of Delacroix) and to maintain fresh water conditions in the sound until the diversion is closed.
- After BSD is closed, the time of recovery of salinity in Breton Sound is essentially independent of the volume of fresh water diverted; recovery is a function of the prevailing wind-driven currents and Mississippi River discharges through the eastern passes.

Figure 3-1. Salinity contours 10 Days after diversion opening.

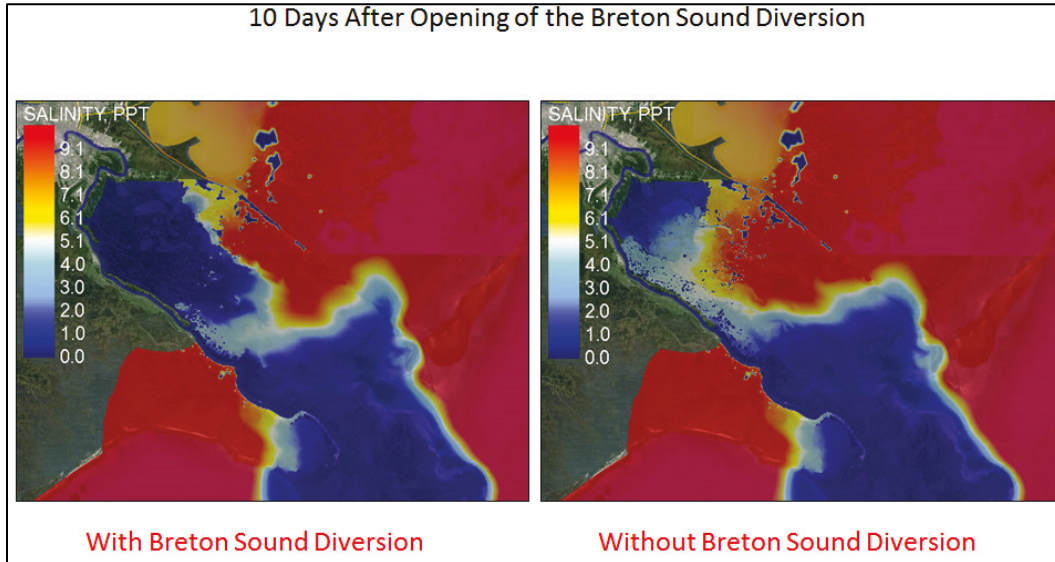


Figure 3-2. Salinity contours 20 days after diversion opening.

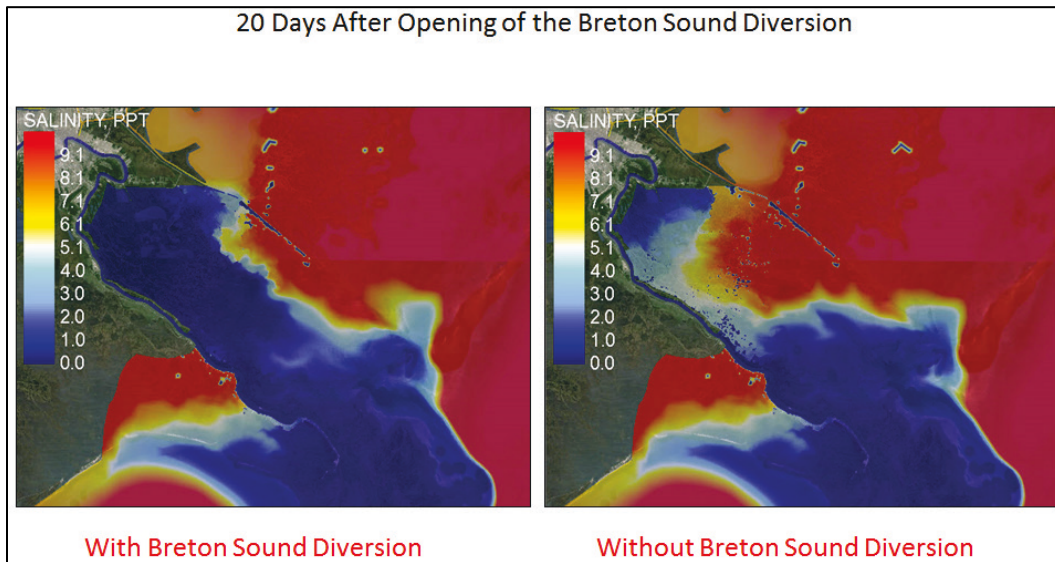


Figure 3-3. Salinity contours 30 days after diversion opening.

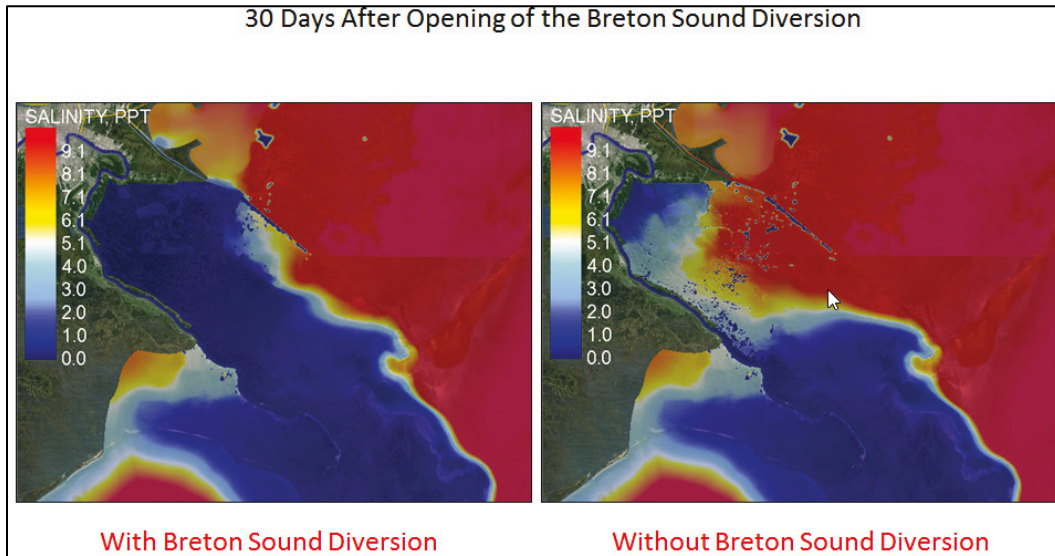


Figure 3-4. Salinity contours 40 days after diversion opening.

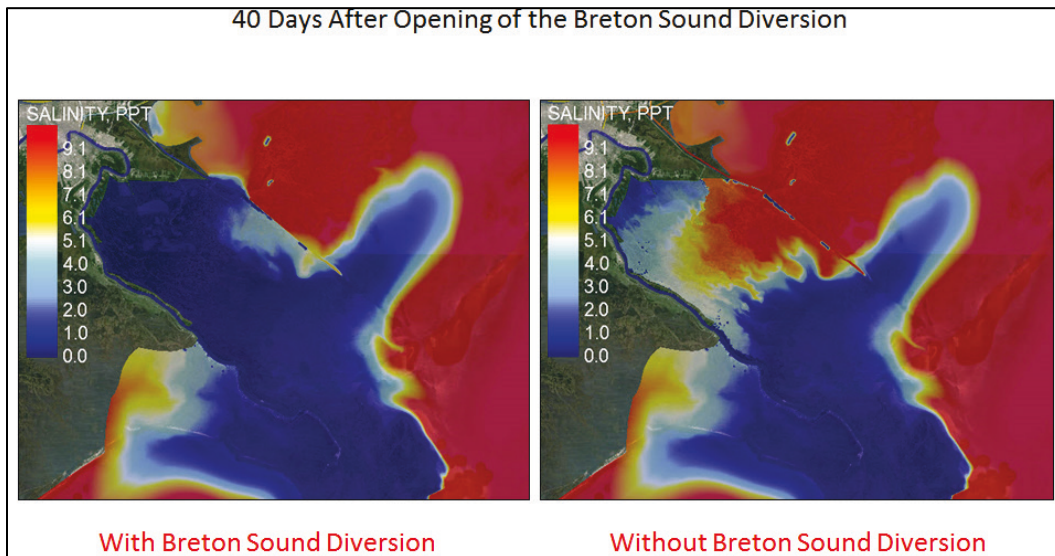




Figure 3-5. Time history of salinity at Bay Gardene.

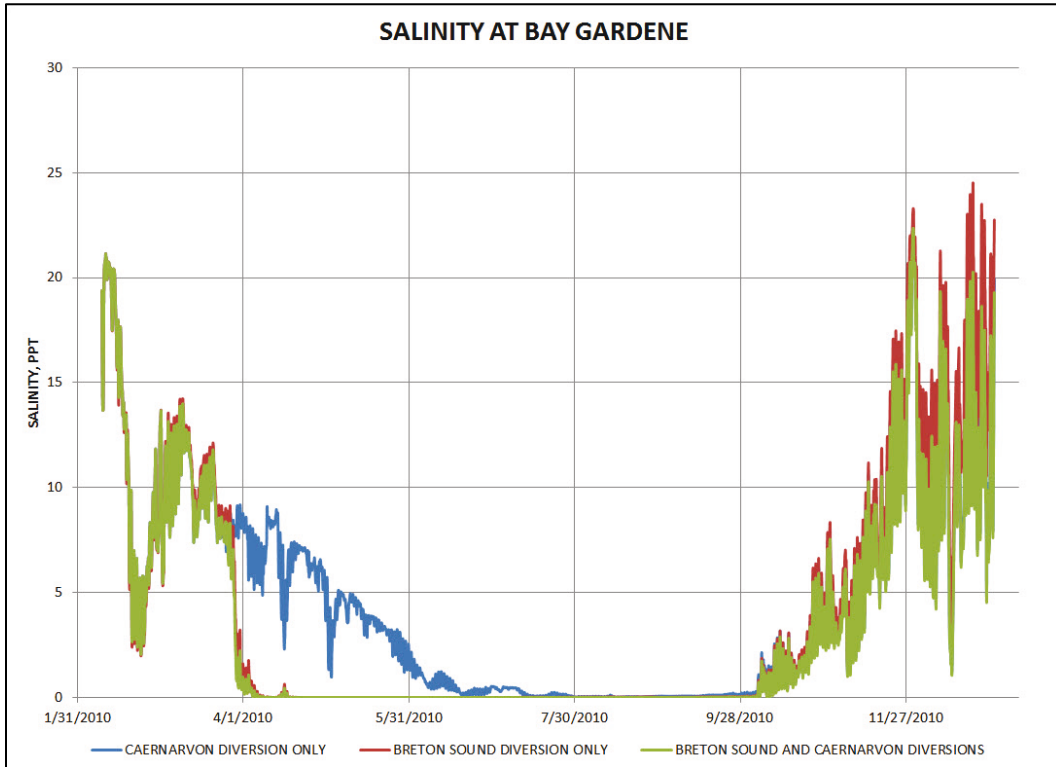
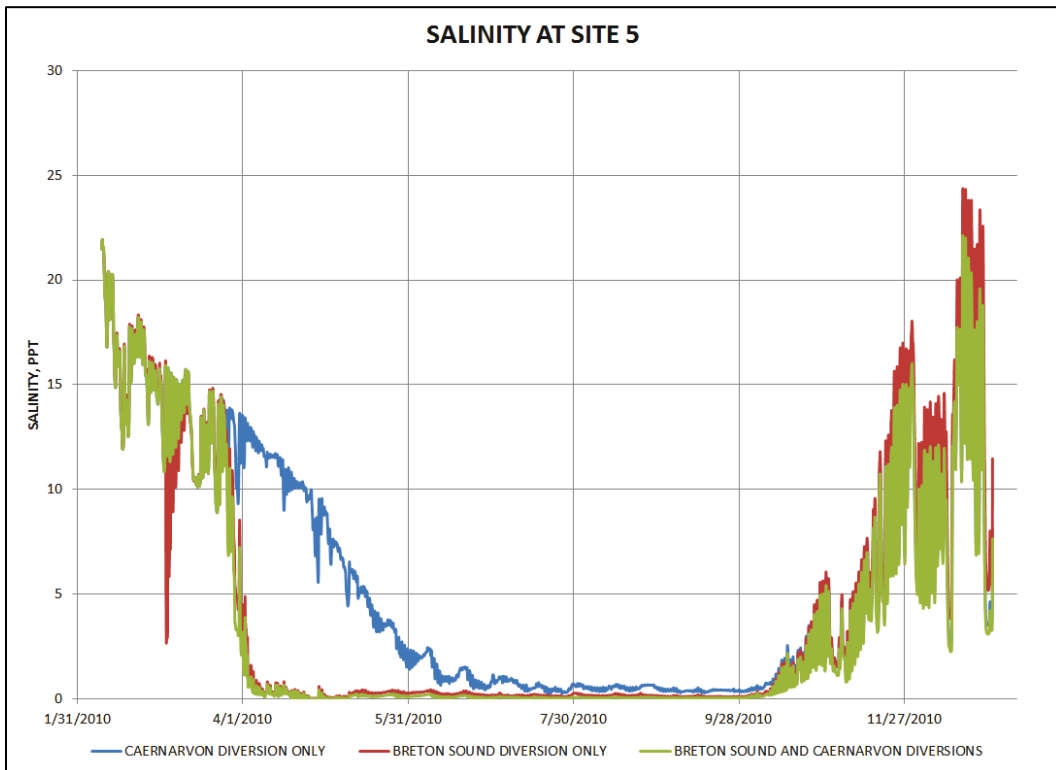


Figure 3-6. Time history of salinity at Site 5.



## 4 Morphologic Modeling

To assess the performance of the BSD, it is necessary to model the long-term morphologic change associated with the diversion. This represents a significant technical challenge, both with respect to the inherent complexities associated with morphological modeling and (even more significantly) the uncertainties associated with such things as the governing processes, the quantification and boundary conditions, and future conditions. This chapter documents the approach taken for this study to model the long-term morphologic impacts of the BSD. The results are provided, with due consideration given to these complexities and uncertainties.

### Approach

To model 50 yr of morphologic change in Breton Sound associated with the BSD, it is necessary to consider the uncertainties associated with each of the boundary conditions and governing processes and how these might change over time. Although there are many boundary conditions that actually influence the system, the boundary conditions of interest for this study include the following:

- water and sediment discharge through the BSD
- water and sediment discharge through the CD
- tides
- winds
- eustatic sea level rise
- subsidence.

The processes of primary interest for this study include the following:

- sediment deposition
- sediment erosion
- primary productivity (i.e., the establishment and growth of wetland vegetation).

Bounding the absolute uncertainty of each of these factors is beyond the scope of this study. Also, modeling 50 yr simulations of the large model mesh for this study is computationally intensive and impractical due to

the time required to run the simulations if a time dilation approach is not adopted.

Therefore, this study was constructed with an approach that simplifies the problem as much as possible while factoring the dominant sources of uncertainty directly into the analyses. The approach is given as follows:

- An inset model mesh was created for Breton Sound. Resolution was added to this mesh in the vicinity of the BSD outfall, to depict the outfall channel and to resolve local morphologic change (see Figure 4-1 and Figure 4-2).
- The model is provided with typical (i.e., approximately average) boundary conditions for water and sediment discharge, tide, and wind. These boundary conditions are repeated every year for 50 yr of analysis.
- A time dilation approach was employed whereby each year is approximated with only 1,000 hours of simulation time. This is done by simulating 1,000 hours in real time, applying all of the boundary conditions (sediment discharge, tide, and wind) during this 1,000 hours. Then, relative sea level rise and primary productivity contributions for the remaining 7,760 hours of the year are applied in one discrete step.
- Based on order-of-magnitude reasoning, the most significant uncertainties with respect to land building are assumed to be those associated with subsidence and eustatic sea level rise (or relative sea level rise, RSLR), and primary productivity.
- The uncertainty associated with RSLR is addressed by performing simulations for three different RLSR scenarios.
- Since primary productivity is modeled as a function of local depth, some level of uncertainty in primary productivity is addressed indirectly via the simulation of three RLSR scenarios. However, a much more sophisticated treatment of primary productivity would be necessary to formally bound the uncertainties associated with this process.
- For this reason, and because of the multitude of assumptions employed in this analysis, the absolute modeled predictions of land/loss gain are subject to a significant amount of uncertainty. Therefore, the modeled difference in land gain/loss between with and without project model simulations are reported and considered reasonable for this study.

Figure 4-1. Inset mesh for morphologic modeling.

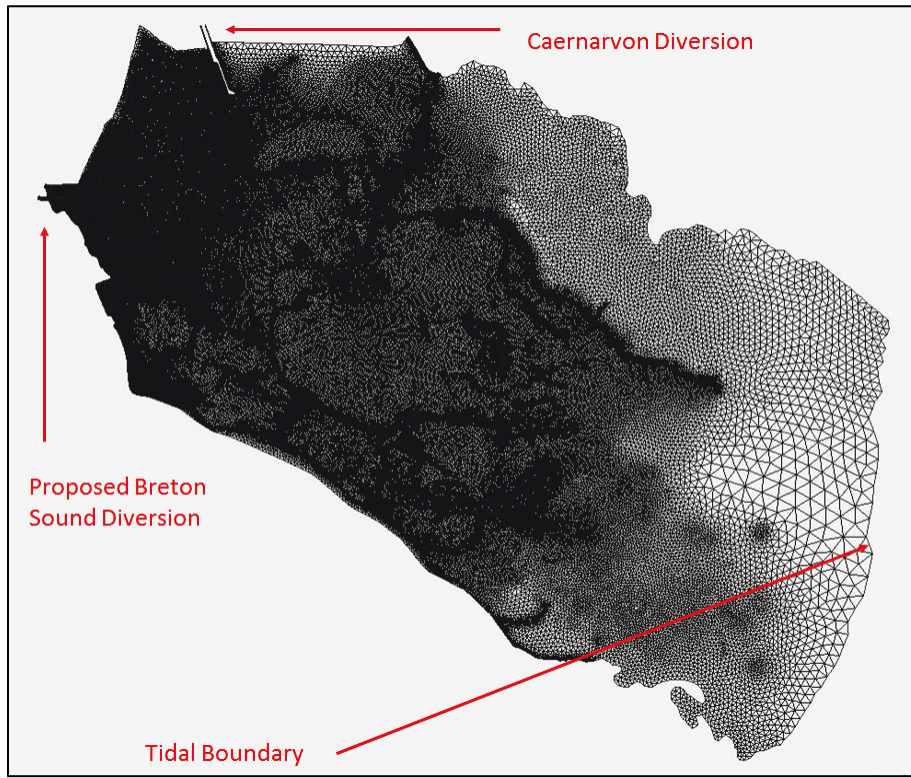
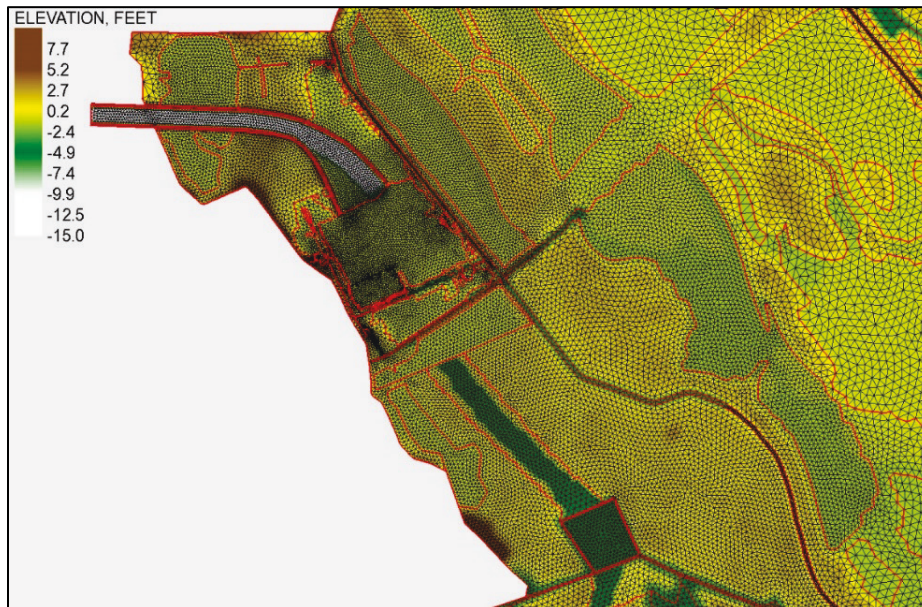


Figure 4-2. Zoom of inset mesh for morphologic modeling at diversion outfall.



## Morphologic model set up

### Sediment properties

The sediment properties of interest for the morphological modeling include properties that are associated with both the morphological model itself, as well as the model that has been used to generate the inflowing sediment boundary conditions. This model is the AdH Lower Mississippi River model, which has been developed as part of the Mississippi River Hydrodynamic Study.

### *Sediment grain classes*

The range of sediment grain classes simulated in the morphodynamic model include the full spectrum of grains that could potentially pass from the Mississippi River into Breton Sound via the diversions. These are given as follows:

- Clay (CLAY)            0.003 millimeter (mm)
- Very Fine Silt (VFM)   0.006 mm
- Fine Silt (FM)         0.011 mm
- Medium Silt (MM)      0.023 mm
- Coarse Silt (CM)       0.045 mm
- Very Fine Sand(VFS)   0.088 mm
- Fine Sand (FS)         0.177 mm
- Medium Sand (MS)     0.354 mm
- Coarse Sand (CS)      0.707 mm.

The transport properties of the sand classes are controlled by expressions given by various researchers. These are listed below:

- Settling Velocity from Cheng (1997)
- Suspended Entrainment from Wright and Parker (2004)
- Bedload Entrainment from van Rijn (Kleinhans and van Rijn 2007)
- Hiding Factor from Egiazaroff (1965).

The process of quantifying silt and clay grain class properties tends to require much more site-specific data than are required to quantify sand class properties. This is due primarily to the cohesive nature of these sediments. Cohesion is influenced by a variety of site-specific factors such as local sediment mineralogy, salinity, and biological factors. However,

this site-specific data are often unavailable, or sparse. In this case, it is useful to consider the objectives of the model to narrow the number of parameters that require accurate specification.

Since the goal of this study is to quantify potential land building associated with the introduction of a diversion, the primary behaviors of interest (with respect to cohesive sediments) are those associated with the sediments inflowing from the diversion rather than those associated with the existing marsh. These behaviors include the initial settling of the sediments discharged from the diversion and the resuspension of these freshly deposited sediments due to tidal currents, and/or wind waves.

Observations of suspended sediment profiles associated from sediments being delivered to Breton Sound via the Caernarvon Diversion indicate settling velocities in the range of the free settling velocities of the individual particles. Hence, in the absence of salt water, a simplifying assumption is made that that the sediments delivered by the diversions are unflocculated. The silt and clay sediments have been assigned properties appropriate for unconsolidated, free settling fine sediment. Sediment is assumed to settle grain by grain (as opposed to settling in flocs) (i.e., settling speeds taken from Stokes Law).

In SEDLIB, the erosion rate of recently deposited sediment is prescribed by the method of Alishahi and Krone (1964). The critical shear for erosion and the erosion rate constant are assumed constant for all grains (i.e., they are properties of the settled sediment bed layer). The values of these are given such that areas of Breton Sound subject to wind-wave stresses (i.e., open water, as opposed in the interior of marshes) will exhibit suspended sediment concentrations on the order of those observed in the field. Hence, the specification of these values is qualitative in nature.

The deposition rate is given by the method of Krone (1962). The critical shear for deposition is assumed proportional to grain size, scaled by the critical shear stress of very fine sand. A summary of the silt- and clay-sized sediment properties is given in Table 4-1.

Table 4-1. Silt and clay sediment grain class properties.

Class	Diameter (mm)	Settling Velocity (mm/sec)	Critical Shear for Erosion (Pa)	Erosion Rate Constant (kg/m <sup>2</sup> -sec)	Critical Shear for Deposition (Pa)
CLAY	0.003	0.009	0.35	0.00001	0.005
VFM	0.006	0.036	0.35	0.00001	0.01
FM	0.011	0.121	0.35	0.00001	0.02
MM	0.023	0.529	0.35	0.00001	0.04
CM	0.045	2.025	0.35	0.00001	0.075

sec = second  
 Pa = Pascal  
 kg = kilogram

**Boundary conditions**

The inflowing sediment boundaries for both the BSD and the CD are taken from an AdH simulation of the operation of the diversions for the 2009 hydrograph. The water and sediment discharge hydrographs for both diversions are given in Figure 4-3 and Figure 4-4.

Figure 4-3. Modeled annual water and sediment inflow hydrograph for the diversion.

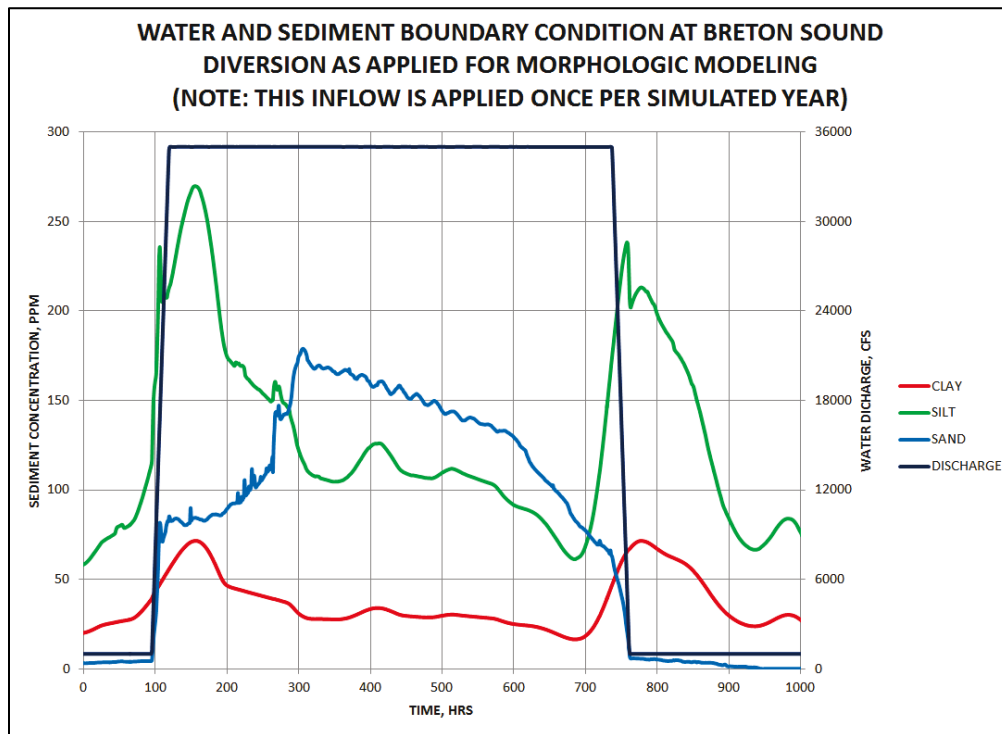
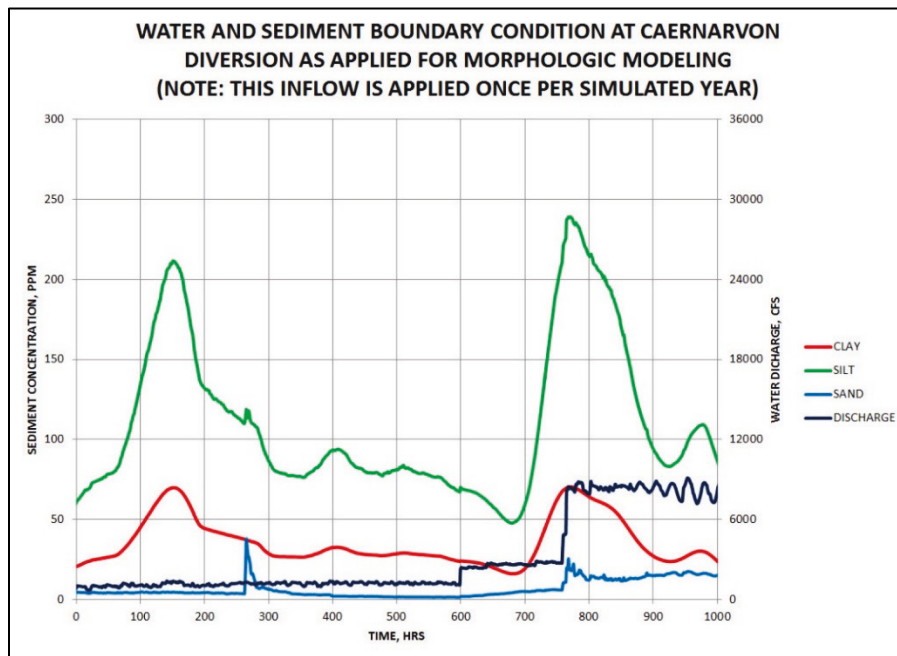


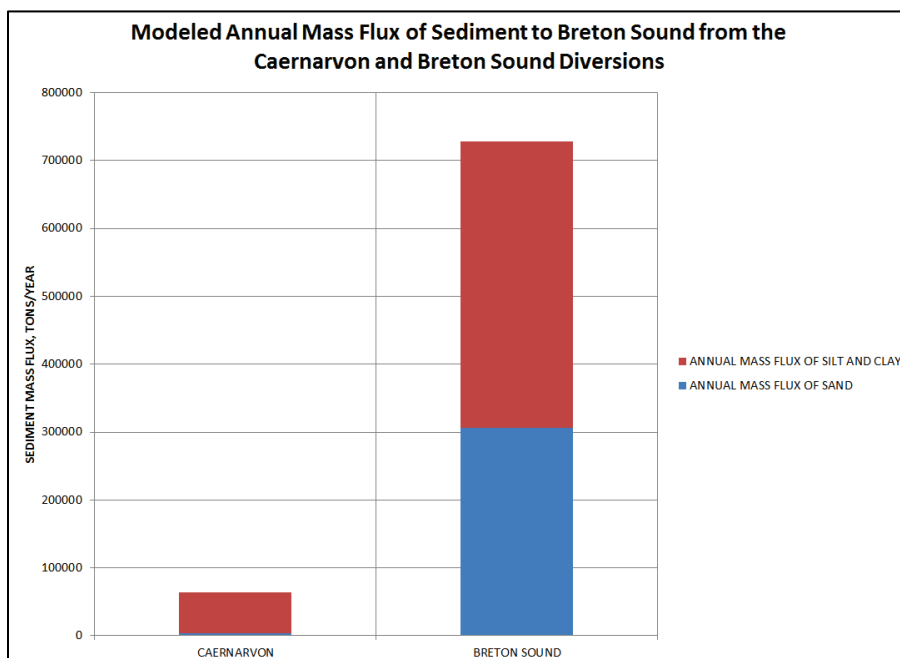


Figure 4-4. Modeled annual water and sediment inflow hydrograph for Caernarvon Diversion.



The modeled annual sediment discharge for the BSD is 728,000 tons/yr, with 42% of that sediment consisting of sand classes. The modeled annual sediment discharge for the Caernarvon Diversion is 64,000 tons/yr, with 6% of that sediment consisting of sand classes. The modeled annual sediment discharges for both diversions are given in Figure 4-5.

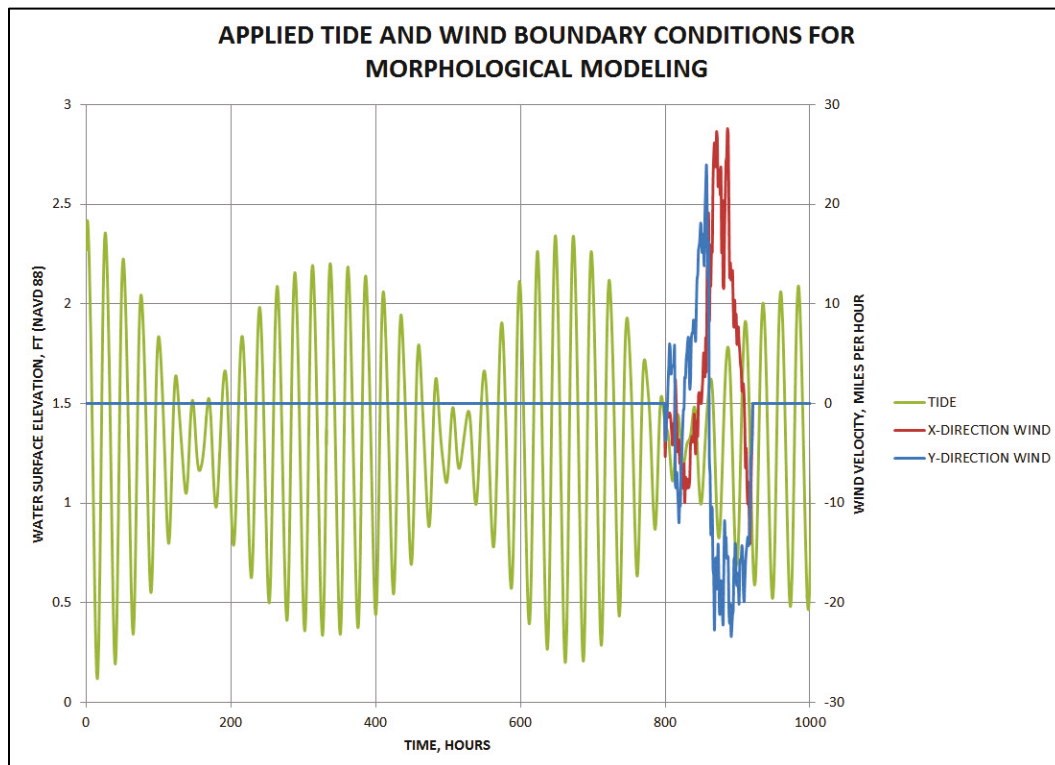
Figure 4-5. Modeled annual mass flux for BSD and CD.



## Tide and wind

To simulate typical tidal conditions, a synthetic tide was constructed using tidal harmonics at the Olga Compressor NOAA gage. A typical storm was also selected and used to simulate the effects of currents and wind waves during storm passage. These boundary conditions are depicted in Figure 4-6.

Figure 4-6. Applied tide and wind boundary conditions for morphological modeling.



## Relative sea level rise

USACE guidance (ETL 1100-2-1, June 2014) (USACE 2014) specifies the following procedures for incorporating relative sea level rise into the project impacts.

Evaluate alternatives using *low*, *intermediate*, and *high* rates of future sea-level change:

- Use the historic rate of local mean sea-level change as the low rate. (The guidance further states that historic rates of sea level rise are best determined by local tide records.)

- Estimate the intermediate rate of local mean sea-level change using the modified National Research Council (NRC) Curve I. Consider both the most recent (Intergovernmental Panel on Climate Change (IPCC) projections and the NRC projections and add those to the local rate of vertical land movement.
- Estimate the high rate of local mean sea-level change using the modified NRC Curve III. Consider both the most recent IPCC projections and the NRC projections and add those to the local rate of vertical land movement.

The Modified NRC curves are based on the curves published by the NRC in 1987 (NRC 1987) with modifications of the coefficients suggested in the IPCC 4th Assessment Report (AR4) (IPCC 2007).

The Modified NRC equation is given below:

$$\eta(t) = (0.0017 + M)t + bt^2 \quad (4-1)$$

where:

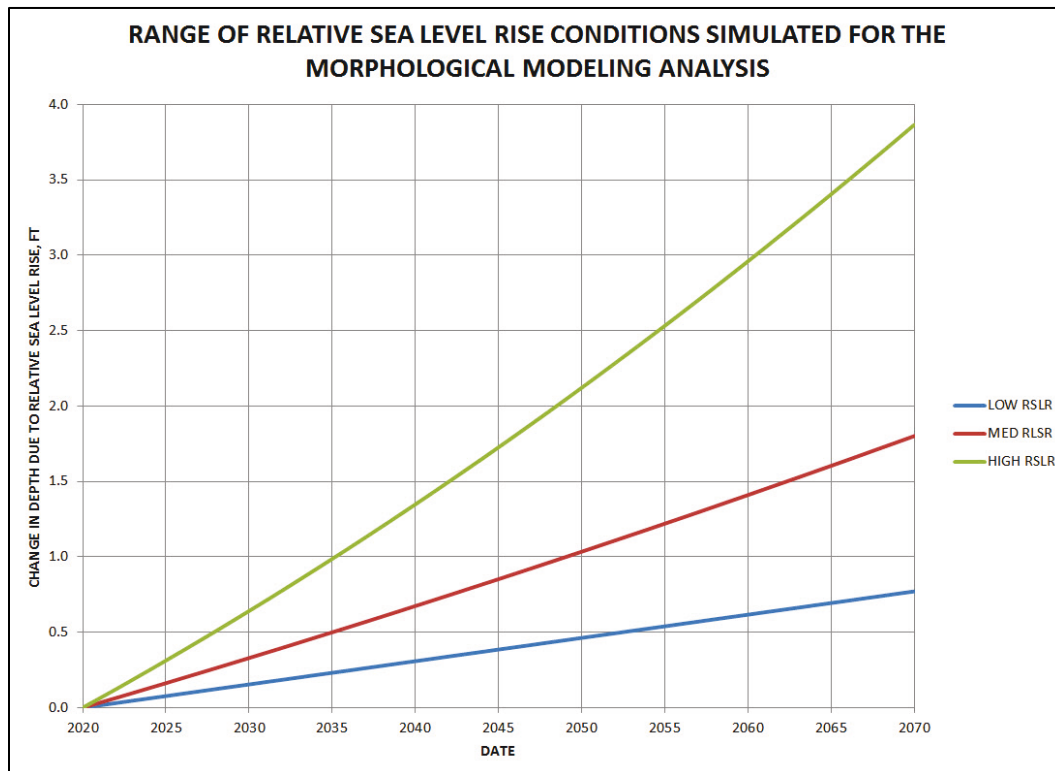
- $\eta(t)$  = the water surface elevation at year  $t$  (meters)
- $t$  = the elapsed time since the baseline year of 1992 (years)
- $M$  = the local rate of subsidence (+) or uplift (-) (meters/year)
- $b$  = the rate of acceleration of eustatic sea level rise (meters/year<sup>2</sup>).

The values of  $b$  are chosen such that the sea level due to eustatic rise at year 2100 is equal to 0.5, 1.0, and 1.5 m, respectively. These values are given in Table 4-2. The values of  $M$  are taken from CPRA estimates of subsidence. The range of estimated subsidence for Breton Sound is 3 to 10 mm/yr. These values are the low and high estimates for this study. The moderate subsidence rate is applied as the average of these two (i.e., 6.5 mm) and are also listed in Table 4-2. The resulting relative sea level rise curves are given in Figure 4-7.

Table 4-2. Values of the rate of acceleration of eustatic sea level rise for each of the Modified NRC curves.

NRC Curve	$b$ (m/yr <sup>2</sup> )	$M$ (m/yr)
NRC I	2.35611E-05	.003
NRC II	6.20345E-05	.0065
NRC III	1.0051 E-04	.01

Figure 4-7. Relative sea level rise curves applied to morphological modeling scenarios.



### Primary productivity

Primary productivity is the rate at which plants produce organic substrate; hence, it is a measure of the ability of plants to contribute to and sustain wetlands. For this study, it is important to characterize primary productivity in terms of the capacity of the plants rather than in terms of the observed behavior of plants. This is because this study is concerned with predicting land gain and loss in terms of the ability for coastal wetlands to keep pace with various rates of relative sea level rise; hence, the historic rates of productivity may not be indicative of the maximum capacity of the plants.

A full treatment of this important process is beyond the scope of this study. Therefore, the approach taken here is to develop and implement a simple algorithm for primary productivity, conceding that this simplification results in considerable uncertainty. However, the model results are reported in terms of relative rates of land change (i.e., with minus without project results) and considered reasonable for this study.

The primary productivity algorithm is based primarily on the results of a study by Kirwen and Gutenspergen (2012). In this study, the researchers conducted marsh organ experiments on *schoenoplectus americanus* and *spartina patens* to determine the correlation between depth of inundation and primary productivity. These results were used to create a simple model in which primary productivity begins at a depth of 0.66 ft and reaches a maximum at a depth of 0 ft. The maximum rate of productivity is converted to a rate of land elevation gain using an average bulk density of organic substrate for Louisiana marshes given by Boudreaux. This value is 136 kg/m<sup>3</sup>.

The resulting maximum rate of primary productivity, expressed in terms of marsh elevation change, is 2.8 centimeters (cm)/yr. Assuming the average rate is half of the maximum (1.4 cm/yr), this rate compares favorably with the observed range for Louisiana coastal marshes of 0.09 to 1.78 cm/yr. The primary productivity algorithm is depicted in Figure 4-8.

## Results

### Qualitative validation to Caernarvon outfall

To determine if the morphological modeling approach adopted here can produce reasonable results, a qualitative comparison was made between 20 yr of predicted land growth in Big Mar and Caernarvon marsh and observations of land growth patterns in the same location. The modeled ground elevations in year 0, year 10, and year 20 of the simulation are shown in Figure 4-9, Figure 4-10, and Figure 4-11, respectively. The observed pattern of land gain is shown in Figure 4-12.

Figure 4-8. Primary productivity algorithm used in morphological modeling scenarios.

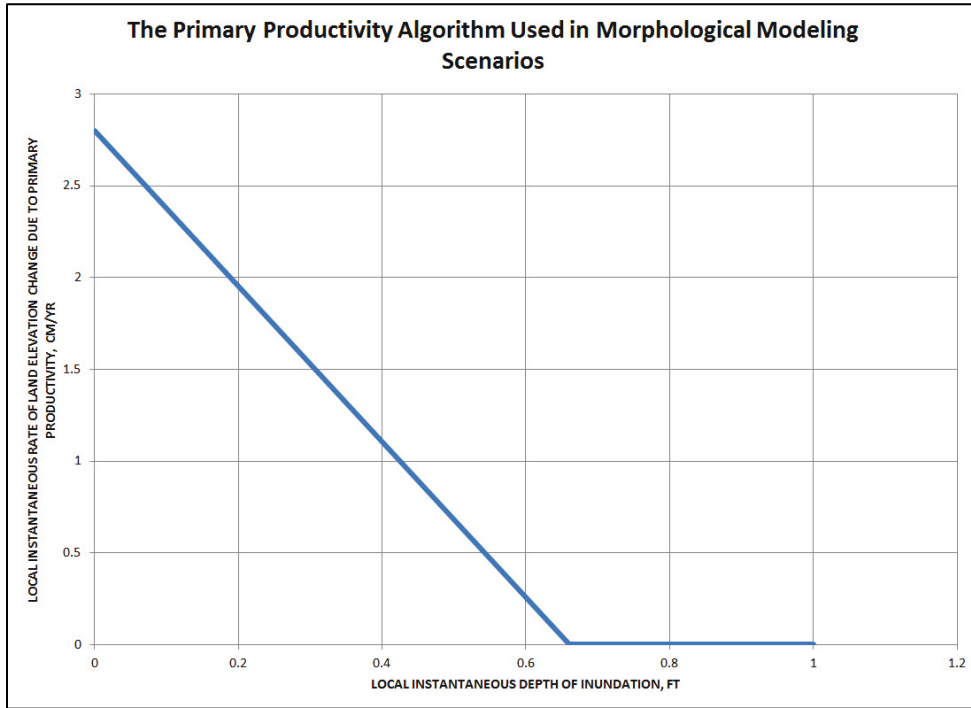


Figure 4-9. Ground elevation at year 0 of morphological model simulation - medium RSLR.

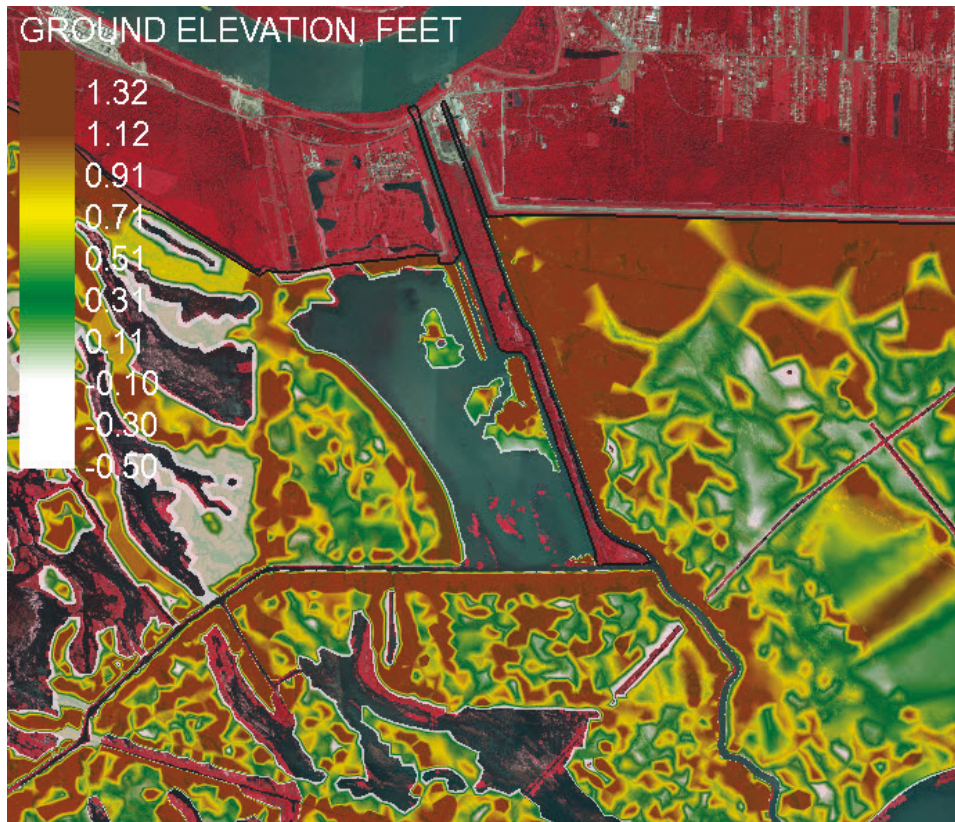




Figure 4-10. Ground elevation at year 10 of morphological model simulation - medium RSLR.

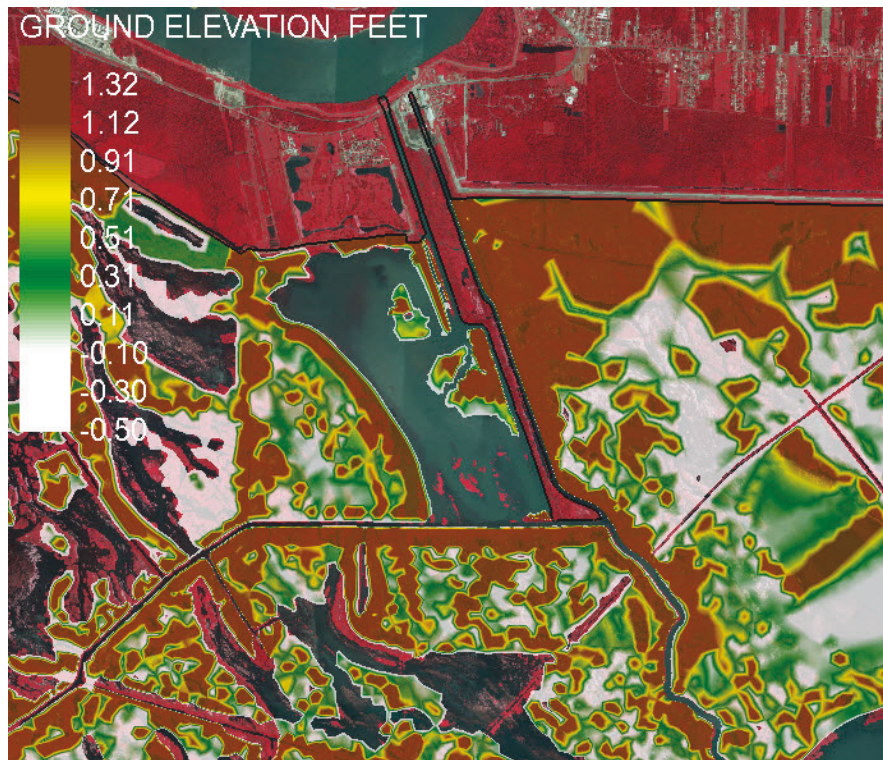


Figure 4-11. Ground elevation at year 20 of morphological model simulation - medium RSLR.

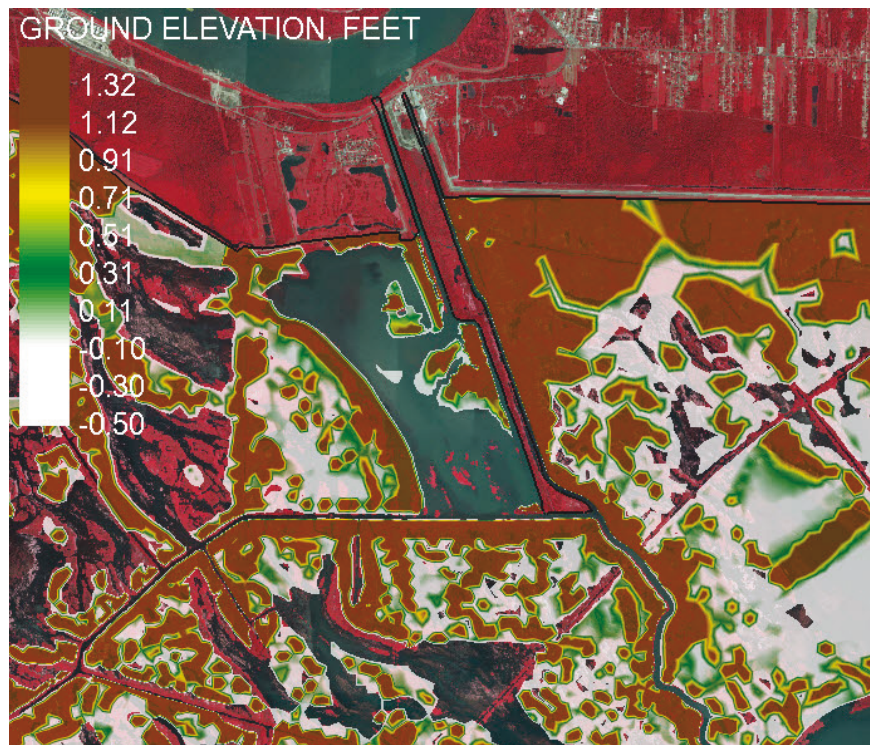




Figure 4-12. Observed pattern of land gain (source: Lake Ponchartrain Basin Foundation).



It is evident that the model is adding land in the location that the observed land gain is occurring. Also, the model depicts regions of the marsh that are deprived of sediment as sinking (due to subsidence) and regions that are emergent as growing (due to primary productivity). This demonstrates the behavior of the basic governing processes that are operating in the model.

#### **Diversion operations and the energy budget constraint**

The patterns of bed displacement (which include changes due to RLSR and primary productivity) associated with the first 5, 10, 15, and 20 yr of BSD operation are given in Figure 4-13, Figure 4-14, Figure 4-15, and Figure 4-16. Only positive (depositional) bed displacement is shown. The development of a sand delta, a primary distributary channel, and vegetated land can clearly be seen. In general, the sandy sediments deposit in a delta at the diversion channel mouth and slowly prograde into the marsh. The silt and clay sediments tend to collect in existing marsh areas and fill in voids in the marsh.

However, although this simulation demonstrates the ability of the diversion to create land, it also shows that the diversion cannot operate at full capacity for the full life cycle of the project. This is because the energy

loss associated with the diversion violates the head constraint at the diversion outfall.

Figure 4-17 depicts the modeled water surface elevation at the control location for the BSD (in the outfall channel, approximately 1 mile downstream of the structure). The control elevation of 5 ft was established as the maximum elevation for which the structure could pass the design discharge of 35,000 cfs.

It is evident that, even at the onset of operations, the water surface elevation is at approximately 4 ft. This is due to the water surface slope in the outfall channel, and more importantly, the significant backwater effects associated with discharging 35,000 cfs into a very shallow, vegetated marsh.

As the simulation progresses, sand deposition at the outfall channel mouth begins to form land. This land obstructs the flow, causing further increases in the water surface elevation. Within 15 years of operation, the water surface elevation has violated the design criteria, and the structure can no longer be operated as designed.

Therefore, to evaluate the structure performance for 50 yr, it was necessary to assume that the material deposited in the outfall channel mouth would be periodically dredged and placed to form new land elsewhere in the marsh. The results of these simulations are given in the next section.

#### **50 yr projections of land gain associated with BSD operations**

Figure 4-18 depicts the land gain associated with 50 yr of operation of the BSD for all three RSLR scenarios. For each RSLR condition, the land gain is computed by subtracting the total emergent land for a simulation without BSD from the total emergent land for a simulation with BSD.

The dashed lines are total land computed directly in the model results. This is land mostly associated with the trapping of silts and clay in existing marshes, and filling voids in those marshes.

Figure 4-13. Bed displacement after 5 yr of operation of BSD.

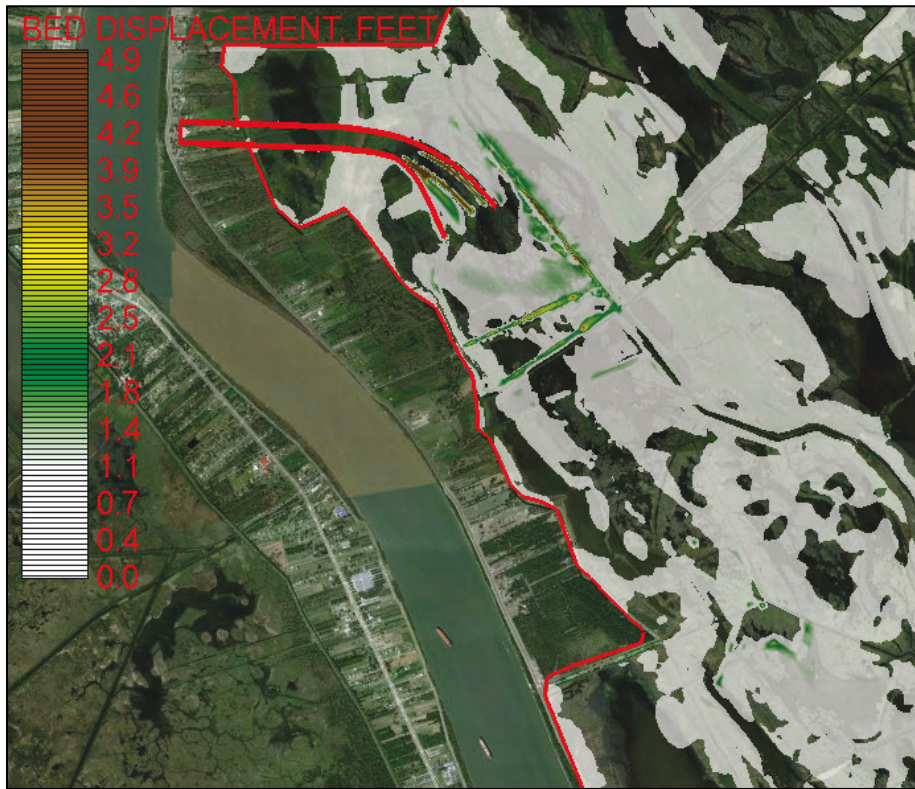


Figure 4-14. Bed displacement after 10 yr of operation of BSD.

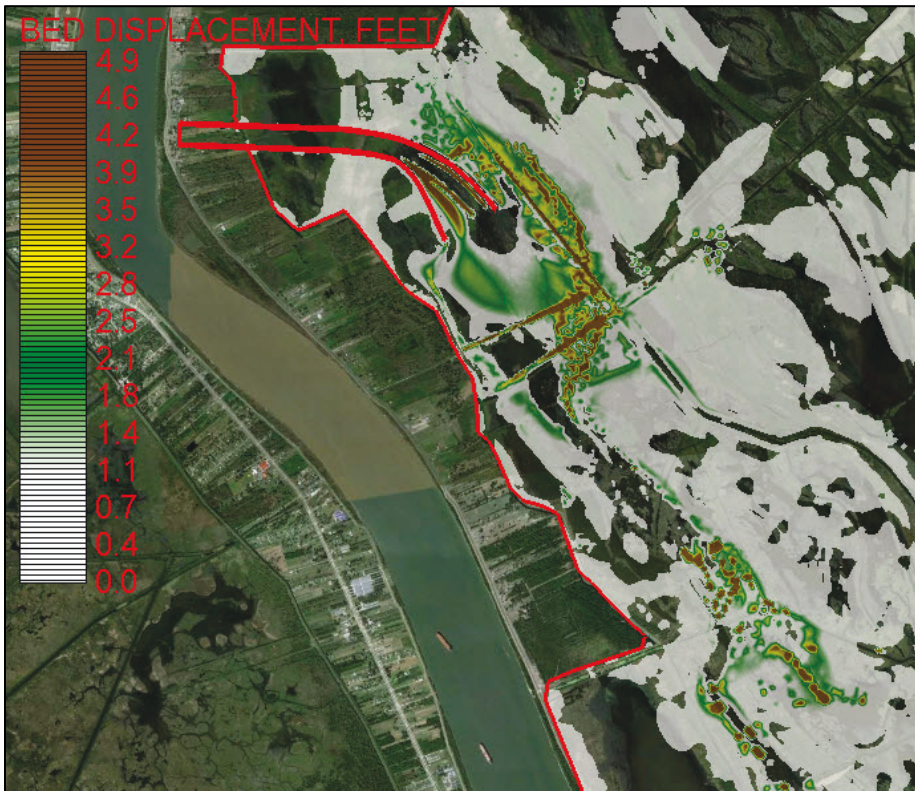




Figure 4-15. Bed displacement after 15 yr of operation of BSD.

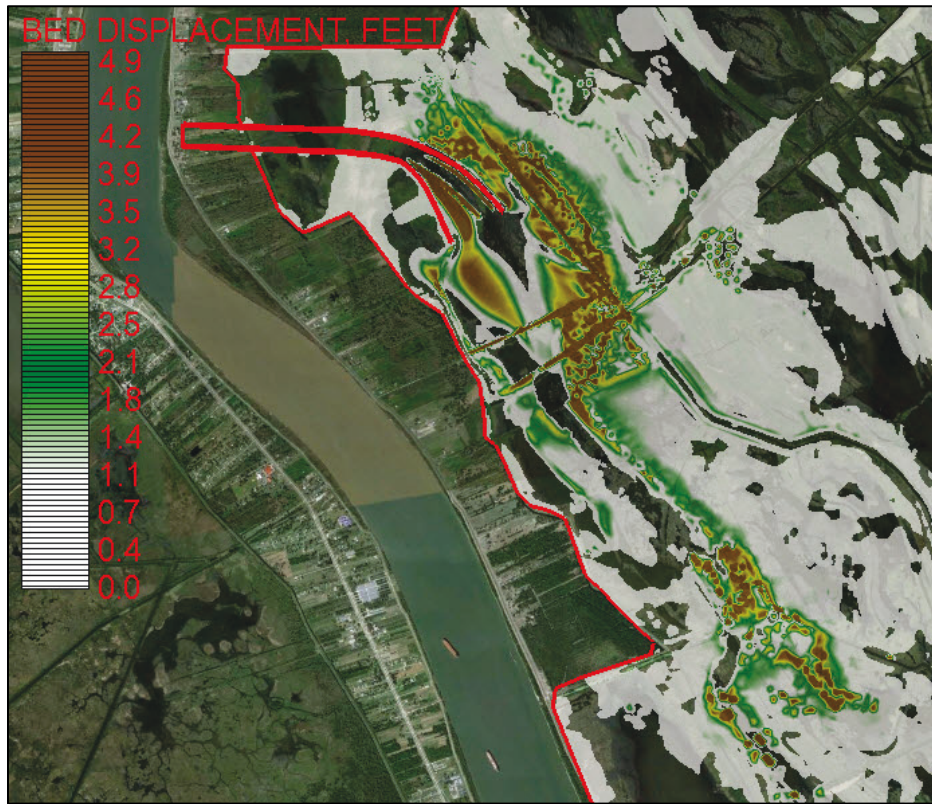


Figure 4-16. Bed displacement after 20 yr of operation of BSD.

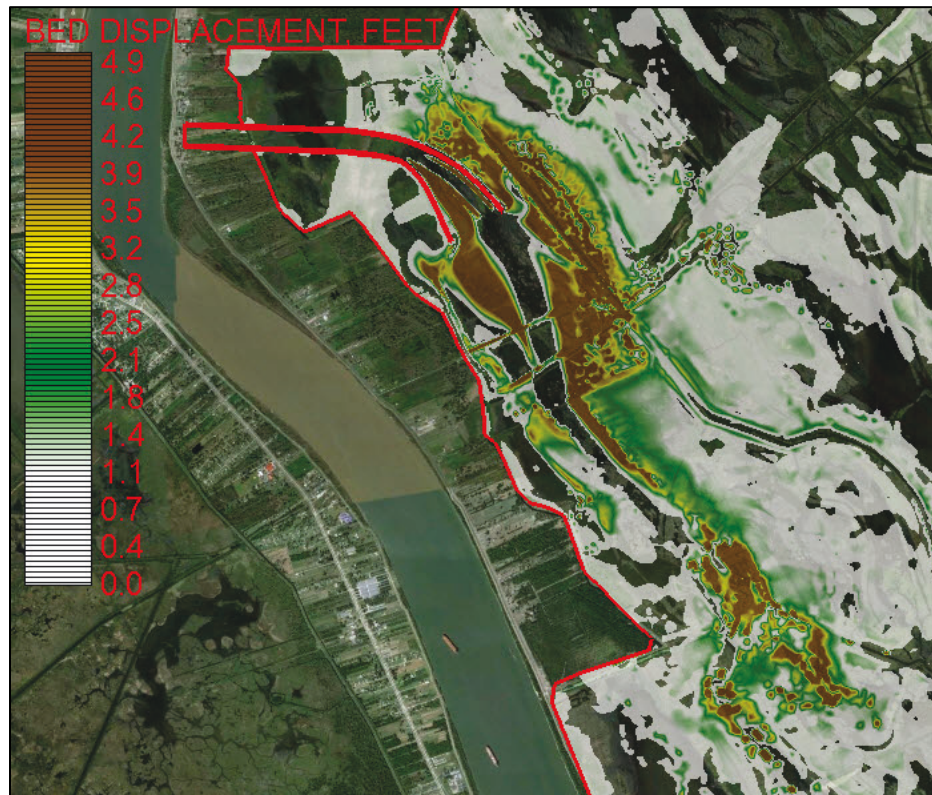


Figure 4-17. Water surface elevation at BSD outfall.

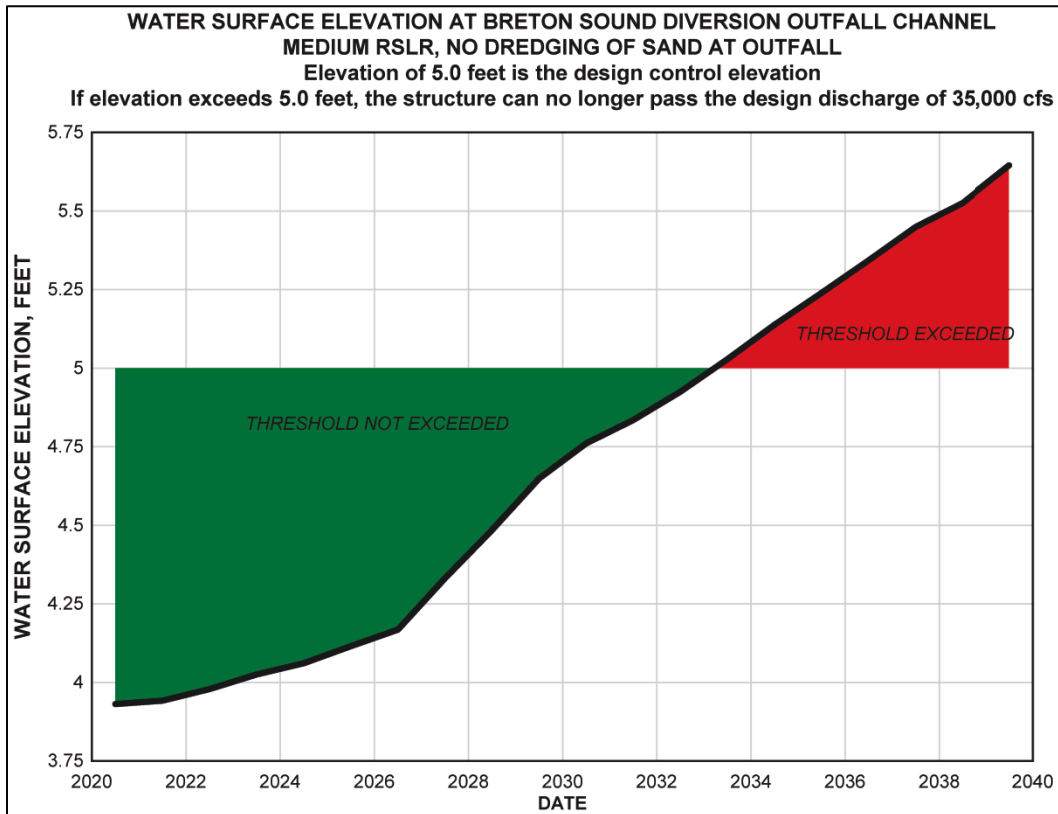
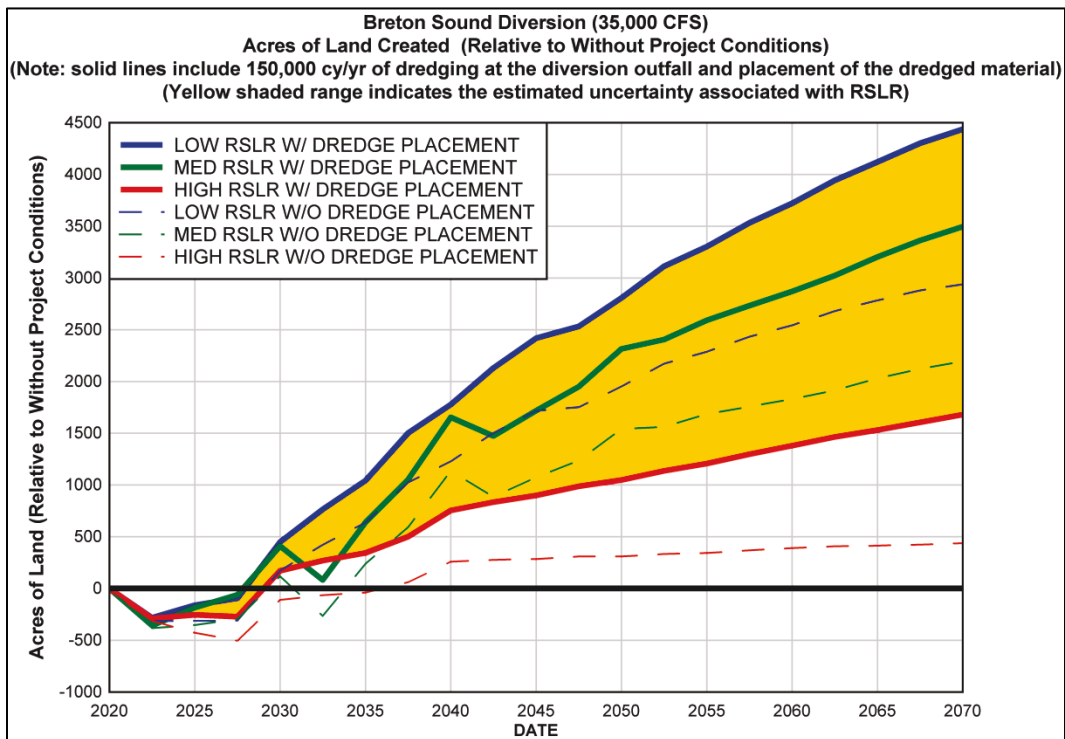


Figure 4-18. Projected land gain associated with the operation of BSD for different rates of RSLR.



The solid lines include the additional land that results from dredging of the outfall channel mouth. This sediment is primarily sandy sediment. The dredging required to keep this location free of sediment is approximately 150,000 cy/yr for every year of operation. For each RSLR scenario, this volume was converted to an approximate amount of equivalent land by assuming a thickness of placement necessary to achieve emergent conditions. This thickness was estimated by first approximating the initial average depth in the vicinity of BSD (3 ft), and then computing the time-averaged value of additional depth associated with RSLR. The final values used in the study are given in Table 4-3.

**Table 4-3. Thickness of dredge placement needed to build land.**

RSLR Scenario	Average Thickness of Dredge Placement Needed to Build Land, $\delta_E$ (ft)
LOW	3.9
MEDIUM	4.5
HIGH	5.4

The shaded region between the low and high RSLR curves is an approximation of the uncertainty associated with the analysis. This does not represent the results of a formal uncertainty analysis but rather is an acknowledgement of the fact that the large uncertainty associated with both subsidence and with potential future eustatic sea level rise is of such significance with respect to land building that this can be used as a proxy estimate of the general uncertainty of the prediction.

Hence, the results of the model indicate that BSD, operated as specified for this study (i.e., 35,000 cfs, only during March and April when the river is flowing with at least 600,000 cfs) will create between 1,600 and 4,450 acres of land over 50 yr of operation relative to the without project condition. This includes the dredging of an average of 150,000 cy/yr of sediment from the outfall mouth for every year of operation and placement of this material elsewhere in the Sound.

Figure 4-19, Figure 4-20, and Figure 4-21 depict the spatial distribution of the land acquired during 50 yr of operation. These plots do not include the placed material; hence, they represent mostly the spatial distribution of land associated with the trapping of silts and clays in existing wetlands, and the filling of voids in those wetlands. There is some conversion of

open water to wetlands, especially just east and southeast of the channel mouth. This is likely due to the deposition of coarse silt and very fine sand.

To estimate the functional efficiency of the operation of the BSD (with respect to the objective of land building), a land building efficiency has been estimated for each RSLR scenario using the following equation:

$$\varepsilon_{LB} = \rho s (1 - p) \frac{A_{CL} \delta_E}{M_{DS}} \times 100\% \quad (4-2)$$

where:

$\varepsilon_{LB}$  = the land building efficiency

$A_{CL}$  = the surface area of the created land

$\delta_E$  = the estimated thickness of deposit needed to create land

$\rho$  = the density of water

$s$  = the specific gravity of the sediment

$p$  = the average porosity of the deposited sediment

$M_{DS}$  = the total mass of sediment discharged through the diversion.

The values of  $\delta_E$  are taken from Table 4-3. The average porosity of the deposited sediment is estimated to be 0.565. The resulting land building efficiency estimates are given in Table 4-4. This indicates that both the low and medium RLSR scenarios are relatively efficient with respect to building land with the sediment diverted from BSD whereas the high RLSR scenario is relatively inefficient. Table 4-4 also gives the percent of land created that is due to dredge placement. Again, a relative small percentage is associated with the low and medium RLSR conditions, and a larger percentage is associated with the high RLSR condition.



Figure 4-19. Spatial distribution of land gain due to the operation of BSD-low RSLR (Note: does not include land from dredge placement).



Figure 4-20. Spatial distribution of land gain due to the operation of BSD - medium RSLR (Note: does not include land from dredge placement).



Figure 4-21. Spatial distribution of land gain due to the operation of BSD - high RSLR  
(Note: does not include land from dredge placement).

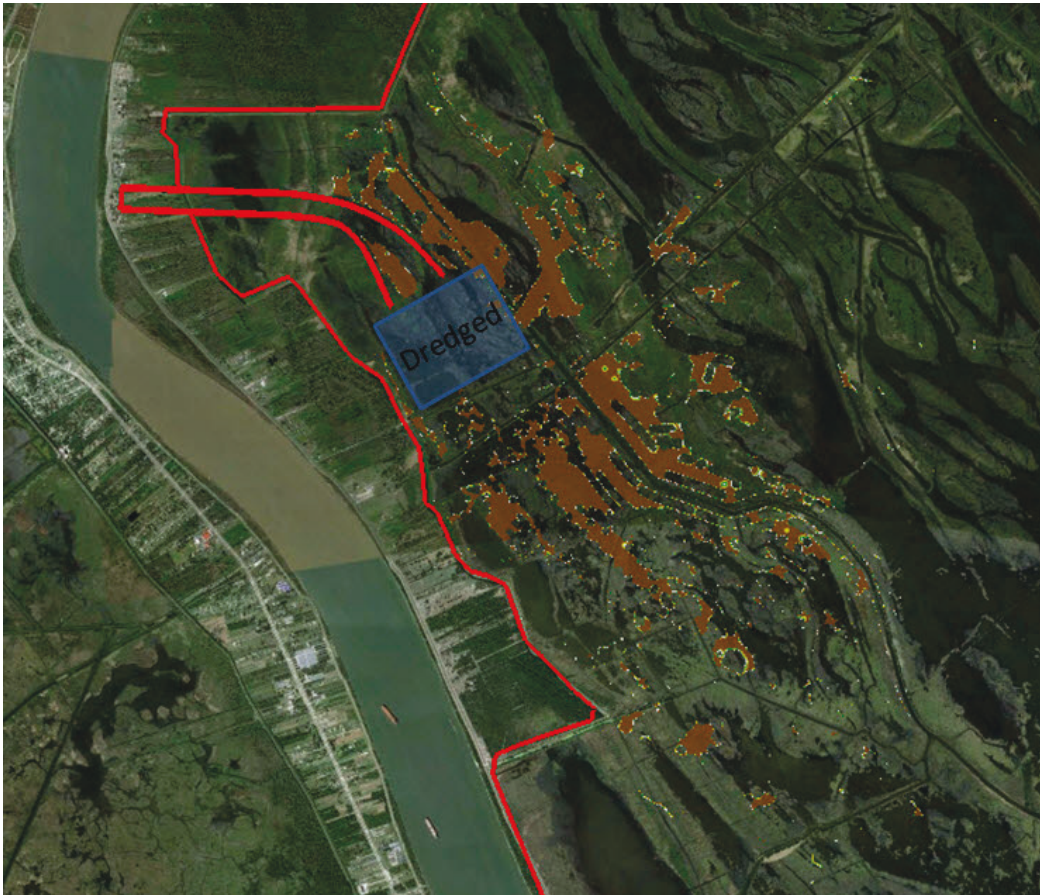


Table 4-4. Land building efficiency and percent of land due to dredge placement.

RSLR Scenario	The Estimated Land Building Efficiency ( $\epsilon_{LB}$ )	Percent of Created Land That Is Due to Dredge Placement
LOW	74.5%	33.8%
MEDIUM	74.0%	37.3%
HIGH	39.1%	74.0%

## 5 Conclusions

The following general conclusions can be derived from this study concerning the effects of the operation of a diversion into Breton Sound.

With respect to salinity, two general statements can be made concerning the expected changes due to operations of BSD as specified on Breton Sound:

- BSD can be expected to rapidly freshen all of Breton Sound (except the region east of Delacroix) and to maintain fresh water conditions in the sound until the diversion is closed.
- After BSD is closed, the time of recovery of salinity in Breton Sound is essentially independent of the volume of fresh water diverted; recovery is a function of the prevailing wind-driven currents and Mississippi River discharges through the eastern passes.

With respect to the land building potential of BSD, this study demonstrates the ability of the diversion to create land, but it also shows that the diversion cannot operate at full capacity for the full life cycle of the project. This is because the deposition of sand at the diversion channel mouth creates a backwater effect that causes the water surface elevation in the outfall channel to exceed the 5 ft elevation prescribed by design constraints. This exceedance occurs within the first 15 yr of diversion operations.

Therefore, to evaluate the structure performance for 50 yr, it was necessary to assume that the material deposited in the outfall channel mouth would be periodically dredged and placed to form new land elsewhere in the marsh.

The results of the morphological modeling indicate that BSD, operated as specified for this study (i.e., 35,000 cfs, only during March and April when the river is flowing with at least 600,000 cfs) is expected to create between 1,600 and 4,450 acres of land over 50 yr of operation relative to the without project condition. This includes the dredging of an annual average of approximately 150,000 cy/yr of sediment from the outfall mouth throughout the life of the project and placement of this material elsewhere in the Sound.



## References

- Alishahi, M. R., and R. B. Krone. 1964. *Suspension of Cohesive Sediments by Wind-Generated Waves*. Technical Report HEL-2-9. University of California: Berkeley Hydraulic Engineering Laboratory.
- Barras, J. A. 2006. *Land Area Change in Coastal Louisiana after the 2005 Hurricanes—A Series of Three Maps*. U.S. Geological Survey Open-File Report 06-1274. [https://www.nwrc.usgs.gov/topics/hurricane/katrina\\_rita/landchange2005/CWPPRA\\_hurricanepres\\_10-18-06\\_vid\\_final.pdf](https://www.nwrc.usgs.gov/topics/hurricane/katrina_rita/landchange2005/CWPPRA_hurricanepres_10-18-06_vid_final.pdf)
- Barras, J. A., P. E. Bourgeois, and L. R. Handley. 1994. *Land Loss in Coastal Louisiana 1956-90*. National Biological Survey, National Wetlands Research Center Open File Report 94-01.
- Berger, R. C., J. N. Tate, G. L. Brown, and G. Savant. 2013. *Adaptive Hydraulics; Users Manual*. <https://chl.ercd.dren.mil/chladh/>
- Brown, G. L. 2012. A quasi-3D suspended sediment model using a set of correction factors applied to a depth-averaged advection diffusion equation. In *Proceedings, IIHR Third International Symposium on Shallow Flows*.
- Brown, G. L., J. N. McAlpin, K. C. Pevey, P. V. Luong, C. R. Price, and B. A. Kleiss. 2019. *Mississippi River Hydrodynamic and Delta Management Study: Delta Management Modeling; AdH/SEDLIB Multi-Dimensional Model Validation and Scenario Analysis Report*. ERDC/CHL TR-19-2. Vicksburg, MS: U.S. Army Engineer Research and Development Center.
- Bunya, S., J. C. Dietrich, J. J. Westerink, B. A. Ebersole, J. M. Smith, J. H. Atkinson, R. Jensen, D. T. Resio, R. A. Luettich, C. Dawson, V. J. Cardone, A. T. Cox, M. D. Powell, H. J. Westerink, and H. J. Roberts. 2010. A high-resolution coupled riverine flow, tide, wind, wind wave, and storm surge model for Southern Louisiana and Mississippi. Part I. Model development and validation. *Monthly Weather Review* 138: 345-377.
- Cheng, Nian-Sheng. 1997. Simplified settling velocity formula for sediment particle. *J. Hydr. Engrg.* 123(2). [https://doi.org/10.1061/\(ASCE\)0733-9429\(1997\)123:2\(149\)](https://doi.org/10.1061/(ASCE)0733-9429(1997)123:2(149))
- CWPPRA Website. 2014. *What is CWPPRA?* Accessed 19 March 2014. <http://lacoast.gov>
- Egiazaroff, L. V. 1965. Calculation of non-uniform sediment concentration. *Journal of Hydraulics Division ASCE* 91(HY4): 225-248.
- Heath, R. E., G. L. Brown, C. D. Little, T. C. Pratt, J. J. Ratcliff, D. D. Abraham, D. Perkey, N. B. Ganesh, K. Martin, and D. P. May. 2015. *Old River Control Complex Sedimentation Investigation*. MRG&P Report No. 6. Vicksburg, MS: U.S. Army Engineer Research and Development Center.

- Intergovernmental Panel on Climate Change (IPCC). 2007. *Climate Change 2007: The Physical Science Basis. Contribution of Working Group I to the Fourth Assessment Report of the Intergovernmental Panel on Climate Change*. Edited by S. Solomon, D. Qin, M. Manning, Z. Chen, M. Marquis, K.B. Averyt, M. Tignor, and H. L. Miller. Cambridge, UK: Cambridge University Press. <http://ipcc-wg1.ucar.edu/wg1/wg1-report.html>
- Johnson, D. R. 2008. *Ocean Surface Current Climatology in the Northern Gulf of Mexico*. Ocean Springs, MS: Gulf Coast Research Laboratory.
- Kirwan, M. L., and G. R. Guntenspergen. 2012. Feedbacks between inundation, root production, and shoot growth in a rapidly submerging brackish marsh. *Journal of Ecology* 100: 764–770.
- Kleinhans, M. G., and L. C. van Rijn. 2002. Stochastic prediction of sediment transport in sand-gravel bed rivers. *Journal of Hydraulic Engineering* 128(4): 412–425.
- Krone, R. 1962. *Flume Studies of the Transport of Sediment in Estuarial Shoaling Process*. University of California, Berkeley: Hydraulic Engineering Laboratory and Sanitary Engineering Research Laboratory.
- Lane, R. L., J. W. Day, B. D. Marx, E. Reyes, E. Hyfield, and J. N. Day. 2007. The effects of riverine discharge on temperature, salinity, suspended sediment and chlorophyll a in a Mississippi delta estuary measured using a flow through system. *Estuarine Coastal and Shelf Science* 74(1–2): 145–154.
- National Research Council (NRC). 1987. *Responding to Changes in Sea Level, Engineering Implications*. Committee on Engineering Implications of Changes in Relative Mean Sea Level, Marine Board, Commission on Engineering and Technical Systems, National Research Council. Washington, DC: National Academy Press. [http://www.nap.edu/catalog.php?record\\_id=1006](http://www.nap.edu/catalog.php?record_id=1006)
- Roberts, H. H. 1997. Dynamic changes of the holocene Mississippi River delta plain: The delta cycle. *Journal of Coastal Research* 13(3): 605–627.
- Schroeder, W. W., O. K. Huh, L. J. Rouse, Jr., and W. J. Wiseman, Jr. 1985. Satellite observations of the circulation east of the Mississippi Delta: Cold-air outbreak conditions. *Remote Sensing of Environment* 18(1): 49–58.
- Sharp, J. A., C. D. Little, G. L. Brown, T. C. Pratt, R. E. Heath, L. C. Hubbard, F. Pinkard, K. Martin, N. D. Clifton, D. W. Perkey, and N. B. Ganesh. 2013. *West Bay Sediment Diversion Effects*. ERDC/CHL TR-13-15. Vicksburg, MS: U.S. Army Engineer Research and Development Center.
- Snedden, G. A., J. E. Cable, C. Swarzenski, and E. Swenson. 2007a. Sediment discharge into a subsiding Louisiana deltaic estuary through a Mississippi River diversion. *Estuarine Coastal and Shelf Science* 71(1–2): 181–193.
- Snedden, G. A., J. E. Cable, and J. W. Wiseman. 2007b. Subtidal sea level variability in a shallow Mississippi River deltaic estuary, Louisiana. *Estuaries and Coasts* 30(5): 802–812.
- U.S. Army Corps of Engineers (USACE). 2014. *Procedures to Evaluate Sea Level Change: Impacts, Responses, and Adaptation*. ETL-1100-2-1. Washington, DC.

Wright, S., and G. Parker. 2004. Flow resistance and suspended load in sand-bed rivers: simplified stratification model. *Journal of Hydraulic Engineering* 130(8): 796–805.

**REPORT DOCUMENTATION PAGE**

*Form Approved  
OMB No. 0704-0188*

The public reporting burden for this collection of information is estimated to average 1 hour per response, including the time for reviewing instructions, searching existing data sources, gathering and maintaining the data needed, and completing and reviewing the collection of information. Send comments regarding this burden estimate or any other aspect of this collection of information, including suggestions for reducing the burden, to Department of Defense, Washington Headquarters Services, Directorate for Information Operations and Reports (0704-0188), 1215 Jefferson Davis Highway, Suite 1204, Arlington, VA 22202-4302. Respondents should be aware that notwithstanding any other provision of law, no person shall be subject to any penalty for failing to comply with a collection of information if it does not display a currently valid OMB control number.  
**PLEASE DO NOT RETURN YOUR FORM TO THE ABOVE ADDRESS.**

<b>1. REPORT DATE</b> March 2019		<b>2. REPORT TYPE</b> Final Report		<b>3. DATES COVERED (From - To)</b>	
<b>4. TITLE AND SUBTITLE</b> Hydrodynamic, Salinity, and Morphological Modeling Study of a Sediment Diversion; An Application of the Adaptive Hydraulics Model/SEDLIB Sediment Transport Library				<b>5a. CONTRACT NUMBER</b>	
				<b>5b. GRANT NUMBER</b>	
				<b>5c. PROGRAM ELEMENT NUMBER</b>	
<b>6. AUTHOR(S)</b>  Gary L. Brown and Kimberly C. Pevey				<b>5d. PROJECT NUMBER</b> 118958	
				<b>5e. TASK NUMBER</b>	
				<b>5f. WORK UNIT NUMBER</b>	
<b>7. PERFORMING ORGANIZATION NAME(S) AND ADDRESS(ES) (see reverse)</b>  Coastal and Hydraulics Laboratory U.S. Army Engineer Research and Development Center 3909 Halls Ferry Road Vicksburg, MS 39180-6199				<b>8. PERFORMING ORGANIZATION REPORT NUMBER</b>  MRG&P Report No. 27	
<b>9. SPONSORING/MONITORING AGENCY NAME(S) AND ADDRESS(ES)</b> U.S. Army Corps of Engineers, New Orleans District 7400 Leake Ave New Orleans, LA, 70118				<b>10. SPONSOR/MONITOR'S ACRONYM(S)</b> USACE MVN	
				<b>11. SPONSOR/MONITOR'S REPORT NUMBER(S)</b>	
<b>12. DISTRIBUTION/AVAILABILITY STATEMENT</b> Approved for public release; distribution is unlimited.					
<b>13. SUPPLEMENTARY NOTES</b>					
<b>14. ABSTRACT</b> A water diversion designed to channel sediment-rich water from the Mississippi River into Breton Sound marsh was evaluated through application of a numerical model. The model was validated to data collected from April to December 2010. After model validation was complete, simulations to understand the effects of the proposed diversion on hydrodynamics, salinity, sedimentation, and land building were conducted. Model salinity results indicate that the proposed diversion will rapidly freshen most of Breton Sound and maintain fresh water conditions in the Sound until the diversion is closed. After closure, the time of recovery of salinity in Breton Sound is a function of the prevailing wind-driven currents and Mississippi River discharges through the eastern passes. With respect to the land building potential, model results indicate that the diversion has the capability to create land, but that the diversion cannot operate at full capacity for the full life cycle of the project. Deposition of sand at the diversion channel mouth creates a backwater effect that causes the water surface elevation in the outfall channel to exceed prescribed design constraints. The outfall channel mouth will therefore need to be periodically dredged and placed to form new land elsewhere in the marsh.					
<b>15. SUBJECT TERMS</b>  Breton Sound (La.), Diversion structures (Hydraulic engineering), Geomorphology, Salinity, Sedimentation and deposition, Sediment transport—Computer simulation					
<b>16. SECURITY CLASSIFICATION OF:</b>			<b>17. LIMITATION OF ABSTRACT</b>	<b>18. NUMBER OF PAGES</b>	<b>19a. NAME OF RESPONSIBLE PERSON</b>
<b>a. REPORT</b>	<b>b. ABSTRACT</b>	<b>c. THIS PAGE</b>			Gary L. Brown
Unclassified	Unclassified	Unclassified	SAR	87	<b>19b. TELEPHONE NUMBER (Include area code)</b> 601-634-4417